MASTERARBEIT | MASTER'S THESIS

Titel | Title

Root Architecture and Root Mechanical Properties of Tōtara, Kānuka, and Poplar Trees Across Auckland Hill Country, New Zealand

verfasst von | submitted by

Anne Margaretha Hendrika Fokker

angestrebter akademischer Grad | in partial fulfilment of the requirements for the degree of

Master of Science (MSc)

Wien | Vienna, 2025

Studienkennzahl lt. Studienblatt | Degree programme code as it appears on the student record sheet:	UA 066 855
Studienrichtung lt. Studienblatt | Degree programme as it appears on the student record sheet:	Masterstudium Geography: Global Change and Sustainability
Betreut von | Supervisor:	Univ.-Prof. Dipl.-Geogr. Dr. Thomas Glade

Acknowledgements

I would like to thank everybody who has been supporting and motivating me throughout this amazing project. First and foremost, I would like to express my gratitude towards my supervisor Thomas Glade for offering me the wonderful and unexpected opportunity to travel to New Zealand and collect ever-lasting memories and experiences. Unfassbar schön war es! Secondly, I would like to thank Raphael Spiekermann and Tom Mackay-Smith from Verdantia Research for facilitating the whole project and believing in me. Raphael for making time to listen, provide feedback, and share his great technical expertise, without him I would not have been able to make it. Tom for our brainstorm sessions, his support and motivation during the data collection, and, not unimportant, allowing me to use the ute to explore New Zealand! Thirdly, a big shout-out to the country's best field work team, Nicola, Simone, Mark, Natalie, and Alisha: endless motivation, dedication, singalongs, and laughter during and after working hours! Lastly, I want to say a special thank you to all my friends, family, and colleagues who have been there for the mental support. Providing me an audience when I needed to get my thoughts organised, or just some motivating words when things were not going as smooth as hoped for. Opa, tante Anita, Lavi, Clemens, Steven, Aoibhin, Max, Lisabelle, Estephany, Felix, any many more, thank you for pulling me through!

Abstract

Vegetation is an important asset for preventing rainfall-triggered landslides across New Zealand pastoral hill country. Trees may stabilize sloped pastures depending on their spatial root distribution and reinforcing capacities. Introduced tree species have been selected for soil stabilisation in the past, but an interest has emerged for the integration of indigenous species into silvopastoral systems. Field data on these species is limited, especially in the context of space-planted trees. This study is directed at the description, quantification, and comparison of the root distribution and root mechanical properties of the introduced *Poplar sp.* (poplar) and the natives *Kunzea ericoides* (kānuka) and *Podocarpus tōtara* (tōtara). Across Auckland Hill Country, 12 trees were assessed for their root architecture. Linear mixed effects models were used to assess root arrangements across species and two soil types. Variability in root architecture was found between the exotic and native species. Overall, the poplar exhibited fewer but coarser roots. The natives showed a mat-like root architecture consisting of very fine roots. No clear differences in architecture were found across the soil types. Field pullout tests of 80 poplar, 79 kānuka, and 79 tōtara roots were performed. A linear mixed effects model as well as exponential regressions were fitted to test the influence of independent factors on root mechanical behaviour. Higher tensile strength values were found in the typic yellow ultic soil compared to the mottled yellow ultic soil. Overall, tensile strength, elastic modus, and survival probability changed with root diameter. All species rendered different fitted coefficients. Findings of the current study are in strong contrast to previous findings. Nevertheless, these results provided first insights into root architecture and root mechanical properties of space-planted poplar, kānuka and tōtara in pastoral hill country. The results may provide a basis for further modelling efforts incorporating root reinforced soils.

Zusammenfassung

Die Vegetation ist ein wichtiger Faktor für die Verhinderung von durch Regen ausgelösten Erdrutschen in den Weidehügeln Neuseelands. Bäume können je nach ihrer räumlichen Wurzelverteilung und ihrer Verstärkungskapazität Hangweiden stabilisieren. In der Vergangenheit wurden eingeführte Baumarten zur Bodenstabilisierung ausgewählt, doch mittlerweile besteht Interesse daran, einheimische Arten in silvopastorale Systeme zu integrieren. Die Felddaten zu diesen Arten sind begrenzt, insbesondere im Zusammenhang mit räumlich gepflanzten Bäumen. Diese Studie befasst sich mit der Beschreibung, Quantifizierung und dem Vergleich der Wurzelverteilung und der mechanischen Eigenschaften der Wurzeln der eingeführten Art *Populus sp.* (Pappel) und der einheimischen Arten *Kunzea ericoides* (Kānuka) und *Podocarpus tōtara* (Tōtara). Im Auckland Hill Country wurden 12 Bäume hinsichtlich ihrer Wurzelarchitektur untersucht. Lineare gemischte Effektmodelle wurden verwendet, um die Wurzelanordnung über verschiedene Arten und zwei Bodentypen hinweg zu bewerten. Es wurde eine Variabilität in der Wurzelarchitektur zwischen den exotischen und einheimischen Arten festgestellt. Insgesamt wies die Pappel weniger, aber gröbere Wurzeln auf. Die einheimischen Arten zeigten eine mattenartige Wurzelarchitektur, die aus feinen Wurzeln bestand. Es wurden keine deutlichen Unterschiede in der Architektur zwischen den Bodentypen festgestellt. Es wurden Feldauszugstests an 80 Pappel-, 79 Kānuka- und 79 Tōtara-Wurzeln durchgeführt. Ein lineares gemischtes Effektmodell sowie exponentielle Regressionen wurden angepasst, um den Einfluss unabhängiger Faktoren auf das mechanische Verhalten der Wurzeln zu testen. Im typischen gelben Ultiboden wurden höhere Zugfestigkeitswerte festgestellt als im fleckigen gelben Ultiboden. Insgesamt veränderten sich Zugfestigkeit, Elastizitätsmodul und Überlebenswahrscheinlichkeit mit dem Wurzeldurchmesser. Alle Arten ergaben unterschiedliche Koeffizienten. Die Ergebnisse der aktuellen Studie stehen in starkem Kontrast zu früheren Erkenntnissen. Dennoch lieferten diese Ergebnisse erste Einblicke in die Wurzelarchitektur und die mechanischen Eigenschaften der Wurzeln von räumlich gepflanzter Pappel, Kānuka und Tōtara in den Weidehügeln Neuseelands. Die Ergebnisse können als Grundlage für weitere Modellierungsbemühungen dienen, bei denen wurzelverstärkte Böden berücksichtigt werden.

Table of Contents

List of Figures

List of Tables

List of Abbreviations

BRR …..…….. Basal root reinforcement

DBH …..…….. Diameter at breast height

F_{max} …… Maximum applied force / Maximum tensile strength

FoS ……. Factor of Safety

LMM ……..... Linear Mixed Effects Model

LRR ……...…… Lateral root reinforcement

MORLE ……. Multiple-occurrence regional landslide events

RAR ……...……..… Root area ratio

RBMw ……... Root Bundle Model with Weibull function

RRM …… Root Reinforcement Model

SSM ……..… Slope Stability Model

UYM …….. Mottled Yellow Ultic

UYT ……... Typic Yellow Ultic

WWM ……. Wu and Waldron's Model

1. Introduction and Problem Statement

Much of Aotearoa New Zealand is prone to high rates of soil erosion. Due to the country's geographical location, the magnitude and frequency of precipitation, steep terrains, and significant recent changes in landcover, New Zealand's soil removal rates are proportionally high (Basher, 2013; Dymond & Shepherd, 2023). When soil renewal rates exceed the rate of removal, soil erosion becomes unsustainable. Specifically on New Zealand's North Island, past clearance of indigenous forests and other human activities have led to increased risks of soil erosion (Page et al., 2000; Glade, 2003). With climate change further inducing the intensity of rainfall events, as well as intensified deforestation, sloped soils are increasingly susceptible to mobilisation (Dymond & Shepherd, 2023). On the North Island, soil erosion rates are estimated to range between 80 and 5000 tonnes/km^2/year (Dymond et al., 2010).

Vegetation plays a crucial role in mitigating the risk of hydrogeomorphological hazards (Schwarz et al., 2010c). Through multiple hydrological and mechanical effects, woody roots contribute to slope stability and enhance the overall cohesion of the soil-root matrix (Vergani et al., 2016). Especially in vegetation-poor pastoral systems, the integration of trees or shrubs can increase the stability of slopes. Generally, the relationship between roots and the soils they occupy are complex, site-specific, and constantly changing (Masi et al., 2021). The level of reinforcement of the soil is strongly determined by the vegetation's root architecture and root mechanical properties. These root characteristics differ between species, densities, and soils, thereby determining the effectivity of the root reinforcement.

Over the last decades, there is a growing interest for holistic landscape management, including more long-term solutions for slope protection (Barton, 2008). To date, important species for slope stability have been predominantly exotic to New Zealand, for example *Poplar sp.* (poplar). This species has been preferred for its low purchasing price and general availability, but also fast growth, compatibility with livestock, and its strong and extensive root system (Mackay-Smith et al., 2021; Satchell, 2018). However, the objective to combat natural hazards and other environmental pressures has been broadened. Complementary to soil stabilization, the enhancement of the cultural value of a landscape, increasing biodiversity and soil quality, and carbon sequestration play an increasingly important role in species selection (Kimberley et al., 2025). Consequently, the reintroduction of native New Zealand tree species is favoured, among others for their longevity.

Extensive research has been conducted on both indigenous as well as introduced tree species in the context of soil erosion (Philips et al., 2023). Across New Zealand, the below-ground extent of trees has been examined and compared to estimate their potential contribution to slope stability (e.g. Marden et al., 2018b; Giadrossich et al., 2020). Commonly studied is the previously mentioned poplar, introduced by Europeans and now prevalent throughout New Zealand due to its versatility and economic benefits (Ngo et al., 2023). The species is easy to propagate via coppicing, low-maintenance, low in costs, and brings up nutrients to the surface through annual shedding of leaves (Sulaiman, 2006). However, due to a high risk of breaking under strong winds as they get older, the recommended felling age of poplar is about fifty years

(Mackay-Smith et al., 2021). Increasingly more indigenous trees and shrubs are being assessed for their root reinforcing capacities (e.g., Lambie et al., 2021; McIvor et al., 2024). Common species such as *Kunzea ericoides* (kānuka) and *Podocarpus tōtara* (tōtara) are endemic to New Zealand, found in forests, shrublands, and abundantly scattered across hill country pasture. Kānuka is a pioneer species, characterised by quick growth on relatively nutrient poor soils; tōtara is a long-lived pioneer that easily propagates, whilst also persisting in climax communities (Dawson & Lucas, 2012). Despite being an abundant native, tōtara has been greatly understudied (Phillips et al., 2023).

Most of existing root strength datasets have been derived from tests performed in a laboratory setting (e.g. Watson & Marden, 2004) or consisted of in-situ field measurements supplemented with laboratory tests (e.g. Ngo et al., 2023). The limited number of in-situ field measurements has been conducted primarily in the southeastern region of the North Island, among others at the Ballantrae Hill Country Research Station (McIvor et al., 2008). Furthermore, research on soil stabilisation by space-planted trees remains limited (Spiekermann et al., 2021; Spiekermann et al., 2022b). Typically, studies were performed on planted trials with a relatively high stem density and were carried out predominantly in free-draining sandy soils or imperfectly drained soils with silt-loam textures (e.g. Marden et al., 2025; Phillips et al., 2014; Schwarz et al., 2016). It has been recognised, however, that individually spaced species develop distinct root growth patterns in the absence of neighbouring competition. Therefore, the mature trees in such space-planted context may be underestimated in their potential contribution to slope stability. Moreover, soil is a key determinant of the root architecture, and assessment across different soils may consequently yield varying root reinforcement values.

To date, no measurements of root system architecture and mechanical properties have been undertaken for mature, widely spaced common native tree species in New Zealand. Likewise, no research has been conducted in the ultic soils dominant across the Auckland Pastoral Hill Country. Hence, site-specific dynamics and behaviour of live root systems under these conditions remain poorly understood. Yet, such data are essential for the development of root reinforcement models that can be integrated into slope stability models, as demonstrated for example by Spiekermann et al. (2023). Obtaining such data allows for comparisons between species and modelling to be undertaken to understand the effectiveness of different species and planting densities across varying soils. The current research aims to close this gap by performing field assessments of the roots of individually spaced natives kānuka and tōtara and introduced poplar species across Auckland Hill Country, New Zealand.

In the following section, the specific research questions and corresponding hypotheses addressing the research gap are presented. Then, a summary of the relevant literature is provided, before explaining the materials and methods directed to answering the research question. The results and the discussion thereof will follow, and at last the concluding remarks are provided. At the end of the document, references and appendices are listed.

2. Research Questions and Hypotheses

The following research questions and corresponding hypotheses have been formulated:

1. **Do the vertical and lateral arrangements of the roots differ between the species across the soil types?**

This question aims to examine and compare the below-ground tree extent across different growth dimensions and soil types. Understanding the trees' below-ground architecture is essential for predicting the root reinforcement of the soil.

H1: There is a difference in root architecture between the natives tōtara and kānuka and the exotic poplar. The natives have a similar root architecture of heart-shaped form, poplar exhibits a plate-like root architecture.

2. **Does the tensile strength of the roots differ between species across the soil types?**

This question aims to assess and compare the mechanical properties of individual tree roots of the species across the different soils. Understanding the trees' mechanical properties is essential for predicting the root reinforcement of the soil.

H1: Root tensile strength of both poplar and kānuka are in line with existing literature. In contrast, the mechanical properties of tōtara are within the range of other softwood tree species native to New Zealand and therefore exhibit a lower range in tensile strength compared to hardwood species such as kānuka.

3. **In what way do independent factors modify the variability of root mechanical behaviour?**

This question is directed at examining the role of the independent factors i) root diameter and ii) species on the roots' mechanical behaviour as described by the Root Bundle Model with Weibull function (RBMw). Furthermore, the aim is to assess how the coefficients of i) maximum tensile force function, ii) the apparent spring constant function, and iii) the survival probability function influence the slope and variability of the curve.

H1: Independent factors root diameter and species are expected to significantly influence the coefficients of the parameters of the RBMw.

3. Theoretical Background

3.1. Soil Erosion in New Zealand

New Zealand experiences above world-average rates of erosion due to its steep terrain, high rainfall, as well as tectonic activity (Basher, 2013). Additionally, New Zealand's history of large-scale clearance of indigenous forests for farming purposes has been a major cause of enhanced erosion vulnerability, particularly on pastoral hills (Glade, 2003). Steep pastoral hill landscapes show an increased loss of sediment, nutrients, and faecal coliforms to waterways when compared to forested landscapes (Dodd et al., 2016). Manaaki Whenua - Landcare Research (2024) estimated that, in 2022, a total of 182 million tonnes of eroded soil washed out into New Zealand's waterways. Throughout the country, though, the average soil erosion rates vary substantially. The country's lowest rates are less or equal to 50 tonnes km^{-2} $year^{-1}$, whereas its highest rates exceed 20,000 tonnes km^{-2} $year^{-1}$. The very northern region of the North Island, the east coast of the North Island, and the west coast of the South Island are considered erosion "hot spots". The average annual cost (derived from a 20-year period) of soil erosion has been estimated at NZ$126 million (Crozier, 2005).

Landslides are a type of soil erosion, defined as the mass downward movement of soil and rock under the effect of gravity (Cruden, 1991). When the dynamic between the forces holding the soil together (resisting forces) and the forces exerting stress on this cohesive matrix (driving forces) changes, slope failure may be initiated. Landslides occur worldwide and are caused by a multitude of conditioning and triggering factors. Natural factors that determine slope stability are geology, morphology, hydrology, soil properties, land use and land cover, seismicity, and volcanic activity of the area (Pacheco Quevedo et al., 2023). Triggers that may lead to slope failure are, for example, precipitation, earthquakes, snow melt, and human activity (Haque et al., 2019). In New Zealand, the temporal and spatial occurrence of landslides is heavily affected by anthropogenic change to the land cover. Crozier (2010) stated the human-induced disturbance of the landscape to be "of equal, if not greater, importance than climate change" considering slope instability (p. 1).

Shallow, rapid slides is the most common form of erosion in New Zealand (Glade, 2003). Such landslides are characterised by planar sliding, with the surface of rupture at about two-meter vertical depth (Basher, 2013). Shallow landslide initiation is the sum of various physical properties and the composition of the soil, as well as climate, vegetation, land use, hillslope hydrology, and ecological processes. Generally, rainfall is the main trigger for shallow landslides (Wieczorek and Glade, 2005). After high-intensity rainfall, multiple-occurrence regional landslides events (MORLEs) are common, consisting of hundreds to thousands of shallow landslides occurring at a high density within a given area. Each individual soil slip is relatively small, with the debris and earth slides consisting of colluvium and weathered bedrock (Crozier, 2017). However, the magnitude of the cumulative effect of such event is very large. Such MORLEs are especially frequent on New Zealand's pastoral lands, which may suffer from major stock losses as well as damage to essential infrastructure (Crozier, 2005). A major landslide event in 2004, encompassing 80,000 soil slips in an area of 16,000 km^2, resulted in

310 destroyed houses, farm damages amounting up to NZ$189 million, and a major state highway closed for over 8 weeks.

3.2. Silvopastoral Systems in New Zealand

Silvopasture is a type of agroforestry commonly implemented in New Zealand (Kemp et al., 2018). Silvopastoral systems are defined as productive systems where grazing is combined with plantation forests. Such systems are established by either space-planting trees in existing pasture or thinning out forests to accommodate for grazing cattle (Knowles, 1991). Such an integrated system allows for an enhanced profitability from ecosystem services. The extensive review by Mackay-Smith et al. (2025) summarizes the wide range of effects. Resulting from the complex relations within a silvopastoral system, a variety of synergies and trade-offs are to be considered. For example, stemflow increases surface runoff and encouraged grazing below the canopy induces soil compaction and water infiltration reduction (Mackay-Smith et al., 2025). Moreover, pasture production and nutritive value are negatively affected with increasing tree age and higher stem densities (Benavides et al., 2009). Furthermore, beneath deciduous trees, light becomes a limiting factor due to canopy closure, resulting in a competitive relationship to the pasture (Guevara-Escobar et al., 2007). Conversely, trees may reduce sediment loss by surface runoff through rainfall interception and throughfall reduction, as well as enhanced water infiltration into the ground (Mackay-Smith et al., 2025). Moreover, the assessment by Mackay-Smith et al. (2021) suggested that the evergreen kānuka seems to exert a facilitating interaction with the herbaceous understory. The enhanced soil quality due to an increased below ground diversity and richness as well as nutrient input by litterfall and livestock excreta may benefit pasture production (Mackay-Smith et al., 2025). Lastly, individually spaced trees can have a positive effect on the reduction or prevention of sediment loss on erosion-prone pastures (Spiekermann et al., 2022b). The connectivity model developed by Spiekermann et al. (2022a) showed that by employing a silvopastoral system on only 6.5% of the productive land, a 34% reduction in sediment delivery can be achieved through the increased slope stability. Other benefits amount to livestock production, crop yield (from fruit bearing trees), timber production, or wind and rainfall protection (Benavides et al., 2009; Kemp et al., 2018).

The tree species selected within a silvopastoral system are tailored to the productive purposes of the land as well as market conditions and governmental policies (Kemp et al., 2018; McGregor et al., 1999). Usually, plantations are either deciduous systems, commonly based on poplar (*Populus spp*.) and willow (*Salix spp.),* or evergreen systems, commonly based on radiata pine (*Pinus radiata*). More novel approaches to silvopastoral land management base their vegetative systems on indigenous species. A common native is the manuka (*Leptospermum scoparium*), among others for honey production (Kemp et al., 2018).

3.3. Vegetation as Protective Measure

Worldwide, forests serve as a protection against diverse geomorphological hazards, such as rockfall, avalanches, bank erosion, and landslides (Mao et al., 2012). More specifically, vegetation has been planted with the purpose of enhancing slope stability and thereby mitigating

soil erosion (Basher, 2013). The relationship between vegetation and slope stability is of complex nature. The cohesiveness of the soil is significantly controlled by (the absence of) vegetation on the slope. Through both reinforcing capacities of the roots as well as alterations to the system's hydrological properties, vegetation governs the cohesion of steep, regolith mantled slopes (Phillips et al., 2021; Sidle & Ziegler, 2017). The magnitude of the vegetation's stabilizing effects differs across both temporal as well as spatial scales (Watson et al., 1999; Schwarz et al., 2012).

The reinforcing effect of vegetation on the slope is most evident at shorter timescales. Trees and forests are found to have an inhibiting effect on landslide occurrence within the 'management' timescale (10^1–10^3 years) but may facilitate slope failure by establishing a thick regolith prone to sliding on the longer term (10^3–10^5 years; Phillips et al., 2021).

On a single-tree scale, both the hydrological as well as mechanical effects of the vegetation on the slope stability are strongly related to tree species, shape, age, and root architecture, among others (Schwarz et al., 2010b). The roots alter the regolith by input of organic matter and the creation of preferential flow paths by the root systems. Furthermore, roots anchor the looser regolith to the more stable substrate, increase soil shear strength, and provide support through buttressing and arching, thereby inhibiting slope failure (Vergani & Graf, 2016). The roots provide additional friction at the root-soil interface, thereby increasing effective colluvium cohesion (Crozier, 2010; Schwarz et al., 2010a). Conversely, increased infiltration capacity due to roots as well as surcharge of trees may facilitate slope failure (Mackay-Smith et al., 2025). Local hydrological effects, such as canopy interception and transpiration, and redistribution of rainwater, may regulate slope mobilisation (Phillips et al., 2021). However, such hydrological mechanisms exert only a limited effect on landslide prevention, as their effectiveness is strongly affected by rainfall (Arnone et al., 2016). On a catchment scale, hydrological processes seem to be more influential, governing the hydrological balance of an entire basin (Murgia et al., 2022). For example, tree foliage facilitates evapotranspiration, thereby regulating water available for infiltration (Vergani et al., 2017).

3.4. Root Reinforcement in the Soil

As briefly mentioned before, a soil mass fails when the shear strength of a soil is exceeded by the driving forces acting upon the soil mass (Schwarz et al., 2015). Shear strength is the balance of cohesion between particles and the resistance against sliding particles. A distinction can be made between the true cohesion and the apparent cohesion of a soil matrix. True cohesion results from the chemical bonds between soil particles, whereas apparent cohesion is a function of the water content within a specific soil (Stokes & Yildiz, 2023). The added cohesion-like strength in a rooted soil is called "additional cohesion due to roots" (Wu et al., 1979). As mentioned before, this additional resistance against shear forces is established through a multitude of root mechanical properties. Determined by the position of the root zone relative to the potential sliding mass, three mechanisms of root reinforcement can be distinguished: 1) basal root reinforcement; 2) lateral root reinforcement; and 3) stiffening of the soil mass (Murgia et al., 2022).

Basal Root Reinforcement

Basal root reinforcement (BRR) considers the roots' force operating on the basal shear plane (Giadrossich et al., 2019). Local shear strength diminishes when the soil bulk density increases and, simultaneously, pore water pressure increases or soil suction along the potential slip decreases. This creates a potential failure plane. When this failure plane is situated in the root zone, roots can significantly limit soil mobilisation (Schwarz et al., 2015). Nevertheless, this effect is found to be confined within the surface soil layers only. With increasing soil depth, the number of roots declines, thereby affecting the intensity of BRR (Murgia et al., 2022).

Lateral Root Reinforcement

Lateral root reinforcement (LRR) acts under tension or under compression at the edges of a landslide, i.e. near the scarp or the toe (Giadrossich et al., 2019). The former exerts tensile force at the scarp of a landslide, where roots act as bridging forces crossing the cracked surface between the sliding mass and the surrounding area. The latter applies compressive force at the toe of a landslide, with roots majorly influencing the redistribution of downward pressing forces of the sliding mass (Schwarz et al., 2015). LRR is especially effective for landslides with areas up to 1000 m^2 (Schwarz et al., 2010c) and is dependent on the spatial distribution of the root network (Cohen & Schwarz, 2017).

Stiffening of the Soil Mass

The roots exert a macroscopic stiffening effect in the soil, leading to a larger redistribution of the forces (Cohen & Schwarz, 2017). Added friction in the root-soil matrix is a result of the root distribution and geometry (Schwarz et al., 2010a). Also in soils under compression, roots have been shown to improve soil stiffness (Schwarz et al., 2015). The stiffening effect enhances BRR and LRR across the mobilised mass.

3.5. Root Properties for Reinforcement

Geometric Factors

Multiple characteristics across different scales are involved when it comes to soil stabilization by trees. On a rhizosphere scale, the root hairs, root exudation, and mycorrhizal fungi affect the shear resistance along the root-soil interface (Mao, 2022). Zooming out to the individual root, the geometry is characterized by the length:diameter ratio, branching, and tortuosity of the root. Root diameter is the main governing factor of root reinforcement, with coarser roots generating larger maximum pullout forces (Schwarz et al., 2010b). Generally, root length increases with root diameter (Schwarz et al., 2010a). Furthermore, the number and order of branches is important for the pullout resistance. Branching is considered when a main root divides into two sub roots. The apex may continue to grow straight and produces a second-order lateral, or two new apices appear at the branching point and replace the former single apex (Schwarz et al., 2010b). Increased branching results in a higher total-root length and surface area, increasing the required pullout force. Schwarz et al. (2011) demonstrated that the presence of branching points doubled the required pullout force. Lastly, the tortuosity of a root is defined by the ratio effective root length (i.e. the sum of length of all straight subsections of a

"zigzagged" or curved root) over the length of the root measured from the origin to the tip of the root (Schwarz et al., 2010b). The tortuosity of a root is found to drastically increase the maximum tensile resistance as well as the displacement of a root till breaking (Schwarz et al., 2011). Scaling up to a root-bundle, orientation, position, and spacing of the roots determine the total reinforcement by the bundle (Mao, 2022). Moreover, the root diameter distribution is an important predictor for global pullout behaviour of a root bundle (Schwarz et al., 2011). Within the plant community, the overall root architecture influences the redistribution of shear stress on the root system (Cohen & Schwarz, 2017). Root systems with a higher density of roots close to the slope surface provide a more enhanced mechanical reinforcement and root water uptake. Moreover, the root demography (i.e. the differences in root systems among the plant population) within the local soil is indicative of the root reinforcement (Mao, 2022).

Mechanical Properties

The root mechanical properties are inherently related to the previously described geometric factors. Firstly, the maximum tensile force that individual roots can withstand, i.e. the tensile strength of a root, differs between species due to varieties in tissue density and cellulose content. The species-specific root tensile strength is derived from the complex interaction between root diameter and friction at the soil-root interface. Determining the friction between the root and soil is complicated, due to its dependence on soil type, water content, cohesive strength, the friction angle, and the shear stiffness at the root-soil interface (Schwarz et al., 2010a). Furthermore, the relative displacement of a root till point of breaking is constituted in the root elasticity. This displacement is described in the Young's modulus of elasticity, quantifying the stress-strain relationship of a root. Stiffer materials will have a higher modulus of elasticity. Lastly, load sharing among the individual roots as well as root failure order determine the mechanical reinforcement capacities of a bundle (Mao, 2022). This is commonly referred to as the roots' survival probability (Schwarz et al., 2013).

3.6. Slope Stability Models

Obtaining empirical data on trees and their reinforcing capacities is time consuming, costly, and intrusive (Phillips et al., 2023). Especially collecting data on a stand scale is near impossible, limiting insights into vegetation induced slope stability. Hence, slope stability modelling is essential for deepening the understanding of the cohesion between roots and the soil. Vice versa, accurate and precise empirical data is required to feed model inputs and enhance model outcomes. Slope stability models (SSM) are either i) conceptual, ii) statistical, or iii) physical models (Murgia et al., 2022). Conceptual models aim to simplify the estimation of slope failure in space and time. Statistical approaches are rooted in the two basic assumptions that future landslides will occur in areas shown to be prone to landslides in the past and environmental variables are to be reived from a digital terrain model of the respective area. Statistical models most commonly employ logistic regressions between the variables. Physically based models are generally compiled of a hydrological module and a mechanical module, quantifying the soil water pressure and soil mechanical parameters, respectively.

Analysis of these variables generates numerical values indicating the state of a slope. Physical slope stability models apply varying dimension effects (1D, 2D, or 3D).

Modelling root reinforcement in the soil is commonly used within slope stability modelling. Boundary conditions characterised in such SSM are, among others, the morphology, lithology, pedology, and vegetation cover. Mechanical and hydrological processes incorporated in the model determine the state of these environmental factors (Murgia et al., 2022). To quantify stability, the Factor of Safety (FoS) of a slope is used as an indicator. The FoS is the ratio stabilizing forces to destabilizing forces and is expressed by a set of various strength variables (listed in Schwarz et al., 2015). Root reinforcement models are incorporated into these larger stability models as a cohesion parameter (van Zadelhoff et al., 2022). Such additional cohesive forces affect the severity of change in the boundary conditions triggered by hydrological and (other) mechanical processes, and thus, affect the FoS of a modelled slope.

3.7. Root Reinforcement Models

Numerous root reinforcement models (RRMs) exist and are incorporated into SSM. All RRMs are physically based, numerical models, with a spatial dimension independent of the SSM it is incorporated into (Murgia et al., 2022). In most models, there is no spatial variability in root reinforcement in the soil (Murgia et al., 2022), however, some other models differentiate between BRR and LRR across different soil depths (e.g., Milledge et al., 2014; Mao et al., 2014). More simplistic models such as the Wu and Waldron's Model (WWM) assume simultaneous breakage of all roots across the shear plane (Mao et al., 2012). Only few RRMs consider the temporal dimension. One example is the Root Bundle Model with Weibull function (RBMw), modelling the progressive breakage of roots over time, determined by mechanical and geometrical variation of individual roots (Schwarz et al., 2013). Parameters of the model are derived from mechanical properties described before. Among others, the maximum tensile strength, the modulus of elasticity, and the survival probability of a root serve as model inputs. Root traits such as diameter, orientation, position, and tortuosity form the foundation of the parameters in the RBMw (Giadrossich et al., 2016).

3.8. Native New Zealand Species

The growing interest for reintegrating native species into the existing ecosystem is no novelty. There is an abundance of New Zealand studies as well as governmental schemes through which a more holistic, sustainable approach to ecosystem management is advocated for (e.g. Marden et al., 2005; Mackay-Smith et al., 2021. Rather than purely productive gains, conservation and regeneration of naturally occurring species are included in reforestation objectives. Kānuka and tōtara grow well in northern New Zealand's conditions and establish easily in the wild**.** These native species are lower growing (northern North Island conditions) compared to some exotic species like radiata pine or poplar, therefore better applicable to windy conditions (Phillips et al., 2023). Pioneer evergreen natives possibly have a more facilitative relationship with the soil and moderate the beneath-foliage climate better than e.g. introduced poplars (Mackay-Smith et al., 2021). Lastly, indigenous species have found to sequester

significant amounts of carbon in stems, branches, foliage, and root mass, with storage rates like that of radiata pine (Kimberley et al., 2021).

3.8.1. Kānuka

The *Kunzea ericiodes* var. *ericoides* (Fig. 1A), commonly known as kānuka, is classified under the taxonomic family of *Myrtaceae* (Allan Herbarium, 2000). Currently, there are ten *Kunzea* species recognised. The genetic gradient between species is found to correspond to the biogeographic boundaries of New Zealand (Heenan et al., 2022). The hardwood kānuka is considered a pioneer species, commonly dominating the early developmental stages of a forest after major disturbance. Reasonable fertility and drainage of the soil are required, as well as sufficient light (Dawson & Lucas, 2012). Soil preferences vary across the biogeographical range. Kānuka populations on the South Island have been found to dominate on stony, sedimentary soil and in frosty or dry climates (Heenan et al., 2022). Populations on the North Island, however, have been found to also establish on cooler, wetter volcanic soils with a higher organic carbon content (Hedley et al., 2013). Kānuka grow between 20 and 30 meters tall, with a trunk diameter at about 60 cm or more. Often, kānuka are multi-trunked from the base. Its average dry wood density is 757 kg m^{-3} (Barton, 2025). The closely related manuka constitutes an asymmetric, heart-shaped root system, where multiple oblique roots grow directly below the stem, in diagonal directions (Marden et al., 2005). Kānuka may live up to a century but are eventually outcompeted by more shade-tolerant species (Dawson & Lucas, 2012).

Kānuka is found to be the most abundant woody species in pastoral hill country (Spiekermann et al., 2021). Kānuka is considered highly valuable, providing firewood and shelter on farms. The species relies on seed dispersal by wind and ground disturbance for growth initiation (Heenan et al., 2022). Kānuka flowers are insect pollinated, and the species is

Figure 1

Kānuka, Tōtara and Poplar Trees

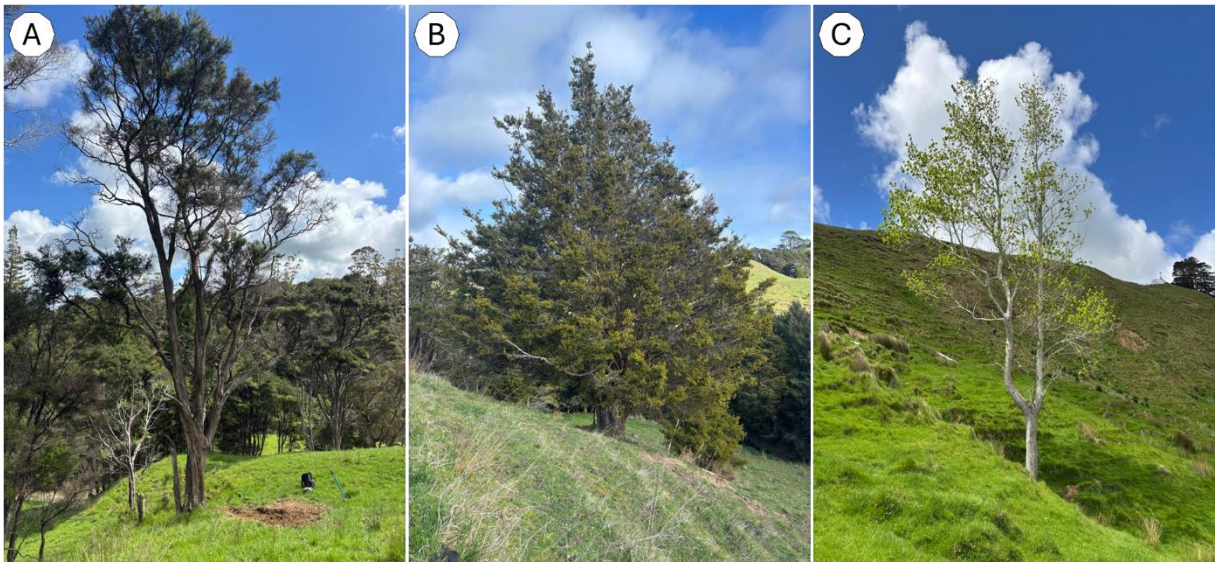

Note. (A) Kānuka in Hoteo, (B) Tōtara in Makarau, (C) Poplar in Hoteo. Photographs by Nicola Wilson.

essential for New Zealand's high quality honey production (Bimbo et al., 2025). Lastly, kānuka has been found to facilitate pasture production under the tree (Mackay-Smith et al., 2022).

Some studies on the mechanical properties of native New Zealand tree roots have included kānuka in their analysis. Watson et al. (1999) and Watson and Marden (2004) assessed the tensile strength of kānuka, measuring average values of 32.5 MPa and 34.2 MPa, respectively. Maximum tensile strength of kānuka roots may range between 15.5 and 80 MPa, depending on the diameter of the root, amongst others. A study by Ekanayake et al. (1997) showed kānuka to be more effective at stabilizing the soil as opposed to the exotic *Radiata pine* during the first eight years of stand growth. This could be attributed to the naturally higher stand density of kānuka as opposed to the pines. After 16 years, however, the reinforcing capacities of kānuka roots start to decline, although very mildly. The more recent study by Spiekermann et al. (2021) confirmed the relevance of kānuka contribution to soil stabilisation and soil conservation at the landscape scale.

3.8.2. Tōtara

The *Podocarpus tōtara* var. *tōtara* (Fig. 1B), commonly known as tōtara or lowland tōtara, belongs to the taxonomical family of indigenous conifers *Podocarpaceae* (Allan Herbarium, 2000). The softwood species is endemic to New Zealand and found throughout the country's lowlands and montane forests up to 480 meters altitude (Dawson & Lucas, 2012). Tōtara is a long-lived pioneer species, suited to the colonisation of disturbed environments such as eroded soils (Quinlan, 2022), but is also commonly found as a climax species in mature forests (Dawson & Lucas, 2012). Often, this species is dominant in well-drained alluvial plains that experience seasonal drought. Generally, tōtara is intolerant of wet and waterlogged soils (Marden et al., 2018a). A study by Bergin and Kimberley (2014) showed that natural regeneration of tōtara was most prevalent on steep slopes deficient of nutrients. Adult trees averagely grow to a 30 m height, with the diameter of the trunk often around two meters, sometimes exceeding four meters (Dawson & Lucas, 2012). Tōtara grow a tap-like root system, where one main vertical root grows directly below the stem of the tree (Marden et al.,). The average wood density of tōtara at age 14 is 446 kg m^{-3} (Bergin et al., 2008). Tōtara are known to live at least 900 years (Dawson & Lucas, 2012).

The seeds of the tōtara are commonly spread by birds and germinate rather easily. Tōtara establishes less successful on flatter, open areas like farmland, as such conditions favour light-competing, fast-growing herbaceous crops. Tōtara growth is favoured by the warming global climate and, due to its unpalatability, is relatively resistant to livestock (Quinlan, 2022). The species is known to produce highly durable timber (Bergin, 2000) and its foliage possesses natural fungicidal properties (Franch & Cambie, 1999). Furthermore, Kimberley et al. (2021) measured continued carbon sequestration to last up to at least 120-year of age.

The Northland Tōtara Working Group has published several reports and documents on the characteristics, management, and harvesting of tōtara as a productive species (e.g., Quinlan, 2022). Despite the reports on tōtara use and growth for productive purposes, publications on the root architecture and/or mechanical properties of tōtara are rather limited (Marden et al., 2018a). Some efforts have been made to document several of the species' root characteristics:

Donaldson (1983) assessed the anatomy of the root wood of various *Podocarpaceae* species on a microscopic level, describing the type and functions of cells within the plant's root. Baylis et al. (1963) described the mycorrhizal nodules on tōtara roots, underlining the importance of the tree's interaction with fungi for optimal tree growth and nitrogen fixation in natural soils. In 2008, Bergin et al. assessed distinct cultivars of tōtara on growth, form, and wood density at a coastal site in New Zealand. Seeds collected from singular trees across 36 different sites throughout New Zealand were planted on replicated trials on the North Island. After 11 years, the grown trees were assessed. The study found tōtara to have developed a genetic differentiation between local tree populations due to the species' spread across a wide range of altitudes and latitudes. Generally, seeds from the northern populations tended to grow faster and with better form than those of southern populations, suggesting a genetic variation resulting from differences in geographic origin. The more recent study by Marden et al. (2018a) described root growth patterns of the first five years. By the age of five, the species had produced long lateral roots extending up to 2.2 m and its root network consisted for almost 80% of roots with a diameter of 1-2 mm. Lastly, Salekin et al. (2025) developed a height-diameter model to allow for more precise estimation of tree volume, biomass, and carbon stocks of tōtara.

3.9. Poplar

The exotic *Populus* spp. (Fig. 1C), commonly referred to as poplar, has been introduced in New Zealand with the arrival of European colonists (Wilkinson, 1999). It is a fast-growing, hardwood species, belonging to the taxonomical family of *Salicaceae*. Since its introduction, farmers have been cultivating various poplar species for, among others, soil erosion, riverbank protection, or shade (McGregor et al., 1999). Poplar plantations can be found in a variety of habitats throughout New Zealand. Best suited are sites with fertile soils and sufficient water availability. The most commonly poplar cultivars require at least 700 mm of precipitation per year and an annual temperature range between 8.5 and 17 degrees Celsius (McIvor, 2023). Poplars can be established through natural seed-fall of from stem cuttings (Sulaiman, 2006). The development of individual poplars is highly variable, determined by external factors such as proximity to other trees or steepness of the hillside (e.g. Douglas et al., 2010; McIvor et al., 2009). Close-spaced poplars may have a diameter at breast height (DBH) ranging between 27.5 and 57.5 cm, where widely spaced poplars grow a DBH between 10 and 75 cm (McIvor, 2023). Poplars are rather low in wood density, with 360 kg m^{-3} (Satchell, 2018). The species develops a plate-like root system, where lateral roots grow in horizontal directions from just below the stem (Phillips et al., 2023). Often, vertical (sinker) roots grow from the long laterals (McIvor and Douglas, 2012). The root systems of poplar develop quickly in New Zealand soils, where growth rates of the laterals may vary between 3.4 and 20 mm per day (Phillips et al., 2014). The biggest threat to poplars worldwide is leaf rust: a fungus that causes premature leaf fall and reduces growth. Some poplar hybrids are rather sensitive to rust (e.g. *Populus euramericana* i. Tasman), whereas others are particularly resistance (e.g. *Populus euramericana* ii. veronese; Sulaiman, 2006). This disease struck poplars in New Zealand early 1970's, tremendously affecting the rate at which poplars were planted for soil conservation purposes (McGregor et al., 1999).

Leaf rust aside, poplars earned their popularity within silvopastoral systems due to a set of beneficial traits for pasture production and soil quality (Phillips et al., 2014). Poplars are easy to propagate, and planting is relatively low in costs. Moreover, their leaf litter ensures a seasonal input of nutrients into the pasture soil (Mackay-Smith et al., 2021). Since poplar foliage is safe for consumption by livestock, grazing by sheep is possible immediately after planting poplar poles, and grazing by cattle after one or two years (Wilkinson, 1999). The trees may then provide shelter against precipitation and sun. Moreover, poplars have shown to increase soil fertility and soil pH and regulate soil temperature (Kemp et al., 2018). However, pasture production under a 30% canopy coverage reduces by 10% during the leaf-carrying period (McIvor and Douglas, 2012).

Due to poplar's abundance in the New Zealand landscape, extensive research on its root architecture and mechanical properties has been conducted. Especially in areas of medium erosion, on hillslopes, and non-uniform slopes, poplar are often opted for (Wilkinson, 1999; Phillips et al., 2014). Poplars have an immaculate ability to dry out and bind together the soil (Guevara-Escobar et al., 2000). When the below-ground extend of poplars interlink, a dense, evenly distributed network of roots greatly reduces soil erosion (McIvor and Douglas, 2012). Schwarz et al. (2016) and Ngo et al., (2023) have assessed poplar's effective root reinforcement across different stem densities and trunk sizes. Modelling efforts in both studies emphasised poplar as an essential species for bioengineered slope stabilisation and landslide prevention. Nevertheless, in the first five years of growth, the root systems are not yet fully developed. To ensure immediate slope stabilization, poplars would need to be planted at a higher density and then thinned afterward (Kemp et al., 2018). Another limitation of poplars stands for soil conservation is their susceptibility to damage by wind, where branches or the stem may break with strong gusts. To prevent such damage, it is suggested to fell poplars before the age of 50 (Mackay-Smith et al., 2021).

4. Materials and Methods

4.1. Site and Tree Selection

For this study, three research sites were selected. Prior to the fieldwork, potential research areas were visually assessed based on a set of requirements using remote sensing data, e.g. land cover data and canopy height models. Criteria were selected to safeguard relevance to the study as well as site-accessibility and the elimination of other practical constraints. The requirements were: i) a dominant soil type in the region, ii) grassland or grazed pasture land cover; iii) abundancy of individually spaced poplar, kānuka, and tōtara trees with properly developed canopy (minimum proximity to other trees at eight meters and minimally ~20 years of age); iv) slopes between 15-30°; v) site accessible to a mechanical digger (only necessary for the recording of the root architecture).

The selected sites were all in the Auckland Region. Makarau represented a Mottled Yellow Ultic soil, Tapora and Hoteo represented a Typic Yellow Ultic soil. Subsequently, individual trees were selected and marked on site. To ensure a complete and comparable dataset for each soil type, similar assessments were carried out across the different research sites. For the root architecture records, i) at Makarau, two kānuka, two tōtara, and two poplars were assessed; ii) at Tapora, two kānuka and two tōtara were assessed; and iii) at Hoteo, two poplars were assessed. For the tensile strength measurements, a comparable number of roots were assessed for each of the different species in both Makarau and Hoteo. The fieldwork described in sections 4.2. and 4.3. was carried out in the winter and early spring, May to Oktober 2025. This timeframe was selected to ensure soils were at field capacity when performing the tensile strength tests, resembling landslide-initiating conditions.

4.2. Root Architecture Records

Across the three different study sites, kānuka, tōtara and poplar of similar age and grown under similar conditions (i.e., slope, aspect, proximity to other trees) were selected. For each species, four individual trees were assessed. The root architecture was sampled employing the trench wall method. Around the stem, two trenches of ~1 meter depth and ~1 meter width were dug out at diameters 1.5 m and 3.5 m. This resulted in four 360° trench walls at 1.5 m, 2.5 m, 3.5 m, and 4.5 m (respectively, Fig. 2A1–4). The roots were counted across the soil profile, between 0 – 105 cm soil depth. The diameter of roots intersecting the wall face were recorded using a measuring rod with seven horizontal sections of a fixed height at 15 cm and adjustable width (Fig. 2A5). The radius of the tree was divided into eight 45° sectors (‘pie slices’). Sectors 1 and 8 were situated upslope with their shared border at 0°, sectors 4 and 5 were downslope, with their shared border at 180°. The eight projected sectors served as a guiding principle for sectioning the root distribution counts along the trench walls. Ultimately, roots were measured in each soil section across sector x, depth y, and distance z.

All roots with a diameter < 1.5 mm were recorded with a clicker and the total count was recorded in a tally. The exact size of each root with diameter > 1.5 mm was measured with a calliper and listed. Sectors that were under water resulting from heavy rainfall were pumped

Figure 2

The Set-Up of the Field Work

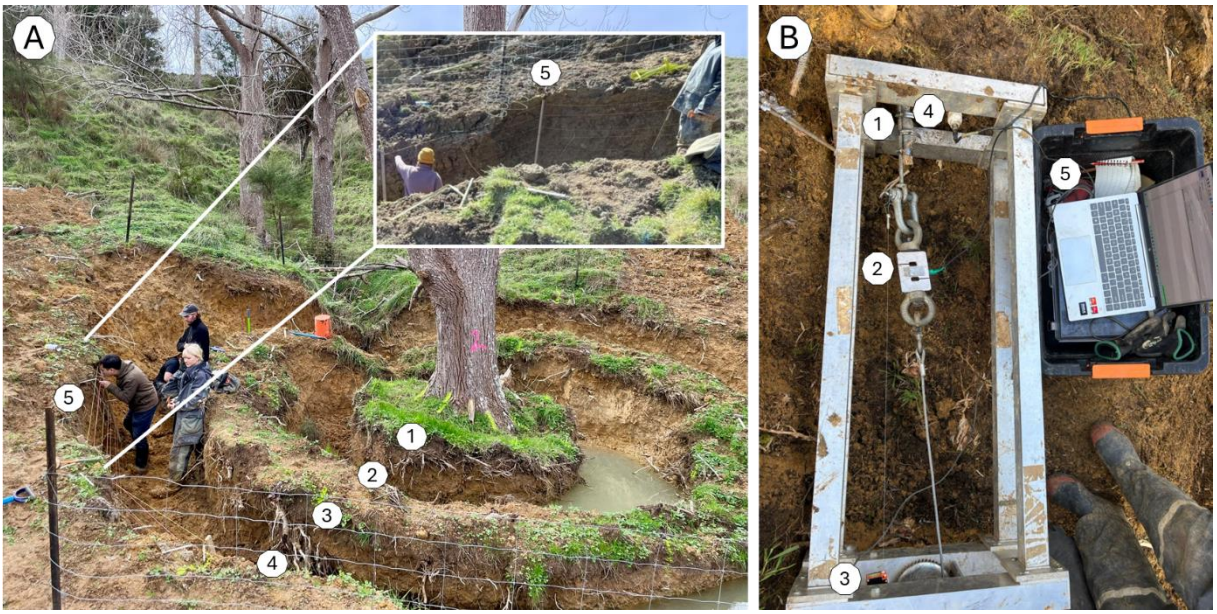

Note. **(A)** Example of the MP2 trench walls at (1) 1.5 m, (2) 2.5 m, (3) 3.5 m, and (4) 4.5 m, and (5) the measuring rod propped up against the trench wall to record the individual soil sections. **(B)** Example of the tensile strength test setup, with (1) the prepped root, (2) the load cell, (3) the extensometer, (4) the soil moisture sensor, and (5) the datalogger and laptop. Photographs by the author.

out and walls were cleared from smudge using a pickaxe. Some of the trench walls collapsed after the heavy rainfall, disallowing the assessment of these damaged sectors. These were recorded as missing values and dealt with at data processing. Additionally, the DBH of each tree was recorded manually.

4.3. Pullout Tests

4.3.1. Procedure

In-field pullout tests were carried out to obtain the mechanical properties of the individual roots. At sites Makarau and Hoteo, at least two individual trees of each species were selected. The roots were dug out manually and were cut loose from the tree they originated from. Soil was carefully removed to uncover enough of the root to enable the montage of the pullout equipment. A shallow trench was dug out to position the pullout machine (Fig. 2B). After coiling the bare roots with metal wire to increase friction, the coiled roots were attached to a metal rod using hose clamps (Fig. 2B1). The metal rod was then hooked to either 200 kg or 2000 kg capacity load cell (Fig. 2B2), depending on the diameter of the subjected root. The other end of the load cell was connected through a snap hook onto a crank handle. Additionally, an extensometer (Fig. 2B3) measuring the displacement of the root was connected to the tip of hook connecting the metal rod and the load cell. Lastly, a soil moisture sensor (Fig. 2B4) was inserted in the trench wall, as close to the root as possible. The crank handle was turned manually, thereby increasing the pulling tension on the attached root opposite from the direction the root had been growing in. Turning of the handle was stopped the moment the root broke or slipped out of the soil. A Campbell Scientific CR1000 data logger (Fig. 2B5) recorded the

applied force (mV), the displacement (mV), and soil moisture content (mV) per second. For each individually assessed root, a file containing the data per second was generated by the CR1000 software. After successful breakage, the diameter of the root at the breaking point, the depth within the soil, and the projection sector in which the root was dug out were recorded manually. Lastly, the DBH of each tree was measured.

4.3.2. Calibration of Sensors

All sensors used for the pullout tests measured a raw voltage (mV). To allow for data analysis, conversion of the raw voltage was required. To obtain the optimal conversion equation, the 250 kg loading cell was calibrated using the calibration method as recommended by the manufacturer. The cell was hung up, and the raw voltage was measured using 1) no weight, 2) four known weights. These points were then plotted and a simple regression derived. The newly obtained regression was comparable to the default calibration regression. The manufacturer's calibration regression was opted for, as this calibration was performed using heavier weights, producing a smaller error.

Similar for the 2000 kg loading cell, a preliminary calibration was performed utilizing a set of known weights up to ~100 kg. Again, the newly obtained regression was compared to the default regression. Since the default, lab-performed calibration allowed to apply controlled forces up to 2000 kg, the manufacturers calibration was opted for.

Both the extensometer as well as the moisture sensor were not recalibrated. Instead, the default calibration equation implemented in the CR1000 software was applied.

4.4. Data Handling and Analysis

4.4.1. Root Architecture

All data logs for the individual trees across the three research sites were compiled into one database. The missing values resulting from damaged sectors were estimated and substituted, based on distributional patterns found across the dataset for the relevant species, sector, depth, and distance from the tree (Walther, 2025).

To quantify the proportion of root cross-sectional area relative to the surrounding soil profile area, the root area ratio (RAR) was calculated using:

$$RAR = \sum_{i=1}^{n} \frac{A_{r,i}}{A_s}$$

where $A_{r,i}$ is root cross section area [m^2] and A_s is soil area [m^2], i is the root diameter class, and n is the number of root diameter classes. Spearman correlations were performed to test for correlations between the DBH and root counts or RAR. Additionally, simple linear regressions were used to fit DBH and RAR. Furthermore, to evaluate patterns in root count and RAR across up- and downslope directions, two-sample *t*-tests and one-way ANOVA-tests were run. These analyses were used to check for significant differences in root arrangement suggested by descriptive comparisons.

Furthermore, due to the many repeated measures of root counts nested within species, a linear mixed model approach was applied to test for relationships (Brown, 2021). Linear mixed effect models (LMM) were composed to assess the relations between the dependent variables (i.e., root counts [n] and RAR [%]) and the independent factors (e.g., arrangement, species, and soil type). To ensure a normal distribution of the residuals, the log-transformed root counts and RAR were used to test for relations. A stepwise forward selection was performed to build an optimized model using the relevant variables. A set of models with varying independent variables and interaction terms was drafted and tested using ANOVA. Between-model comparisons were made using the Akaike Information Criterion (AIC). The AIC tests for relative model fit using the log-likelihood, where a lower AIC score indicates a better model fit compared to other models in the tested set (Burnham & Anderson, 2004). The selected models complied with $AIC_{(selected)} - AIC_{(minimum)} \leq 5$. A Shapiro-Wilk tests of the residuals was performed to confirm normality of the selected log-transformed models. The model fit was checked for significance applying a 95% CI. In the final models, the tree key was set as the random intercept variable to account for the repeated measures for each individual tree. All models were run repeatedly, rotating the species that was set as reference level within the models. All data were compiled and analysed in Microsoft Excel and RStudio. Mos relevant R packages used were "tidyverse", "lme4" and "lmerTest". The complete R script is provided in Appendix A.

4.4.2. Root Mechanical Properties

All individual root pull-out tests across the species and soil types were cleaned and merged into one dataset. The start of each root's testing phase, the maximum applied force (F_{max}), the drop after the F_{max}, and the relative displacement during measurement were derived for each pull-out test in the dataset. The quality of each measurement was assessed based on i) the slope between the F_{max} and the drop force (i.e., a clean break is characterised by a steep slope; a slippage or fail by a gradual slope) and ii) the noise between the start of the testing phase and the maximum applied force (i.e., how much interference was there during the testing phase). A random selection of testing phases was plotted for visual inspection. Any abnormalities were checked and reclassified when necessary. Moreover, tests that were classified as "poor" or "unclear" were assessed manually and reclassified when required. Poor tests were excluded from further data analysis.

The distribution of the maximum tensile strength data across the species was visually inspected using boxplots. Data points numerically distant from the interquartile range of the dataset were not treated as outliers, since they provide valuable information about the relationship between root strength and root diameter, particularly for larger root diameters. Moreover, to quantify the force endured by a single root in relation to its diameter, the stress was calculated using:

$$\sigma = \frac{F_{max,meas}}{A_r}$$

where σ is stress [Pa], $F_{max.meas}$ is the measured maximum tensile force [N], and A_r is the area of the respective root [m^2]. One-way ANOVA tests were run to check for significant differences in F_{max} and σ values between the species.

Considering the many repeated measures of F_{max} nested within species, again a linear mixed effect model (LMM) was applied (Brown, 2021). Multiple LMMs were composed to assess the relations between the dependant variable (i.e., maximum tensile force [N]) and the independent factors (i.e., root diameter, species, and soil type). A stepwise forward selection was performed to build an optimized model employing the relevant variables. A set of LMM models with varying independent variables and interaction terms was drafted and tested with ANOVA. Again, model comparisons were assessed using the AIC, with $AIC_{(selected)} - AIC_{(minimum)} \leq 5$. A visual inspection as well as a Shapiro-Wilk tests of the residuals were performed to confirm normality of the selected log-transformed model. The test indicated a normal distribution of the residuals for the maximum tensile force, albeit not significant ($W = .99$, $p \sim 0.14$). Considering the good model fit ($\Delta_{AIC} = 0.61$ and $p < .001$), it was decided to stick with the preliminary model selection. Variance at the individual tree-level was zero, therefore the species was set as the random intercept variable to account for the repeated measures for each species. The model was run repeatedly, rotating the species that was set as the reference level.

Moreover, the root mechanical data was fitted to the parameters of the RBMw, using a set of equations according to Giadrossich et al. (2016) and Ngo et al. (2023). First, the power-law regression between the maximum tensile force and the root diameter was fitted to the data:

$$F_{max}(\phi) = C(\phi) F_0 \phi^{\alpha}$$

where F_{max} is the maximum tensile force [N], ϕ is root diameter [m], F_0 is a scaling factor, and α is the exponent shape factor. The constant C was defined as:

$$C(\phi) = \frac{1}{2}\left[1 + \mathrm{erf}\left(\frac{\phi - \phi_m}{\phi_{sd}\sqrt{2}}\right)\right]$$

Where *erf* is an error-function built in the R package "pracma", ϕ_m and ϕ_{sd} are coefficients corresponding to the mean and standard deviation of the cumulative normal distribution of the root diameter. Followingly, the apparent secant spring constant was computed by the ratio of maximum tensile force over the displacement at failure:

$$k = k_0 \, \phi^{\beta}$$

with spring constant k [N/m], k_0 as a spring constant scaling factor, ϕ for root diameter [m] and β as the spring shape factor. Then, the survival function with Weibull distribution is given by:

$$S(\Delta x^*) = exp\left[-\left(\frac{\Delta x^*}{\lambda}\right)^{\omega}\right]$$

where Δx^* is the normalized displacement, and ω and λ are the shape and scaling factors. These shape and scaling factors were found by, first, calculating the normalized displacement at failure using:

$$\Delta x^* = \frac{\Delta x_{max}^{data}}{\Delta x_{max}^{fit}(\phi)}$$

and

$$\Delta x_{max}^{fit}(\phi) = \frac{F_0}{k_0}\phi^{\alpha-\beta}.$$

Followingly, the survival distribution value, S_i, was derived for each root:

$$S_i = \frac{n_i}{N}$$

with n_i given by ranking the roots in ascending order of normalized displacement and N being the total number of roots ranked. Then, the computed S_i values were fitted to the function $S(\Delta x^*)$ using a non-linear least square method to obtain the parameters ω and λ. Eventually, the survival probability function over the normalized displacement was generated for each species. Again, all data were compiled and analysed in Microsoft Excel and RStudio. The relevant R packages were "tidyverse", "lme4", "lmerTest", "stats", "minpack.lm", and "pracma". The complete R Script is provided in Appendix B.

5. Study Site

5.1. Geography of the Region

The Auckland Region is situated on the northwestern side of New Zealand's North Island, about 13° latitude south of the Tropic of Capricorn (Chappell, 2013). The Auckland Region is one of sixteen governmental sections, in which the country's most populous city Auckland is located (Fig. 3). The area encompasses about 4,940 km^2 and is bordered east and west by the Tasman Sea (Stats NZ, 2025). The non-urbanized surface of the region, generally referred to as the Auckland hill country, is characterized by its hilly topography. The relief does not exceed above 1,000 m a.s.l. and generally constitutes rolling to steep slopes (8–35°, Manaaki Whenua - Landcare Research, 2025a). Preceding the arrival of humans, Auckland Region was largely covered by indigenous mixed forest. It is estimated that over half of the area was occupied by tall podocarp evergreen, alternating with low-growing broadleaf species

Figure 3

Erosion in the Auckland Region, New Zealand

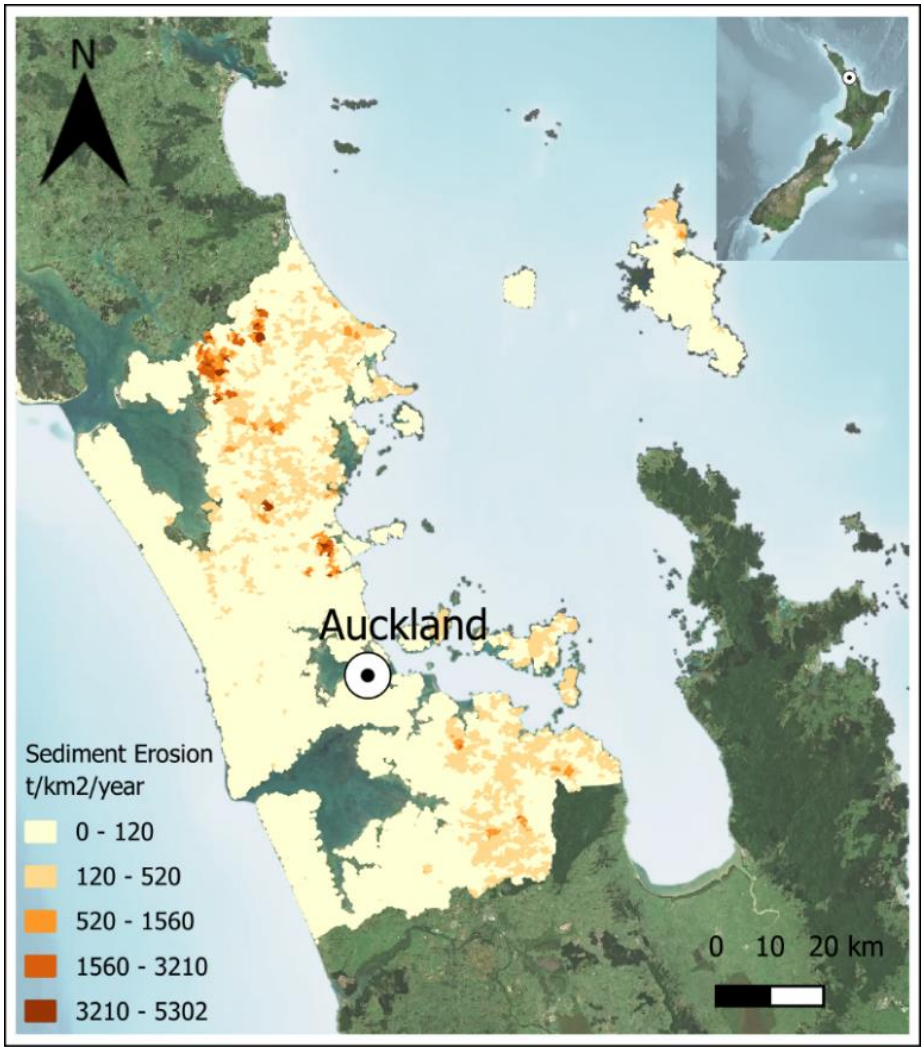

Note. Datasets downloaded from the Manaaki Whenua - Landcare Research data portal (2025a).

(Auckland Council, 2025). Since initial large-scale clearings, the prevailing land cover has been governed by social and economic drivers. Over time, vegetation shifted between grazed (exotic) grassland, regenerated (native/exotic) shrub or bush, and planted forest (Dodd et al., 2016). The dominant soil type in the region is classified as ultic (Manaaki Whenua - Landcare Research, 2025). Erosion rates in the area average from less than or equal to 120 up to more than 5,000 tonnes per km^2 y^{-1} (Fig. 3). In the Auckland Region hill country, three study sites were selected to carry out the tree assessments (Fig. 4; Table 1). The sites are situated in an area characterised by high producing exotic pasture, exotic forests, and indigenous natural land cover.

Figure 4

The Region with Marked Study Sites and Their Land Cover Type

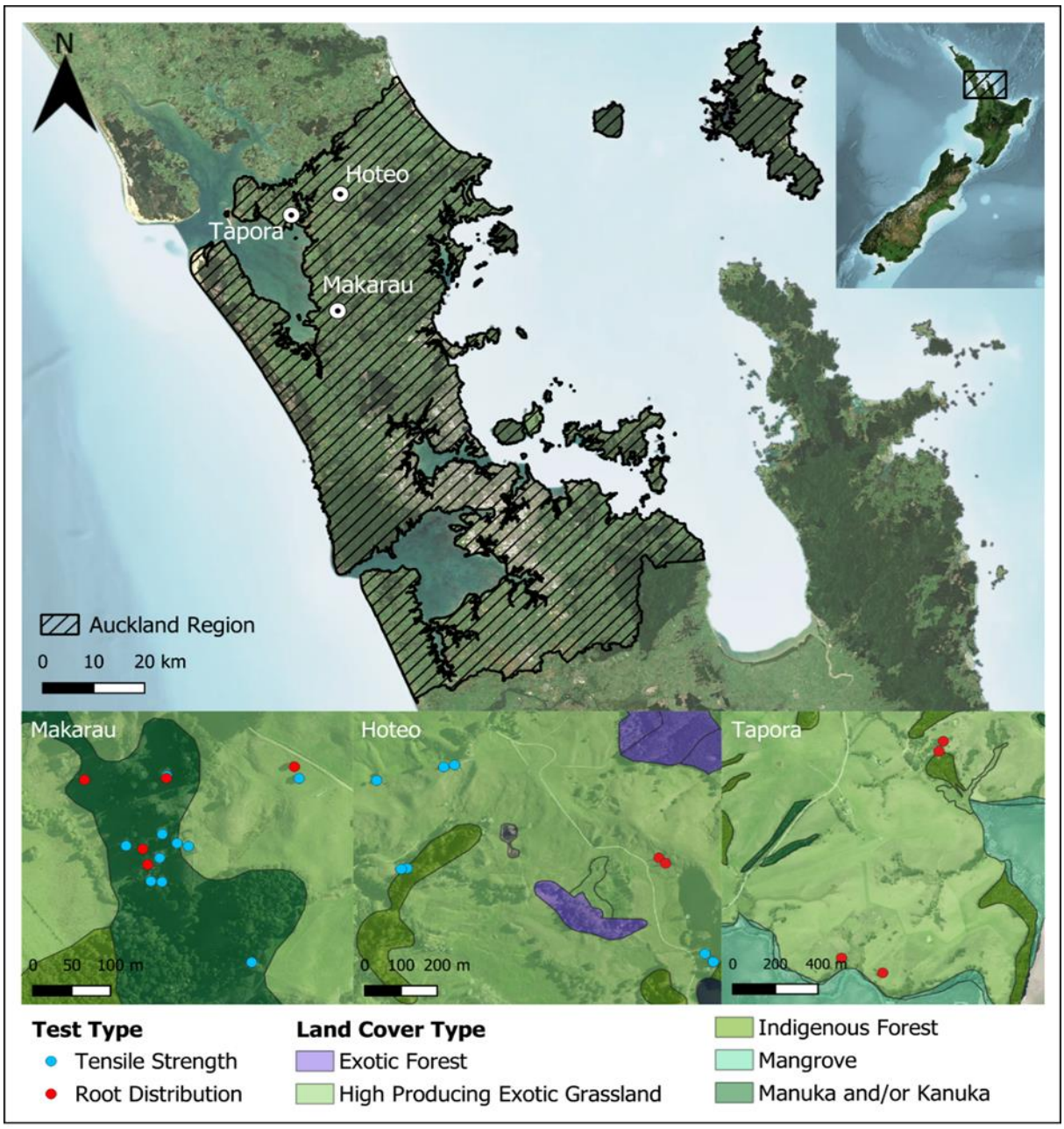

Note. Datasets downloaded from the Manaaki Whenua - Landcare Research data portal (2025a).

Table 1

Site Characteristics

Site	Coordinates	Soil Type[a]	Slope[b]	Aspect[c]	pH[d]	Soil Temp.[e]
Hoteo (H)	19424885.0, 4346687.4	Typic Yellow Ultic (UYT)	Varying from Rolling (8–15°) to Steep (26–35°)	South–west	4.5 – 5.9	15 – 22 °C
Makarau (M)	19423624.4, 4377748.1	Mottled Yellow Ultic (UYM)	Strongly rolling (16–20°)	South–west	4.5 – 5.7	15 – 22 °C
Tapora (T)	19412468.0, 4352191.6	Typic Yellow Ultic (UYT)	Moderately steep (21–25°)	South–west	4.5 – 5.4	15 – 22 °C

Note. All datasets were downloaded from the LRIS Portal by Manaaki Whenua - Landcare Research (2025a).

[a] Dominant soil type; Dataset "NZLRI Soil"

[b] Dataset "NZLRI Slope"

[c] Dataset "NZEnvDS Aspect (degrees) v1.0"

[d] Dataset "NZLRI pH"

[e] Mean annual soil temperature; Dataset "FSL Soil Temperature Regime"

5.2. Climatic Conditions

Chappell (2013) compiled a detailed report describing the climatic conditions of the Auckland Region for the National Institute of Water and Atmospheric Research, from which the information in the following paragraph is derived. Auckland Region is subject to a coastal, subtropical climate. The region receives about 2000 bright sunlight hours per year. Summers are warm and humid. Winters are mild with most of the area receiving only a few frosts per year. The mean annual temperature in the region ranges between 12 and 16 °C. Precipitation is plentiful throughout the year. Most of the Auckland Region receives between 1100 and 1500 mm of rainfall y^{-1}. Around 30% of the annual rainfall precipitates in the winter months (June-August). Windy conditions are most frequent and severe in spring. Predominantly, the airflow in Auckland comes from southwest direction, coming off the Carper Harbour. Auckland's heaviest rainfalls to occur when strong eastern winds prevail. Tropical cyclones are uncommon in the area. However, storms resulting from tropical cyclones elsewhere occur about once or twice per year, characterized by strong easterlies paired with heavy precipitation.

5.3. Soil Types

Two soil types were assessed in the current study. The description of the soils was provided in the New Zealand Soil Classification (NZSC) by Hewitt (2010) and supplemented by information from the Manaaki Whenua - Landcare Research online national soil map (2025b). Both soil types belong to the order of Ultic soils, which are commonly found in the northern North Island of New Zealand. In general, Ultic soils are strongly developed soils, mainly formed from old sedimentary rock. Two subgroups of Yellow Ultic soil have been selected for the current study: Typic Yellow Ultic soil and Mottled Yellow Ultic soil.

5.3.1. Typic Yellow Ultic Soil

At both Hoteo as well as Tapora, a Typic Yellow Ultic soil (UYT) was present (Fig. 5A). Typic refers to typical, meaning that UYT soils correspond to the general characteristics of the yellow ultic soil group. Characteristic for yellow ultic soils is the soft, clayey topsoil, which is susceptible to damage by cattle or compaction during wet periods. As the name suggests, the subsoil horizons have a yellow or yellow-brown colour. Generally, the yellowish subsoil is well-structured and clay enriched. Yellow ultic soils have a very thin eluvial (E) horizon (the layer between the topsoil and the subsoil). When a E horizon is present, it is clay depleted.

The selected soils are strongly weathered, acidic soils. At the study sites, the measured pH ranged between 5.7 – 7.3. Ultic soils are derived by strong, prolonged weathering of quartz-rich, sedimentary rock. Below the topsoil, usually a mixture of minerals such as kaolinite, halloysite, aluminium-interlayered vermiculite and smectite is present. Typically, cation reserves such as potassium, magnesium, and phosphorus are low and concentrations of weatherable minerals are small. Ultic soils are generally strongly leached. At the study site, measured potassium, magnesium, and sodium were low (respectively, < 1 milliequivalent (me) 100 g^{-1}, 1.3–5 me 100 g^{-1}, and < 1 me 100 g^{-1}). Measured calcium was higher, ranging between 9.3–34.6 me 100 g^{-1} soil. Typically, UYTs are moderately to imperfectly drained. A complete overview of the chemical composition of the soil at Hoteo and Tapora can be found in Appendix C.

Figure 5

Soil Profiles at Tapora and Makarau

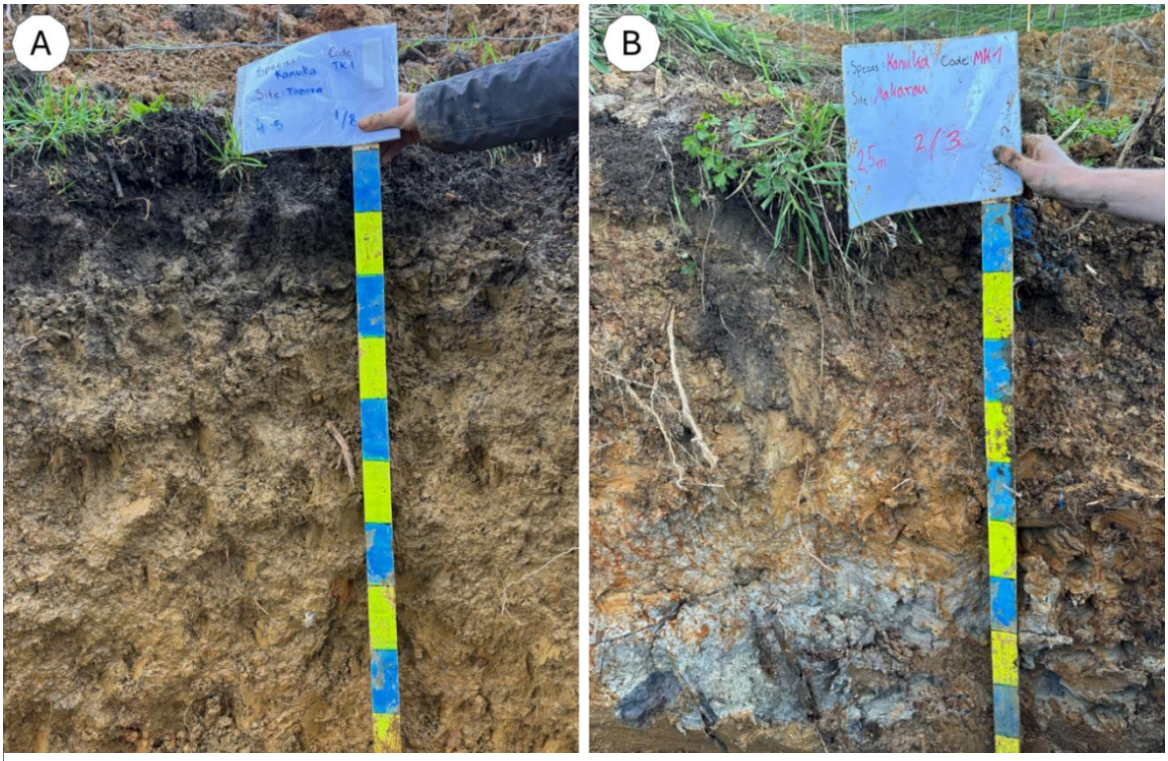

Note. (A) A Typic Yellow Ultic soil profile at Tapora and (B) a Mottled Yellow Ultic soil profile at Makarau. Photographs by Nicola Wilson.

5.3.2. Mottled Yellow Ultic Soil

The soil at Makarau is of Mottled Yellow Ultic type (UYM) (Fig. 5B). Different from the UYT, the UYMs have a mottled profile form, meaning that differently coloured specks or dots, i.e. mottles, are visible in the subsoil. The mottles are formed by the reduction and solubilisation of iron and/or manganese, which are then deposited and precipitate in the form of oxides within the redox-mottled horizon. The pH at the research site ranged between 5.2 and 6.1. Cations in the soil were higher concentrated, with potassium 0.4–2 me 100 g^{-1}, calcium 10–20 me 100 g^{-1}, magnesium 1–9 me 100 g^{-1}, and sodium 0.25–1.3 me 100 g^{-1}. Usually, UYM soils are imperfectly drained. Other characteristics of the soil correspond to the description of the typic yellow ultic soil. A complete overview of the chemical composition of the soil at Makarau can be found in Appendix C.

6. Results

6.1. Root Architecture

The distribution of roots was sampled to assess the spatial variability of roots across the two soil types for each individual tree (Table 2). A total of 117,000 roots were counted across four tōtara, four kānuka, and four poplars. The total root count differed significantly between species ($p < .01$). Generally, tōtara produced the largest number of roots across both soils, with the overall maximum count (MT2 with 17,121 roots) reported in the UYM soil. Kānuka generated the lowest root count in the UYM soil (5,625 roots), whereas poplar generated the lowest root count in the UYT soil (4,608 roots). The overall maximum RAR was calculated in the UYM soil for MP1, with a total root area occupying 2.30% of the total wall area around the tree. In the UYT soil, tōtara generated the highest RAR with 0.92%. The smallest RAR was found in the UYM soil for MK2 (0.21%). DBH was neither correlated with the total root count nor with the RAR ($p > .1$).

6.1.1. Vertical Arrangement of the Roots

Root Counts

The overall variance of the root counts (Fig. 6A) could not be well explained by the fixed and random effects of the LMM ($R^2 = .37$). Nevertheless, some significant effects were

Table 2

Summary of Tree Specifications

Tree Key[a]	DBH[b] (m)	Slope[c] (°)	Total Root Count	Small Root Count[d]	Total Root Area (m^2)	RAR[e] (%)
			Mottled Yellow Ultic Soil			
MK1	0.83	17.9	6,987	6,987	0.14	0.33
MK2	0.59	19.6	5,625	5,280	0.09	0.21
MP1	0.89	23.0	7,725	6,504	0.91	2.30
MP2	0.89	19.3	10,175	9,080	0.52	1.32
MT1	0.86	14.9	10,329	9,961	0.52	1.27
MT2	0.98	18.9	17,121	16,400	0.34	0.81
			Typic Yellow Ultic Soil			
TK1	0.66	19.5	10,887	10,487	0.13	0.32
TK2	0.67	10.6	6,743	6,273	0.11	0.26
TP1	0.76	25.3	4,608	4,329	0.13	0.33
TP2	0.64	24.7	5,596	5,191	0.18	0.46
TT1	0.51	16.5	17,431	17,022	0.34	0.84
TT2	0.64	18.0	13,773	13,452	0.38	0.92

[a] Tree key ABX is derived from (A) the soil type: M = Mottled Yellow Ultic Soil and T = Typic Yellow Ultic Soil; (B) the species: K = Kānuka, P = Poplar, and T = Tōtara; and (X) the unique tree number.
[b] Diameter at Breast Height
[c] Slope of surface surrounding the tree
[d] Roots with diameter ≤ 5 mm
[e] Root Area Ratio

found. A complete list of model interactions is presented in Appendix D1. The root count has been found to systematically decrease with soil depth ($p < .001$). For all species and soil types, the smallest number of roots was counted in the lowest layer (90+ cm). In both soils, more than half of the roots were concentrated in the upper 45 cm of the soil profile for all trees, excluding TK1 and TK2. The mean count of the kānuka in UYT was 3,782 roots for the first 45 cm of soil and another 5,033 roots in the sections below. Thus, an increase in root count with soil depth was found. The depth profiles (i.e. the change in root count across depths) were significantly different between the species and soil types ($p < .001$). The tōtara root counts remained relatively high at deeper soil depth, across both soil types. For kānuka, two significantly different ($p < .001$) depth profiles were observed between the two soil types. The kānuka roots counts in the UYM soil immediately declined with depth, whereas the counts in the UYT soil first increased before dropping to a low at maximum depth. For poplar, the patterns across the soils were significantly different, albeit less strong ($p < 0.05$).

Root Area Ratio

The variance in the RAR (Fig. 6B) could not be well explained by the fixed and random effects of the LLM ($R^2 = .28$). Nonetheless, species-specific RAR patterns across the soil profile were observed. A complete list of model interactions is presented in Appendix D2. Overall, the RAR decreases with soil depth ($p < .001$). Moreover, the change in RAR across depth was significantly different between the species across the soil types ($p < 0.01$). The within-species depth-pattern differed significantly between the soil types for poplar ($p < .001$) as well as tōtara ($p < .01$). Tōtara produced the overall maximum RAR in the uppermost soil layer, with mean

Figure 6

Mean Root Count and RAR for Each Species Across Soil Depth and Soil Type

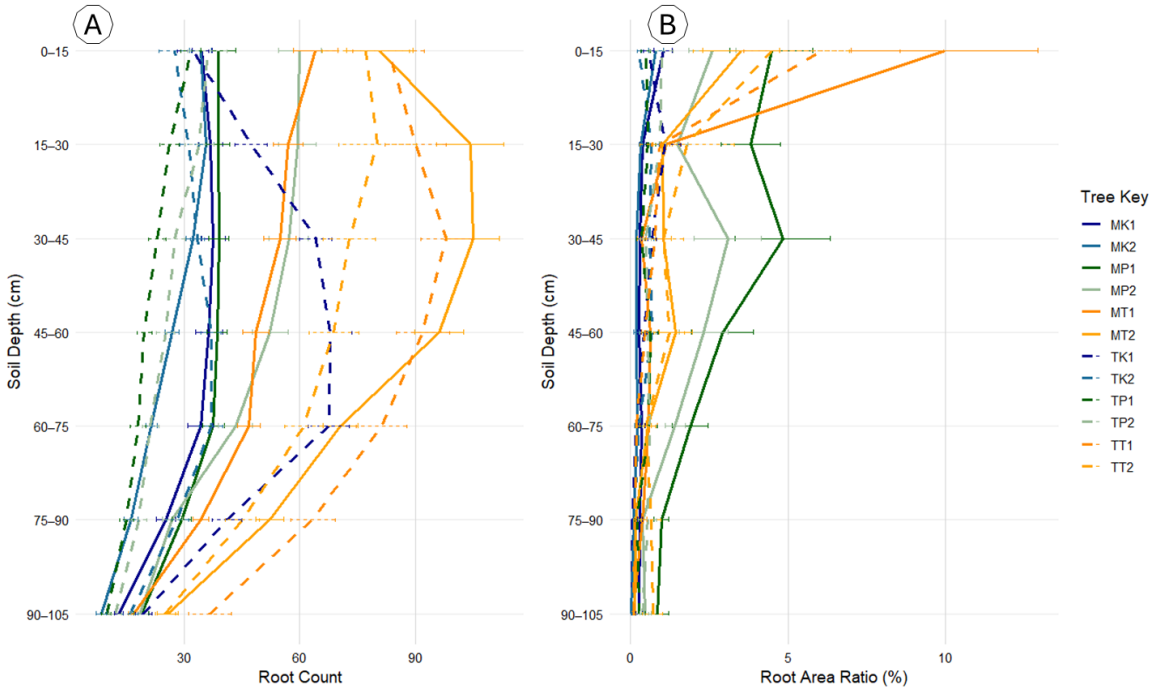

Note. The values for count and RAR are averaged to represent one measured soil section (i.e. soil section at sector *x*, depth *y*, and distance *z*, see Methods 4.2.).

RAR of 4.4% in the UYM soil and 3.1% in the UTM soil. These high RAR values were indicative of a higher proportion of coarse roots in this layer as opposed to deeper soil depths, considering the change in counted roots (Fig. 6A). At lower depths, the RAR values of tōtara ranged between 0.1% and 1.0%. For poplar, a difference in RAR between the soils was visible: in the UYM soil, the RAR ranged between 2.0% and 4.9% in the first half of the soil, whereas the RAR in the UYT soil did not pass 1.9% across all depths. Kānuka varied less in RAR across soil depths, with all RAR values ranging between 0.0% and 0.6%. Kānuka also produced the overall lowest RAR with the species' highest value at 0.6%. Kānuka did not produce significantly different RAR depth-patterns between the two soil varieties ($p > .1$).

6.1.2. Lateral Arrangement of the Roots (Distance)

Root Counts

Overall, the variance of the root counts (Fig. 7A) could not be explained by the fixed and random effects of the model ($R^2 = .27$). However, with distance from the stem, the number of root counts changed significantly ($p < .001$), regardless of species or soil. Furthermore, the distance-profile differed significantly between species ($p < .001$). A complete list of the model interactions is presented in Appendix D3. For tōtara, generally, the number of roots increased with distances further away from the stem. In the UYM soil, the mean number of tōtara roots reported in the 1.5 m radius was 2,508, opposed to 4,306 roots in the outer trench wall. Similarly, for the UYT soil, the mean tōtara root count increased from 2,967 at 1.5 m to 4,982 at 4.5 m distance from the tree. The pattern for tōtara was not significantly different between

Figure 7

Mean Root Count and RAR for Each Species Across Distance and Soil Type

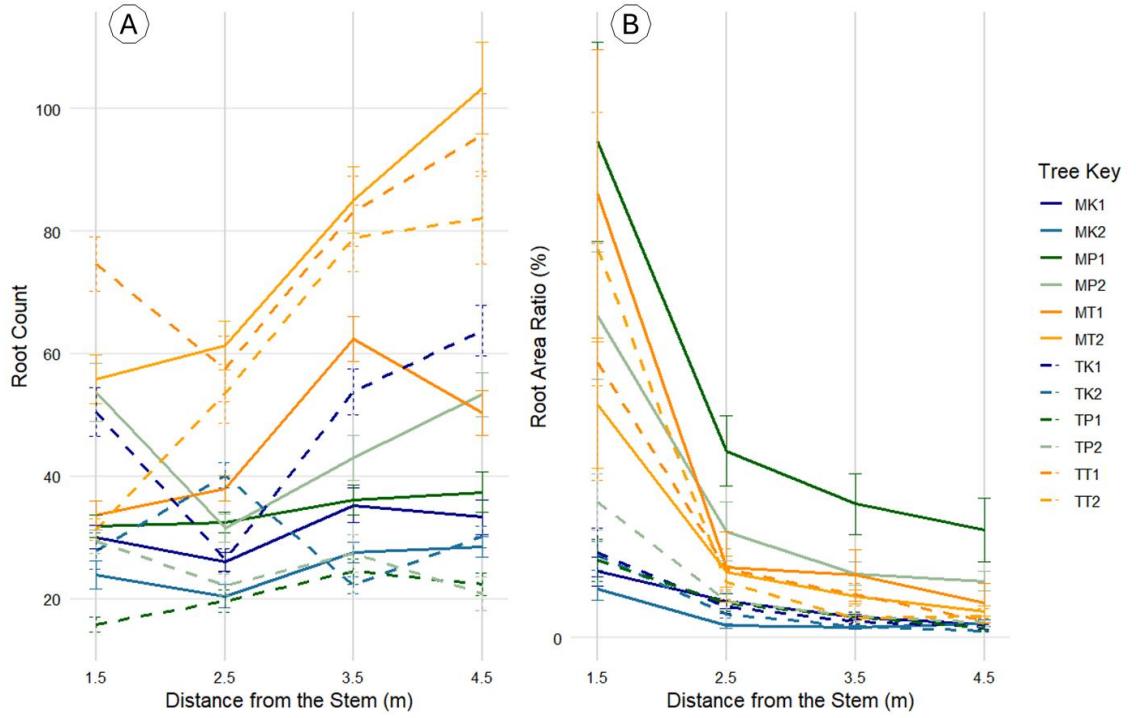

Note. The values for count and RAR are averaged to represent one measured soil section (i.e. soil section at sector *x*, depth *y*, and distance *z*, see Methods 4.2.).

the two soil types ($p > .1$). Similar for kānuka, a pattern across the soils was not statistically distinguishable ($p > .1$). For all radii across both soils, the mean kānuka root count lay between 1,304 and 2,629. The pattern of poplar root count with distance differed significantly between the two soils ($p < .01$). In the UYM soil, the mean poplar root counts varied between 1,794 and 2,543 roots. In the UYT soil, this varied between 1,174 and 1,453 roots.

Root Area Ratio

The fixed and the random effects in the LLM could not capture the variance in overall RAR ($R^2 = .24$; Fig. 7B). Nevertheless, overall species-specific patterns of RAR were found to be significantly affected by both the distance from the stem as well as soil type ($p < .001$). A complete list of model interactions is presented in Appendix D4. The RAR for tōtara was the highest in the first radius around the stem in both soil types. However, root numbers at this radius were among the lowest (Fig. 7A), indicating a shift from fewer, coarser roots, to a finer root network with greater root count further away from the stem. The poplar in the UYM soil generated the maximum overall RAR, with 5.2% of the total soil area in the 1.5 m trench occupied by roots. Like tōtara, the RAR of the poplar in the UYM soil dropped drastically from 1.5 m to 2.5 m, indicating a decline in coarser roots in the 2.5 m trench wall. In the UYT soil, such a steep drop was not visible for poplar. Nevertheless, the distance patterns of poplar did not return significant differences between the soil types ($p > .1$). Conversely, the RAR patterns of kānuka differed significantly across soils ($p < .001$).

6.1.3. Lateral Arrangement of the Roots (Sectors)

Root Count

The LMM did not fit the data well ($R^2 = .26$; Fig. 8). No systematic effect of sector on the overall root count was observed. A complete list of model interactions is presented in Appendix D5. In Appendix D6, a visualisation of the counts across sector for each unique tree can be found. Distinguishing between upslope and downslope sectors did also not result in a significant overall effect on root count ($p > .1$). However, the interaction between sector and species yielded a significant relationship, suggesting a species-specific pattern of root counts across the sectors ($p < .001$). Furthermore, the root count in the respective sectors was distinct for the different species across the two soil types ($p < .01$). Poplar displayed a significantly different sector profile across the two soils compared to both natives ($p < .001$). Between kānuka and tōtara, no significant difference in soil-specific sector profile was found ($p > .1$).

Root Area Ratio

The model showed a poor fit to the data ($R^2 = .14$, Fig. 9) and no overall significant effect of the sector on the RAR was found. Nevertheless, the effect of the sectoral arrangement was found to differ significantly between species ($p < .01$), and specifically within species between soil types ($p < .001$). A complete list of model interactions is presented in Appendix D7. Moreover, in Appendix D8, a visualisation of the RAR across sector for each unique tree can be found. For poplar, the RAR across the sectors differed significantly from the natives ($p < .001$) and between the two soil types ($p < .001$). In the UYM soil, the RAR of poplar did

Figure 8

Mean Root Count for Each Species Across Sector and Soil Type

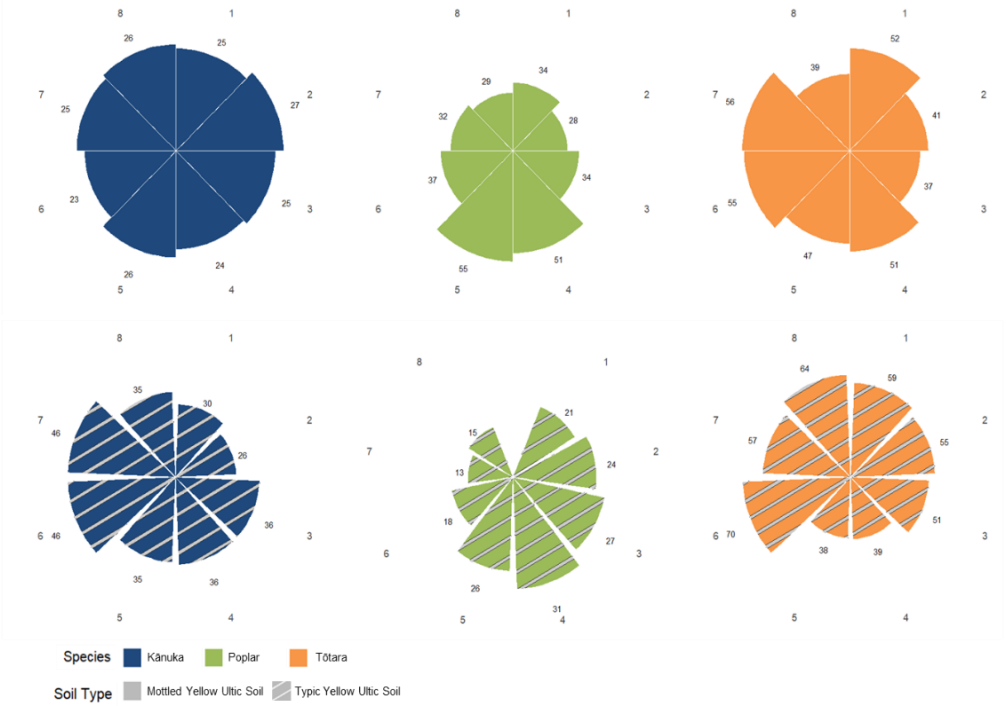

Note. The mean root count was summarized per species, in the sectors at 1.5 and 2.5 m away from the stem, the out two radii (3.5 m and 4.5 m) were filtered out for display purposes.

Figure 9

Mean RAR (%) for Each Species Across Sector and Soil Type

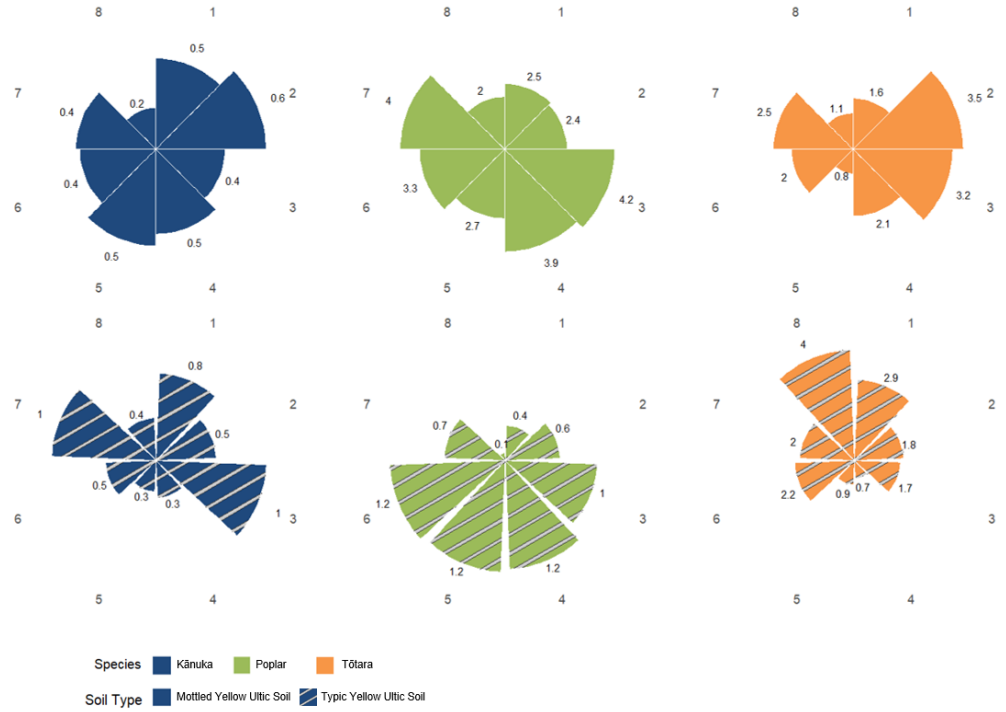

Note. The mean RAR was summarized per species for the sectors at 1.5 and 2.5 m away from the stem, the out two radii (3.5 m and 4.5 m) were filtered out for display purposes.

not differ significantly between the sectors ($p > 0.1$). In the UYT soil, the poplar's downslope sectors consisted of more coarse roots, resulting in a significantly higher RAR compared to its upslope sectors ($p < .001$). Within-species differences in RAR between the two soil types were found tōtara ($p < .05$) but not for kānuka ($p > 0.1$). Differentiating for up- and downslope arrangement did also not return a significant pattern in RAR for kānuka ($p > 0.1$). Tōtara, in UYM soil, displayed a higher root density on the right sided half of the slope. In UYT soil, the tōtara roots are arranged predominantly on the upslope side, with the biggest difference in RAR between sector 8 and sector 4, with respectively 4% and 0.7% of the soil occupied by root area. Nonetheless, distinguishing by up- and downslope sector did not significantly explain the differences in tōtara's RAR ($p > .1$).

6.2. Root Mechanical Properties

The mechanical properties of 238 roots were quantified. The quality of the tests was visually assessed (Fig. 10) and, where necessary, manually reclassified. Following the prerequisites for the test quality classification, in total, 98 tests were categorized as "good" quality, and 117 tests were considered a "medium" quality test. The remaining 22 tests were of "poor" quality (Table 3). The maximum tensile strength (F_{max}) differed significantly between

Figure 10

Selection of Tensile Strength Testing Curves of the Kānuka in UYT soil

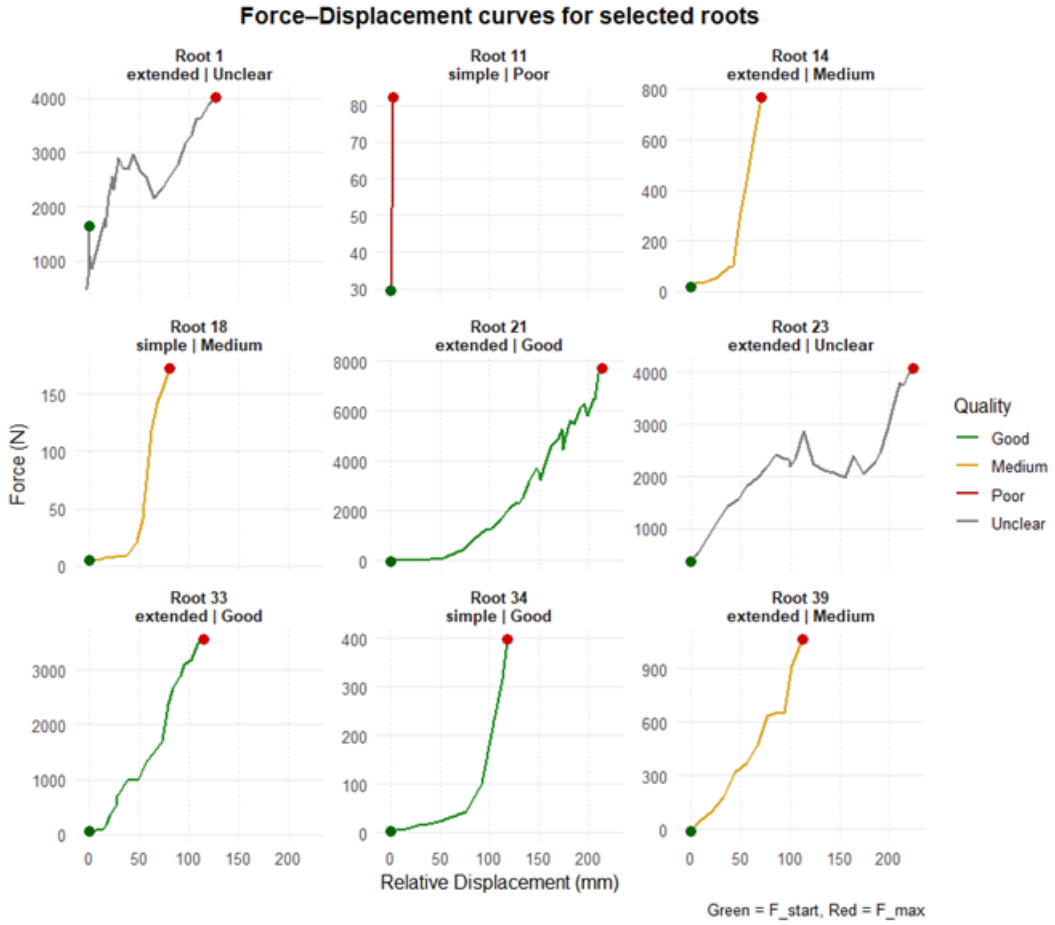

Note. To display, testing phases for nine roots were randomly selected based on "root_ID" (e.g., "1").

Table 3

Summary of Root Tensile Strength Data

Species	Roots	Mean F_{max} (N)	Max. F_{max} (N)	Stress (MPa)	Good[a]	Medium[a]	Poor[a]
			Mottled Yellow Ultic Soil				
Kānuka	38	2,234.19	10,869.48	0.44 – 12.14	15	21	2
Poplar	40	967.71	4,698.00	0.20 – 3.76	21	16	3
Tōtara	38	701.38	4,088.94	0.12 – 3.34	16	14	8
			Typic Yellow Ultic Soil				
Kānuka	41	2,552.95	9,849.24	0.02 – 10.85	11	26	4
Poplar	40	1,630.99	5,904.64	0.01 – 10.00	14	23	2
Tōtara	41	1,746.02	5,815.39	0.45 – 4.03	21	17	3

[a] Test quality

species ($p < .01$). The kānuka in the UYT soil yielded the highest mean F_{max}. Kānuka in the UYM yielded the largest F_{max} withstood by a root in the current study. The tōtara in the UYM soil yielded the lowest mean and maximum applied F_{max} on the roots among all species and across both soil types. The stress endured by individual roots differed significantly between species ($p < .001$). Kānuka yielded the widest range in stress across both soil types.

6.2.1. Descriptives

The distribution in maximum tensile strength of the roots differed between species, with kānuka yielding the largest range (Fig.11A). Generally, the maximum force under which a root snapped was higher for roots with larger diameters, for all species. A larger number of roots below 20 mm were measured, resulting in a right-skewed dataset, as smaller root diameters typically obtain lower tensile strength values. These observations were considered part of the natural variability of the data rather than extraordinary or error values. A non-linear distribution of the F_{max} across root diameters is visible (Fig. 11B).

6.2.2. Linear Mixed Effects Model

The LMM fitted the log-transformed maximum applied force data relatively well ($R^2 = .71$; Fig. 12). A significant positive correlation was found between F_{max} and root diameter. On average, the F_{max} of a root increased with 11.6% per mm diameter increase, regardless of soil type and species ($p < .001$). Moreover, the increase of force per unit diameter was significantly stronger in the UYT soil compared to the UYM soil ($p < .05$). For tōtara, the increase in maximum force per mm diameter increase was about three times higher in the UYT as compared to the UYM ($p < .001$). Other species-specific interactions in the model did not return strong, significant interactions (Appendix E).

Figure 11

The F_{max} for Each Species across Root Diameters and Soil Types

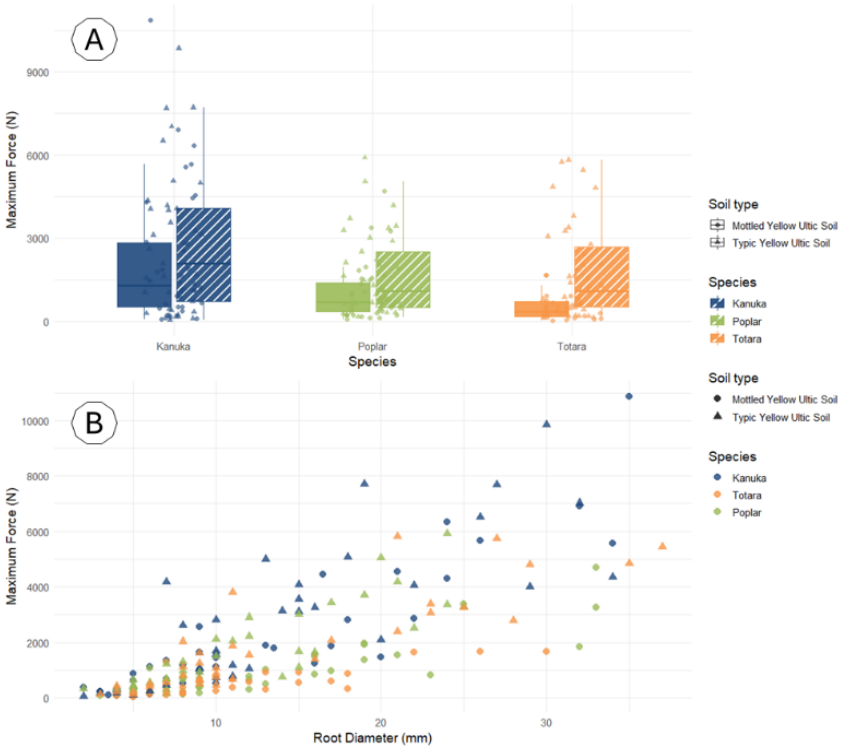

Figure 12

The LMM of F_{max} for Each Species across Root Diameters and Soil Types

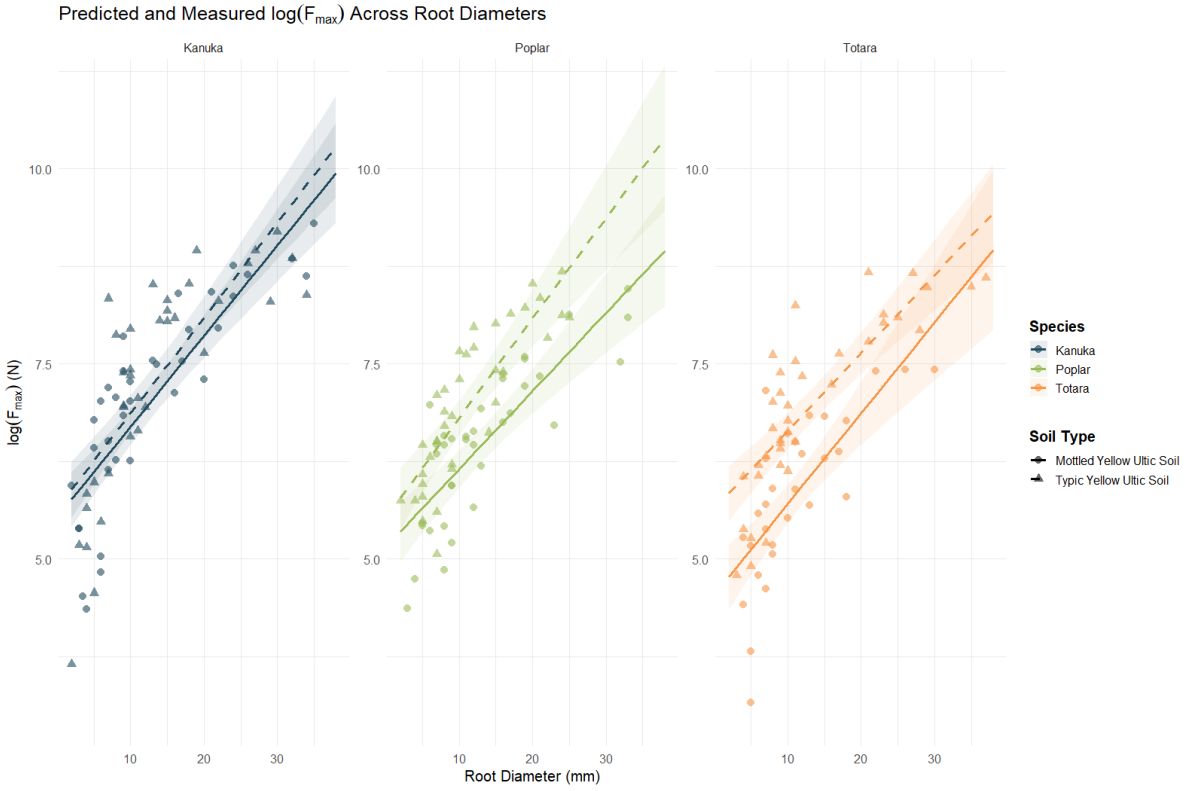

Note. Note the y-axis logarithmic scale. The individual datapoints represent the collected field data. The regression lines represent the predicted relationships between the F_{max} and root diameter across the species and soil types.

6.2.3. Parameter Fitting of the RBMw

Maximum Tensile Force at Failure

For each species, the field data was fitted using the power-law relationship between maximum applied force and root diameter (Fig. 13, Table 4). All three curves presented a clear increase in tensile strength with increasing root diameter. All models had a reasonable fit, with the R^2 ranging between .58 and .72. The Goodness of Fit was the highest for kānuka, however, the datapoints were less clustered around the predicted values (RSE = 1335 N) compared to poplar and tōtara (respectively, 861 N and 892 N). For kānuka, a significant shape factor (α) was derived ($p < .05$). Kānuka's α was the highest, suggesting a stronger increase in maximum applied force with diameter compared to the other two species. For both kānuka and poplar, the slope of the curve decreases slightly for the higher root diameters. Furthermore, the F_0 of the two natives were higher than that of poplar, indicating a higher base-strength for these species. However, these values were not significant.

Figure 13

Fitted F_{max} with Cumulative Normal Distribution Function for Each Species

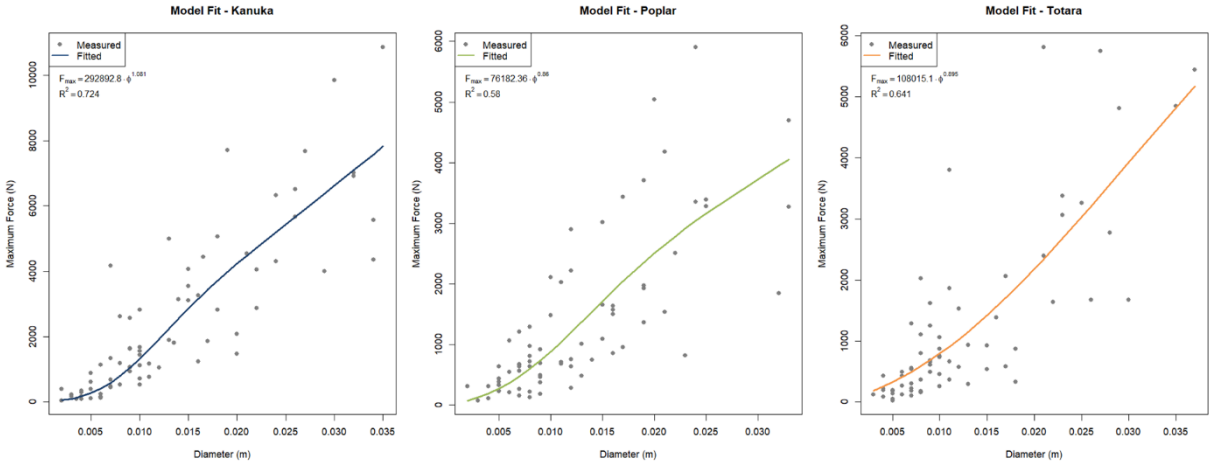

Note. Note the different y-axes.

Table 4

Summary of the Fitted Function for F_{max}

Species	R^2	df	RSE[a]	F_0	α
Kānuka	.72	69	1335	292,893	**1.08****
Poplar	.58	69	861	76,182	0.86
Tōtara	.64	64	892	108,015	0.90

[a] Residual Squared Error
* $p < .05$ ** $p < .01$ *** $p < .001$

Apparent Spring Constant

For each species, the ratio between maximum root tensile strength over the displacement generated a prediction of the apparent spring constant across root diameters (Fig. 14; Table 5). All curves presented an increase in force per displacement with increasing root diameters. For all species, the fit of the model was relatively poor ($.36 \leq R^2 \leq .48$). Despite the poor fit, the yielded root spring constant shaping factors (β) were significant for all species. The slope was the strongest for tōtara, with a β of 1. Moreover, the spring scaling factor (k_0) yielded a significant value of 819,539 ($p < .05$) for kānuka. The spring constant yielded the highest scaling factor for tōtara, where the force per displacement increased with ~1.2×10^6 per unit increase in root diameter.

Figure 14

Fitted Spring Constant Equation for Each Species

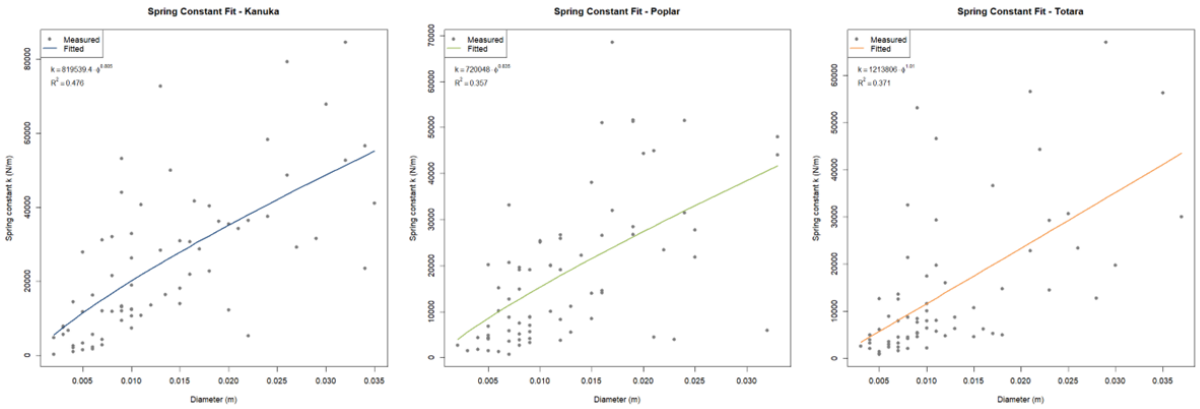

Note. Note the different y-axes.

Table 5

Summary of the Fitted Spring Constant

Species	R^2	df	RSE[a]	k_0	β
Kānuka	.48	70	14.58	**819,539***	**0.80*****
Poplar	.36	71	12.66	720,048	**0.84*****
Tōtara	.37	65	12.31	1,213,806	**1.00*****

[a] Residual Squared Error

* $p < .05$ ** $p < .01$ *** $p < .001$

Weibull Survival Function

The root survival rate was computed for each species (Fig. 15, Table 6). With increasing displacement of the root, the probability of a root surviving the force applied to it declines. The function showed a very good fit for all species (R^2 ~ .99). The steepest decline in survival probability was found for poplar, where the shaping factor ω fitted a value of 2.27. Once failure is initiated, the failure rate of poplar roots increases quickly. The highest fitted λ was found for kānuka, meaning that the displacement at which survival becomes less likely is larger for this species compared to the others. The small λ for tōtara indicates a small displacement scale, tolerating only minimal displacement before root failure starts.

Figure 15

Fitted Weibull Survival Function for Each Species

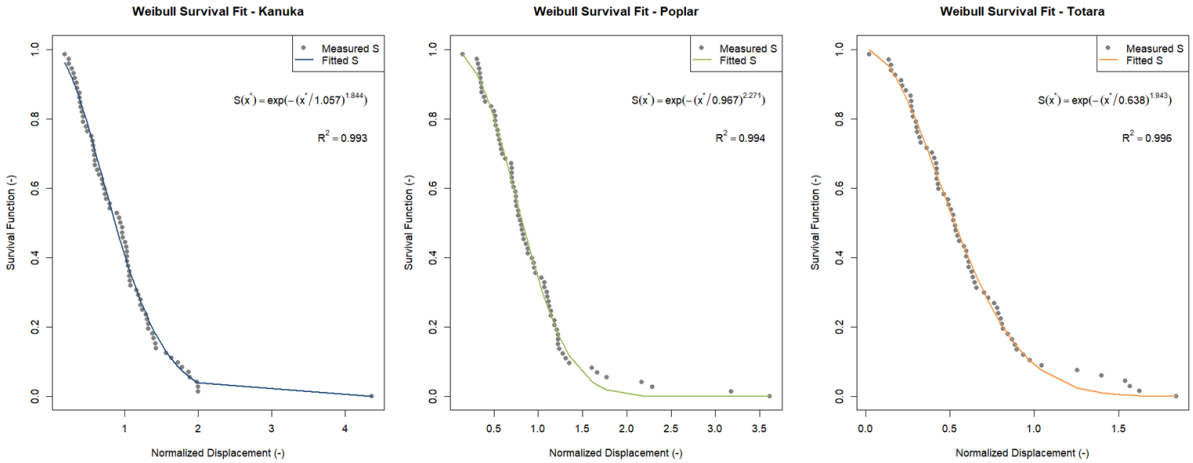

Note. Note the different x-axes.

Table 6

Summary of the Fitted Survival Function

Species	R^2	df	RSE[a]	λ	ω
Kānuka	.99	71	0.02	**1.06*** **	**1.84*** **
Poplar	.99	71	0.02	**0.97*** **	**2.27*** **
Tōtara	.99	66	0.02	**0.64*** **	**1.94*** **

[a] Residual Squared Error

* $p < .05$ ** $p < .01$ *** $p < .001$

7. Discussion

This study evaluated the differences in root architecture and root mechanical properties of kānuka, tōtara, and poplar across two different soil types. Explorative allometric analyses were performed, aimed to test for significant differences between species as well as within species across different soil types. The study was directed at identifying potential influencing factors and providing new or additional evidence on the root distribution and tensile strength of three tree species relevant to New Zealand's pastoral hill country.

This chapter discusses the main findings in relation to the three research questions:

1. **Do the vertical and lateral arrangements of the roots differ between the species across the soil types?**
2. **Does the tensile strength of the roots differ between species across the soil types?**
3. **In what way do independent factors modify the variability of root mechanical behaviour?**

Subsection 7.1. is structured around research question 1, comparing the root architecture of the species and across the soil types. Where comparable data was available, links to previous studies are made. Subsection 7.2. is dedicated to answer both questions 2 and 3, where the reported root mechanical behaviour of the current study were discussed and interpreted. Overall plausibility of the results was weighed and, where possible, compared to findings of existing literature. At last, limitations of the current study, implications of the findings, and suggestions for future research are presented in sections 7.3. to 7.5.

7.1. Root Architecture

Overall, tōtara yielded a much greater total root count opposed to the other two species. However, the RAR of tōtara was not the highest compared to the other species. For example, in the UYM, the RAR of tōtara was lower than that of poplar. This disparity between root count and RAR is indicative of a dense network of finer roots, commonly present in the root systems of indigenous species of New Zealand (Phillips et al., 2023). Poplar, contrastingly, showed lower root counts, but the highest RAR (in the UYM soil), implying the presence of fewer, coarser roots. Furthermore, no correlation of the total number of roots or RAR to the DBH was found. Philips et al. (2014), however, concluded that root number, mass, and length are largely explained by the tree's DBH. It is likely that the species sample size was not sufficient to correlate these tree characteristics adequately.

The LMMs could not adequately explain the variance in root count or RAR for any partitioning direction (i.e. vertical and lateral, in terms of distance and sectors; $.14 \leq R^2 \leq .37$). Despite the poor fit of the models, it was shown that both the root distribution and RAR significantly change with variation in the vertical arrangement. The slopes of the root counts across depth varied between species. Overall, the root count declined beneath the first 45 cm of soil. Generally, across both soil types, a higher root density was observed closer to the stem. This was regardless of species. The higher root density in the upper 45 cm of the soil confirmed

insights from existing literature, e.g., Douglas et al. (2010) on poplars, and Marden et al. (2018a) and Phillips et al. (2023) on different New Zealand natives. Watson et al. (1995) found larger, vertical (sinker) roots at 1 m radius around the stem of indigenous species. Given that the closest soil face was located at 1.5 m away from the stem, it is possible that important vertical roots were not recorded for kānuka and tōtara.

Moreover, the root count and RAR changed with distance from the tree. The RAR was the largest in the first radius around the stem, regardless of species and soil type. For tōtara, the RAR decreased with distance from the tree, whilst the number of roots increased. Such a far-reaching, mat-like root architecture compiled of finer roots is in line with existing literature on indigenous species (e.g., Phillips et al., 2023). The root count and RAR of kānuka were less variable and somewhat consistent across the two soil types. For poplar, Ngo et al. (2023) calculated the RAR at 1.5 m distance around the stem. Reported findings ranged between 0.02 to 1% of root occupation in the soil, for trees with a DBH between 0.41–0.56 m. Moreover, proximity to other trees, in their study around 3.5 m, strongly determined DBH and RAR. The findings in the current study exceed these values tremendously, with 0.99 to 6.35% of poplar root occupation in the 1.5 m radius, for trees with DBH between 0.64–0.89 m. The reported DBH and RAR of the current study, however, were not correlated to each other. Trees studied were individually spaced (proximity to surrounding mature trees about 8 meters), possibly allowing for the development of a higher root density.

The arrangement of the roots across the different sectors did not return an overall significant pattern in the distribution of root counts and RAR. The study on 12 indigenous early colonising trees and shrubs by Marden et al. (2018b) concluded a highly variable arrangement of the roots, with some areas completely devoid of roots. A clear, predictable arrangement of the roots of indigenous New Zealand species is, thus, challenging. Nevertheless, a clear distinction could be made in the sectoral arrangement between the two natives and poplar. While no significant sectoral pattern could be identified for the natives in either of the soil types, the poplars showed a clear distinction in root arrangement between upslope and downslope in the UYT soil. Such a skewness in root development is found more often for poplars on slopes, where roots tend to grow in the direction of higher moisture contents and lower slope and wind resistance (Phillips et al., 2023). For example, McIvor et al. (2009) mapped the root distribution of 11.5-year aged poplars on a slope, differentiating between upper-slope (32.0°; DBH 18.9 cm), mid-slope (28.6°; DBH 27.2 cm) and downslope (21.8°; DBH 29 cm) locations. The poplars on the upper- and mid-slope sections (steeper sections) showed an uneven spread of roots, with clustering in sector 1 and 8 and in sector 4 and 5. The downslope poplars showed a rather even spread. In the current study, the poplars in the UYM soil were situated on a 23.0° slope (MP1, DBH 89 cm) and a 19.3° slope (MP2, DBH 89 cm). Comparable to the results of the downslope poplars by McIvor et al. (2009), the poplars displayed a relatively even spread of the root counts and RAR across the different sectors. The poplars in the UYT soil were grown on a 25.3° slope (HP1, DBH 76 cm) and a 24.7° slope (HP2, DBH 64 cm), similar to the McIvor et al. (2009) mid-slope range. Likewise, there was more clustering of the roots for the UYT poplars. However, this clustering was concentrated in the downslope sectors (3 till 6), and only

very few and small roots were found in sectors 1 and 8. Hence, clustering in opposite sectors like in McIvor et al. (2009) was not observed.

Phillips et al. (2014) found that the root growth rate varied greatly between comparable studies, emphasizing the effects of slight differences in soil type, temperature, moisture availability and competition with surrounding vegetation, including smaller vegetation like weeds and grasses. In the current study, there was variation between environmental and geomorphological factors of the research sites as well as between the selected trees (e.g., exposure, slope, drainage and chemical composition of the soil, proximity to other types of vegetation, etc.) that have not been further considered in the analysis. Moreover, there was a great within-species differences in DBH (and thus tree age). This variability among the assessed trees was reflected in the statistical analysis. The ability to draw significant conclusions considering the root architecture across the species and soil types was limited by the variation across the aforementioned conditions. Nevertheless, a clear distinction in the lateral arrangements of the roots was observed. With distance from the tree, the fine-root network densified for all tōtara as well as some of the kānuka trees. Such a mat-like structure was not observed for poplar. Across the sectoral arrangement, a division between the indigenous species and the poplar was found. Where poplar displayed a rather even arrangement, both tōtara and kānuka varied greatly in root distribution across the sectors. The vertical arrangements did not differ between species, with each species displaying a higher root density in the upper soil layers. Across soil types, no clear effects could be distinguished.

7.2. Root Mechanical Properties

Overall, the maximum tensile strength (F_{max}) range and stress (σ) found in the current study are low compared to previous findings. For example, Watson and Marden (2004) concluded mean σ to range between 8 and 52 MPa across twenty different indigenous New Zealand species. Specifically for kānuka, reported σ values ranged between 18 and 76 MPa. The measured tolerated σ of the kānuka roots in this study did not exceed 12.14 MPa, i.e. about a sixth of previously reported findings. Furthermore, in the study by McIvor et al. (2011), poplar σ values ranged between 19–90 MPa. Their reported maximum σ was, thus, almost a ten-fold larger than the maximum σ of the current study (10.00 MPa). Important to note, strength data yielded in previous studies for similar species and contexts had been predominantly derived from tests performed in laboratory setting. Typically, roots were collected from planted trials and not immediately assessed on-site (Phillips et al., 2023). Hence, varying field conditions affecting the root growth, such as slope, soil type, moisture content, and exposure, as well as inconsistency using field equipment were controlled for. As underlined by Schwarz et al. (2013), only in-situ pullout tests (as opposed to laboratory tests) incorporate the effect of root tortuosity and soil-root interaction. Thus, very likely, these effects have caused the low measurements of F_{max} in the current fieldwork.

7.2.1 Linear Mixed Effect Model

A linear mixed effect model was performed to test for the effects of species, soil type and root diameter on the maximum tensile force (F_{max}). The model explained the variation in

F_{max} well (R^2 = .71). Both the root diameter and soil type returned significant effects on the F_{max}, in line with existing literature (e.g., Ngo et al., 2023; Schwarz et al., 2011). Since all other interactions lack significant effects, root diameter and soil type likely explain most of the variation in measured F_{max}. From the LMM fit, it could be concluded that the rotos in the UYT soil yielded a distinct stronger increase in force per unit diameter compared to the ones in the UYM soil. Hence, a clear effect of soil type on the measured tensile strength can be concluded. No distinct effect of species on the slope between F_{max} and root diameter could be identified through the LMM. Possibly, the measurements per species in each soil were too few to derive a significant relationship.

7.2.2. Parameter Fitting RBMw

The data were fitted to the different parameters of the RBMw, following the methods proposed by Giadrossich et al. (2016) and Ngo et al. (2023). First, all fitted F_{max} equations had a moderate fit ($.58 \leq R^2 \leq .72$), with kānuka yielding the strongest predicted increase in F_{max} with increasing root diameter. The base-strength (F_0) of kānuka was the highest among the three species, albeit not significant. Moreover, the largest and only significant α was fitted for kānuka, suggesting a much stronger increase of F_{max} for roots with larger diameters. The F_0 for tōtara was moderate, laying between the values yielded for kānuka and poplar. This is in line with expectations, as softwood species like tōtara generally demonstrate a weaker relationship between F_{max} and root diameter (e.g. Watson & Marden, 2004). However, studies on the mechanical properties of softwood species are limited, hence a thorough comparison remains open. The fitted coefficients for poplar differed substantially from previous findings. In the current study, the coefficients F_0 and α found for poplar were respectively 10.8×10^4 and 0.86. The data fitted in the work by Ngo et al. (2023) yielded $F_0 = 2.9 \times 10^6$ and α = 1.55. In their study, a much stronger and clearer exponential effect of the root diameter on the maximum tensile force was derived. Considering their goodness-of-fit (R^2 = .88), the calibration of their parameters using pullout data was more accurate, with the curve predicting the maximum tensile forces well. Nonetheless, it has been shown that the parameter fitting using test-data from smaller roots (< 5 mm) leads to an overestimation of the tensile strength at larger root diameters (Giadrossich et al., 2020). Hence, cautious interpretation of the modelled outcomes as well as consideration of the input data are important when assessing the fitted F_{max} equation. To date, previous studies where pullout data of kānuka and tōtara were fitted to the parameters of the RBMw do not exist, hence, further cross-literature comparisons of the calibrated coefficients cannot be made.

The fit of the spring constant was rather weak ($.36 \leq R^2 \leq .48$) but yielded significant values for the shape factor β for all species. The model could best explain the displacement measured for kānuka, with significant values for both k_0 and β. The β was the highest for tōtara, suggesting the steepest positive curve for the elastic modus with diameter. Furthermore, albeit not significant, the spring scale factor k_0 was the highest for tōtara, indicating a stronger base elasticity of the roots compared to the other species. k_0 was the lowest for poplar at $\sim 7{,}2 \times 10^5$. Ngo et al. (2023) reported a higher value for the poplar's k_0 (9.7×10^6), suggesting a higher base elasticity of the roots assessed in their study. In their study, no value for β was fitted.

Giadrossich et al. (2016) also found larger coefficients, with a k_0 of 5.49×10^9 and a β of 2.1. However, their fit was performed for the roots of a different hardwood tree species, thus a direct comparison to the hardwood species in this study cannot be made. Moreover, their tests were performed in the lab, so influence of root tortuosity and root-soil interaction are controlled for when measuring the displacement. This may have led to the higher force per displacement values.

Lastly, the survival function was fitted for each species, using the calibrated scaling factor λ and shape factor ω. All equations showed an excellent fit ($R^2 \sim 0.99$) to the observation data. Kānuka performed best, with the highest tolerance for initial displacement (highest λ) and the least steep survival decline (lowest ω) compared to the other species. Tōtara displayed the quickest failure initiation, with a λ of 0.64. Poplar showed the poorest survival likelihood, with the sharpest decline in survival probability (highest ω) and a relatively low tolerance for displacement (relatively low λ). Comparing the parameters to the findings of Ngo et al. (2023), again, the current study found rather conservative values for poplar. In the Ngo et al. (2023) study, the scaling factor was higher ($\lambda = 1.53$) and the shaping factor was lower ($\omega = 1.83$), resulting in a less quick and strong decline in survival rate over displacement of the root. Seeing as the current study's survival function was derived from the weaker parameter fittings for F_{max} and k, consequently, there is a higher failure probability.

In all, the coefficients of the three base functions of the RBMw showed a great variety between the species. For each species, a different relationship between the root diameter and the maximum force as well as the elastic modus was observed. Furthermore, the fitted coefficients led to different curves for the survival probability function across the species.

7.3. Limitations of the Fieldwork Design

To allow for the assessment of the root distribution, the entire root systems had to be exposed using a mechanical digger. This led to damage and possibly displacement of the roots. Excavation methods such as sluicing with compressed air (e.g., Marden et al., 2025) could prevent such alternations but are extremely costly and require the whole tree to be removed out of the soil. In planted trails, such a method can be opted for. In the natural stands assessed in this study, however, it was aimed for minimal alterations to the privately owned land. Trenches were filled up afterwards assessments and grass seeds were sown in to minimize traces of the conducted fieldwork.

Furthermore, due to a soil slip, no distribution counts were collected for fours sectors across the 3.5 m and 4.5 m trench walls for MP1, sector 4 in the MT2 3.5 m wall, and sector 5 in the MK1 3.5 m wall. The missing values for these sectors were substituted using mathematical imputation to predict the root counts based on patterns across the other sectors of the respective tree. However, especially for MP1, this computation was limited by the absence of the root counts in these four sectors (i.e. the counts in trench wall 1.5 m and 2.5 m). Lastly, due to prolonged rainfall, the downslope trenches of the poplars in the UYM filled up with water and required pumping. Precise assessment of the sectors bordering the high water was hindered due to the remnants of the mud pools covering up the roots exposed on those walls.

Due to inexperience, the first tests had a higher failure rate. For tōtara in the UYM soil, there was more interference during testing. Slippage of the root along the rod, among others, generated a higher ratio of poorly conducted tests for tōtara. Moreover, in-situ failures (i.e. tests that were aborted in the field) were higher for tōtara than in subsequent assessments. The quality of in-field testing depends on several factors. The characteristics of the sampled root (e.g. length of the sample and root moisture content) as well as the experimental set-up (e.g. clamping of root ends and pullout speed) determine the result of a test (Giadrossisch et al., 2017). The lengths of the uncovered root varied greatly between species, between 10 cm for some tōtara roots till about 30 cm for longer poplar roots. The influence of the root geometry and structure on the pull-out test performance was optically evident during field work. Poplar had generally quite long, straight, and bendable roots. This aided the preparation of the roots for the field tests. Also, the poplar roots appeared to branch more often than the natives, distributing the applied force over multiple roots further down in the soil. Occasionally, bundles with relatively coarse second-order apices were pulled out from deeper in the soil (Fig. 16A). Both kānuka and tōtara had flaky, brittle roots with high tortuosity that were not easy to bend. Due to the high tortuosity, straight sections of the roots appropriate for root tensile strength testing were more difficult to find. Rather than growing several coarser apices like poplar, the natives developed fibrous, densely packed shoots directly from the main apex, occasionally pulling out whole bundles of soil (Fig. 16B). Nevertheless, such factors provide valuable input allowing for root reinforcement modelling as close to reality, including the effects of tortuosity and the root-soil interaction (Schwarz et al., 2013). Lastly, Cofie and Koolen (2001) found average tensile forces to increase with higher pullout speeds. In the current project, speed could not be applied in a controlled, consistent manner.

Figure 16

Root Bundles of Poplar (A) and Tōtara (B) Pulled out of the Soil

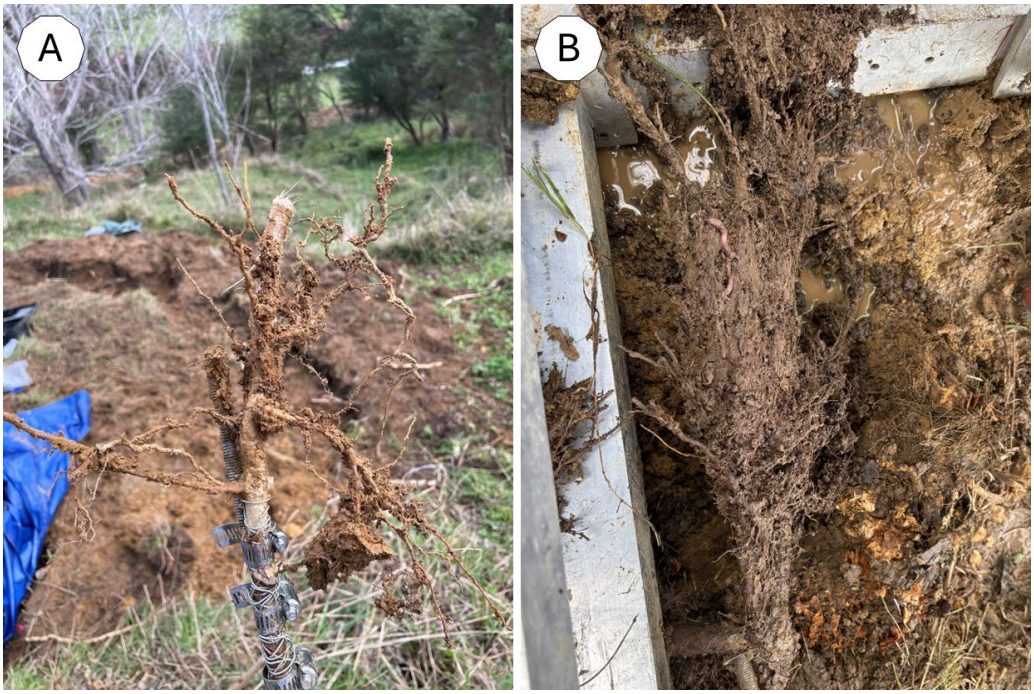

7.4. Implications of the Study

Insights of the current study, combined with the vast amount of existing literature, may serve as a basis for practitioners striving for holistic management of erosion prone slopes. Essential is to focus on long-term solutions, safeguarding the resiliency and sustainability of a landscape. Therefore, mixed species silvopastoral systems may offer several benefits (Marden et al., 2018b). A diverse demography of root systems optimizes the varying lateral and vertical reinforcing effects enacted by different species (Phillips et al., 2023). Findings of the current study confirm that such a variation in root systems is found across the studied species. Native species with a longer lifespan, such as kānuka and tōtara, may provide a long-term solution to soil erosion. They are more resistant to wind gusts, which is particularly important with New Zealand's strong westerly winds (Phillips et al., 2023). Furthermore, it has been demonstrated that kānuka retains its reinforcing capacities long after clear-felling of a slope (Watson et al., 1999). However, low-density monocultures of kānuka likely do not effectively contribute to soil stabilisation (Marden et al., 2020). On the contrary, fast-growing exotics like poplar ensure rapid protection after plantation and have generally greater root reinforcing capacities, also at lower stand densities. In the silvopastoral context, cattle grazing could aid maintaining optimal light input at near-ground levels, to facilitate the growth of otherwise outcompeted seedlings (Bergin & Kimberley, 2014). Moreover, kānuka has been shown to increase pasture production beneath the canopy in summer-dry climates (Mackay-Smith et al., 2022) and poplar may provide supplementary fodder during drier summer months (Suleiman, 2006). Lastly, native birds and potentially other species may benefit from increased indigenous landcover. Dobson (2024) counted increased occurrence of farm birds with densifying kānuka cover, highlighting the potential synergy between bioengineered slope stabilisation, economic gains, as well as conservation goals associated with root reinforced slopes.

7.5. Lookout and Future Research

The data sampled in this study can serve as an input for subsequential RRMs. Calibration and validation of a Root Distribution Model (RDM), used e.g. by Ngo et al. (2023), may be performed using the root distribution data obtained in this study. Variations in root counts and RAR across DBH and distances from the tree could be assessed (Schwarz et al., 2016). Subsequently, the individual root mechanical data could be used as a proxy to determine the root reinforcing capacity of a bundle of roots, for example using the RBMw as proposed by Schwarz et al. (2013). The fitted parameters of the non-linear regressions for the tensile force, spring constant, and the survival function of the current study can serve as inputs for such a model. The data presented here could be supplemented with previous findings, to generate a better model fit. For example, future research could fit the reported kānuka data by Watson and Marden (2004) to these parameters. Cross-literature comparisons of the relationship between root tensile strength and root diameter can then be made.

Many modelling efforts for slopes reinforced by poplar roots exists. Studies employing indigenous species to model the effects on slope stability are, however, limited. Especially for the understudied tōtara, root reinforcing effects at the stand scale are yet to be explored. Hence, future research could calibrate the RBMw to a stand scale using a RDM derived from the current

distribution data. From the single-root system, the stabilizing effects of kānuka, tōtara, or poplar root bundles on the stand or slope scale can be evaluated. Stand densities corresponding to the silvopastoral context can be modelled to extract the reinforcing effects of space-planted tōtara and kānuka in pastures. The outcome across varying stand densities can be evaluated and may, eventually, serve as an input for slope stability models for analysis at regional scale (van Zadelhoff et al., 2022).

To better understand the influences of environmental and geomorphological factors, trials with control sites should be set up. Independent factors such as the slope, position, aspect, exposure, or wind effects could then be studied in greater detail. Especially for the lesser-studied indigenous species, further controlled assessment of the root distribution and root mechanical properties is required. Moreover, the effects of soil type and soil moisture content could be assessed in greater detail. In slope stability analysis, root reinforcement is often modelled as a soil cohesion component (Masi et al., 2021). In such models, total soil cohesion decreases with increasing soil moisture content. Root moisture content is, thus, not modelled separately. However, the study by Yang et al. (2016) concluded root moisture content to have a direct, significant effect on the tensile strength. Slight loss of root water content could enhance tensile strength, whereas too much water loss reduced root elasticity and thereby the tensile strength. Another study by Zhang et al. (2019) mentioned the responsiveness of roots to the surrounding water content, with roots extracting water from the soil when the soil moisture content is high, and vice versa, desiccating when soil moisture is low. Therefore, the relationship between the varying soil moisture contents across the soils and the measured tensile strength should be further assessed. Potential trends in root mechanical behaviour of tōtara, kānuka and poplar under these varying conditions could be identified.

Lastly, few studies have linked mycorrhizal activity to root growth and, indirectly, root reinforcement of the slopes (e.g., Mao, 2022). Root growth and plant maturing rates have been shown to benefit from mycorrhizal activity. By stimulating growth rates, mycorrhizae abundance may decrease the required time to reach structural reinforcement of a slope, i.e., a root network sufficiently developed to stabilise the soil. Davis et al. (2013) concluded that, in open grassland, kānuka establishment is limited by the absence of native arbuscular mycorrhizae. Hence, further investigation of the role of mycorrhizal status is essential to understand root development of young trees in a silvopastoral context.

8. Conclusions

This study evaluated the root architecture and root mechanical properties of individually spaced tōtara, kānuka, and poplar across two different soils dominant in New Zealand's pastoral hill country. A variability in the lateral arrangements of the roots was observed. A significant difference in vertical arrangement was not found. Overall, the poplar demonstrated fewer but coarser roots. The natives showed a mat-like root architecture, with a high count of very fine roots further away from the tree stem. The ability to draw significant conclusions considering the root architecture across the species and soil types, however, was limited by the variation in environmental conditions and tree-specific traits. Root mechanical behaviour different between the species. Rendered tensile strength values in the current study were relatively low. The LMM could not conclude a significant influence of the species on the tensile strength curve. For all species, higher tensile strength values were reported in the UYT soil compared to the UMY soil. Generally, the tensile strength increased with root diameter for all species. Moreover, the force over displacement was found to increase with root diameter, regardless of species. Lastly, the survival rate differed strongly between species. Poplar has been found to be least tolerant to displacement and showed the steepest decline in survival probability after initiated failure. Kānuka performed best, with a more gradual decline and higher initial displacement toleration. However, findings of the current study are rather conservative compared to existing literature on the mechanical behaviour of roots. Nevertheless, these results presented key insights into root architecture and root mechanical properties of widely spaced, mature poplar, kānuka and tōtara across UYT and UYM soils. In-situ tensile strength assessment provides unique, close-to-reality information, acknowledging the influences of environmental factors such as root tortuosity and compressive forces by the soil-root matrix. Many opportunities for future research remain open. The data of the current study should be used for further slope stability modelling and data collection could be replicated to test under controlled circumstance. Eventually, a deepened understanding of root behaviour of tōtara, kānuka and poplar may guide the selection of species in mixed silvopastoral systems.

References

Allan Herbarium. (2000). *New Zealand Plant Names Database*. Manaaki Whenua – Landcare Research. http://nzflora.landcareresearch.co.nz

Arnone, E., Caracciolo, D., Noto, L. V., Preti, F., & Bras, R. L. (2016). Modeling the hydrological and mechanical effect of roots on shallow landslides. *Water Resources Research*, *52*(11), 8590-8612. https://doi.org/10.1002/2015WR018227

Auckland Council. (2025). *Ecosystem Potential Extent*. https://data-aucklandcouncil.opendata.arcgis.com/datasets/815e40f26936442c92d7c617f22f3484_0/explore

Barton, I. (2008). *Continuous Cover Forestry - A Handbook for the Management of New Zealand Forests* [Report]. Tāne's Tree Trust. https://www.tanestrees.org.nz/site/assets/files/1069/continous_cover_forestry_-_web.pdf

Barton, I. (2025). *Species Profiles – Kanuka.* Tāne's Tree Trust. https://www.tanestrees.org.nz/species-profiles/kanuka/

Basher, L. R. (2013). *Erosion processes and their control in New Zealand*. In J. R. Dymond (Ed.), *Ecosystem services in New Zealand: Conditions and trends* (pp. 363–374). Manaaki Whenua Press. https://www.landcareresearch.co.nz/assets/Publications/Ecosystem-services-in-New-Zealand/2_7_Basher.pdf

Baylis, G. T. S., McNabb, R. F. R., & Morrison, T. M. (1963). The mycorrhizal nodules of podocarps. *Transactions of the British Mycological Society*, *46*(3), 378–384. https://doi.org/10.1016/S0007-1536(63)80031-5

Benavides, R., Douglas, G. B., & Osoro, K. (2009). Silvopastoralism in New Zealand: Review of effects of evergreen and deciduous trees on pasture dynamics. *Agroforestry Systems*, *76*(2), 327–350. https://doi.org/10.1007/s10457-008-9186-6

Bergin, D. O. (2000). Current knowledge relevant to management of *Podocarpus tōtara* for timber. *New Zealand Journal of Botany*, *38*(3), 343–359. https://doi.org/10.1080/0028825X.2000.9512687

Bergin, D. O., & Kimberley, M. O. (2014). Factors influencing natural regeneration of totara (Podocarpus totara D.Don) on grazed hill country grassland in Northland, New Zealand. *New Zealand Journal of Forestry Science*, *44*(1), 13. https://doi.org/10.1186/s40490-014-0013-8

Bergin, D. O., Kimberley, M. O., & Low, C. B. (2008). Provenance variation in Podocarpus totara (D. Don): Growth, tree form and wood density on a coastal site in the north of

the natural range, New Zealand. *Forest Ecology and Management*, *255*(5–6), 1367–1378. https://doi.org/10.1016/j.foreco.2007.10.053

Bimbo, F., Nico, K., & de Meo, E. (2025). Assessing the Quality and Floral Variety Market Value: A Hedonic Price Model for Honey. *Sustainability (Switzerland)*, *17*(9), 3903. https://doi.org/10.3390/su17093903

Brown, V. A. (2021). An Introduction to Linear Mixed-Effects Modeling in R. *Advances in Methods and Practices in Psychological Science, 4*(1), 1–19. https://doi.org/10.1177/2515245920960351

Burnham, K. P., & Anderson, D. R. (2004). Multimodel Inference: Understanding AIC and BIC in model selection. *Sociological Methods & Research*, *33*(2), 261–304. https://doi.org/10.1177/0049124104268644

Chappell, P. R. (2013). *The climate and weather of Auckland* (NIWA Science and Technology Series No. 60, pp. 1–40). National Institute of Water and Atmospheric Research. https://webstatic.niwa.co.nz/static/web/Auckland_Climate_NIWA.pdf

Cofie, P., & Koolen, A. J. (2001). Test speed and other factors affecting the measurements of tree root properties used in soil reinforcement models. *Soil and Tillage Research*, *63*, 51–56. https://doi.org/10.1016/S0167-1987(01)00225-2

Cohen, D., & Schwarz, M. (2017). Tree-root control of shallow landslides. *Earth Surface Dynamics*, *5*(3), 451–477. https://doi.org/10.5194/esurf-5-451-2017

Crozier, M. J. (2005). Multiple-occurrence regional landslide events in New Zealand: Hazard management issues. *Landslides*, *2*(4), 247–256. https://doi.org/10.1007/s10346-005-0019-7

Crozier, M. J. (2010). Deciphering the effect of climate change on landslide activity: A review. *Geomorphology, 124*(3–4), 260–267. https://doi.org/10.1016/j.geomorph.2010.04.009

Crozier, M. J. (2017). A proposed cell model for multiple-occurrence regional landslide events: Implications for landslide susceptibility mapping. *Geomorphology*, *295*, 480–488. https://doi.org/10.1016/j.geomorph.2017.07.032

Cruden, D. M. (1991). A simple definition of a landslide. *Bulletin of the International Association of Engineering Geology - Bulletin de l'Association Internationale de Géologie de l'Ingénieur*, *43*(1), 27–29. https://doi.org/10.1007/BF02590167

Davis, M., Dickie, I. A., Paul, T., & Carswell, F. (2013). Is kanuka and manuka establishment in grassland constrained by mycorrhizal abundance? *New Zealand Journal of Ecology*, *13*(2), 172-177. http://www.jstor.org/stable/24060778

Dawson, J & Lucas, R. (2012). *Field guide to New Zealand's native trees*. Craig Potton.

Dodd, M., Mcdowell, R., & Quinn, J. (2016). A review of contaminant losses to water from pastoral hill lands and mitigation options. *NZGA: Research and Practice Series*, *16*, 137–147. https://doi.org/10.33584/rps.16.2016.3269

Donaldson, L. A. (1983). Anatomy of root wood in Araucariaceae and some Podocarpaceae indigenous to New Zealand. *New Zealand Journal of Botany, 21*(3), 221–227. https://doi.org/10.1080/0028825X.1983.10428553

Douglas, G. B., McIvor, I. R., Potter, J. F., & Foote, L. G. (2010). Root distribution of poplar at varying densities on pastoral hill country. *Plant and Soil*, *333*(1), 147–161. https://doi.org/10.1007/s11104-010-0331-4

Dymond, J. R., Betts, H. D., & Schierlitz, C. S. (2010). An erosion model for evaluating regional land-use scenarios. *Environmental Modelling & Software, 25*(3), 289–298. https://doi.org/10.1016/j.envsoft.2009.09.011

Dymond, J., & Shepherd, J. (2023). *Update to Highly Erodible Land and Estimated Long-term Soil Erosion data sets for Environmental Reporting* (Contract Report: LC4365). Manaaki Whenua – Landcare Research. https://environment.govt.nz/publications/update-to-highly-erodible-land-and-estimated-long-term-soil-erosion-data-sets-for-environmental-reporting

Ekanayaka, J., Marden, M., Watson, A. J., & Rowan, D. (1997). Tree roots and slope stability: A comparison between *Pinus radiata* and *kānuka*. *New Zealand Journal of Forestry Science, 27*(2), 216–233. https://www.scionresearch.com/data/assets/pdffile/0009/59508/NZJFS2721997EKANAYAKE216-233.pdf

Franich, R. A., & Cambie, R. C. (1999). Essential Oil Constituents of *Podocarpus totara* Leaves. *Journal of Essential Oil Research*, *11*(4), 507–510. https://doi.org/10.1080/10412905.1999.9701197

Giadrossich, F., Cohen, D., Schwarz, M., Ganga, A., Marrosu, R., Pirastru, M., & Capra, G. F. (2019). Large roots dominate the contribution of trees to slope stability. *Earth Surface Processes and Landforms*, *44*(8), 1602–1609. https://doi.org/10.1002/esp.4597

Giadrossich, F., Cohen, D., Schwarz, M., Seddaiu, G., Contran, N., Lubino, M., ... & Niedda, M. (2016). Modeling bio-engineering traits of Jatropha curcas L. *Ecological Engineering*, *89*, 40–48. https://doi.org/10.1016/j.ecoleng.2016.01.005

Giadrossich, F., Schwarz, M., Cohen, D., Cislaghi, A., Vergani, C., Hubble, T., ... & Stokes, A. (2017). Methods to measure the mechanical behaviour of tree roots: A

review. *Ecological engineering*, *109*, 256-271. https://doi.org/10.1016/j.ecoleng.2017.08.032

Giadrossich, F., Schwarz, M., Marden, M., Marrosu, R., & Phillips, C. (2020). Minimum representative root distribution sampling for calculating slope stability in pinus radiata d.Don plantations in New Zealand. *New Zealand Journal of Forestry Science*, *50*, 5. https://doi.org/10.33494/nzjfs502020x68x

Glade, T. (2003). Landslide occurrence as a response to land use change: a review of evidence from New Zealand. *Catena*, *51*(3-4), 297-314. https://doi.org/10.1016/S0341-8162(02)00170-4

Guevara-Escobar, A., Edwards, W. R. N., Morton, R. H., Kemp, P. D., & Mackay, A. D. (2000). Tree water use and rainfall partitioning in a mature poplar–pasture system. *Tree Physiology, 20*, 97–106. https://doi.org/10.1093/treephys/20.2.97

Guevara-Escobar, A., Kemp, P. D., Mackay, A. D., & Hodgson, J. (2007). Pasture production and composition under poplar in a hill environment in New Zealand. *Agroforestry Systems, 69*(3), 199–213. https://doi.org/10.1007/s10457-007-9038-9

Haque, U., da Silva, P. F., Devoli, G., Pilz, J., Zhao, B., Khaloua, A., Wilopo, W., Andersen, P., Lu, P., Lee, J., Yamamoto, T., Keellings, D., Jian-Hong, W., & Glass, G. E. (2019). The human cost of global warming: Deadly landslides and their triggers (1995–2014). *Science of the Total Environment*, *682*, 673–684. https://doi.org/10.1016/j.scitotenv.2019.03.415

Hedley, C. B., Lambie, S. M., & Dando, J. L. (2013). Edaphic and environmental controls of soil respiration and related soil processes under two contrasting manuka and kānuka shrubland stands in North Island, New Zealand. *Soil Research*, *51*(5), 390–405. https://doi.org/10.1071/SR12248

Heenan, P. B., McGlone, M. S., Mitchell, C. M., Cheeseman, D. F., & Houliston, G. J. (2022). Genetic variation reveals broad-scale biogeographic patterns and challenges species' classification in the *Kunzea ericoides* (kānuka; Myrtaceae) complex from New Zealand. *New Zealand Journal of Botany*, *60*(1), 2–26. https://doi.org/10.1080/0028825X.2021.1903946

Hewitt, A. E. (2010). *New Zealand soil classification* (3rd ed.). Manaaki Whenua Press. https://github.com/lauren-obrien/nzsc_v3

Kemp, P. D., Hawke, M. F., & Knowles, R. L. (2018). Temperate agroforestry systems in New Zealand. In A. M. Gordon, S. M. Newman, & B. R. W. Coleman (Eds.), *Temperate agroforestry systems* (2nd ed., pp. 224–236). CAB International. https://doi.org/10.1079/9781780644851.0224

Kimberley, M. Graeme, M., & Bergin, D. (2025). *Carbon and biodiversity in the understory vegetation of New Zealand's exotic tree plantations.* Tāne's Tree Trust. https://www.tanestrees.org.nz/site/assets/files/2425/carbon_and_biodiversity_in_the_understory_vegetation_of_new_zealands_exotic_tree_plantations.pdf

Kimberley, M., Bergin, D., & Silvester, W. (2021). *Carbon sequestration by native forest - Setting the record straight*. Tāne's Tree Trust. https://www.tanestrees.org.nz/site/assets/files/1069/carbon_sequestration_by_native_forest_-_web.pdf

Knowles, R. L. (1991). New Zealand experience with silvopastoral systems: A review. *Forest Ecology and Management*, *45*(1), 251–267. https://doi.org/https://doi.org/10.1016/0378-1127(91)90221-G

Lambie, S. M., Awatere, S., Daigneault, A., Kirschbaum, M. U. F., Marden, M., Soliman, T., Spiekermann, R. I., & Walsh, P. J. (2021). Trade-offs between environmental and economic factors in conversion from exotic pine production to natural regeneration on erosion prone land. *New Zealand journal of forestry science*, *51*, 14. https://doi.org/10.33494/nzjfs512021x163x

Mackay-Smith, T. H., Burkitt, L., Reid, J., López, I. F., & Phillips, C. (2021). A Framework for Reviewing Silvopastoralism: A New Zealand Hill Country Case Study. *Land*, *10*(12), 1386. https://doi.org/10.3390/land10121386

Mackay-Smith, T. H., López, I. F., Burkitt, L. L., & Reid, J. I. (2022). Kānuka Trees Facilitate Pasture Production Increases in New Zealand Hill Country. *Agronomy*, *12*(7), 1701. https://doi.org/10.3390/agronomy12071701

Mackay-Smith, T. H., Spiekermann, R. I., Richards, D. R., Harcourt, N., & Burkitt, L. L. (2024). An integrative approach to silvopastoral system design: perspectives, potentials and principles. *New Zealand Journal of Agricultural Research*, *68*(2), 218–258. https://doi.org/10.1080/00288233.2023.2298922

Manaaki Whenua - Landcare Research. (2024). *Estimated long-term soil erosion: Data to 2022.* https://www.stats.govt.nz/indicators/estimated-long-term-soil-erosion-data-to-2022/

Manaaki Whenua - Landcare Research. (2025a). *Land Resource Information Systems Portal* https://lris.scinfo.org.nz/

Manaaki Whenua - Landcare Research. (2025b). *S-map – New Zealand's national digital soil map.* https://datastore.landcareresearch.co.nz/dataset/s-map

Mao, Z. (2022). Root reinforcement models: classification, criticism and perspectives. *Plant and Soil*, *472*(1), 17–28. https://doi.org/10.1007/s11104-021-05231-1

Mao, Z., Bourrier, F., Stokes, A., & Fourcaud, T. (2014). Three-dimensional modelling of slope stability in heterogeneous montane forest ecosystems. *Ecological Modelling*, *273*, 11–22. https://doi.org/10.1016/j.ecolmodel.2013.10.017

Mao, Z., Saint-André, L., Genet, M., Mine, F. X., Jourdan, C., Rey, H., Courbaud, B., & Stokes, A. (2012). Engineering ecological protection against landslides in diverse mountain forests: Choosing cohesion models. *Ecological Engineering*, *45*, 55–69. https://doi.org/10.1016/j.ecoleng.2011.03.026

Marden, M., Lambie, S., & Phillips, C. (2018a). Biomass and root attributes of eight of New Zealand's most common indigenous evergreen conifer and broadleaved forest species during the first 5 years of establishment. *New Zealand Journal of Forestry Science*, *48*(1), 9. https://doi.org/10.1186/s40490-018-0113-y

Marden, M., Lambie, S., & Phillips, C. (2020). Potential effectiveness of low-density plantings of mānuka (Leptospermum scoparium) as an erosion mitigation strategy in steeplands, northern Hawke's bay, New Zealand. *New Zealand Journal of Forestry Science*, *50*, 10. https://doi.org/10.33494/nzjfs502020x82x

Marden, M., Lambie, S., & Rowan, D. (2018b). Root system attributes of 12 juvenile indigenous early colonising shrub and tree species with potential for mitigating erosion in New Zealand. *New Zealand Journal of Forestry Science*, *48*(1), 11. https://doi.org/10.1186/s40490-018-0115-9

Marden, M., Mason, N. W. H., Lambie, S., & Rowan, D. (2025). Total plant biomass, carbon stock, and species-and age-specific allometry for 12 of New Zealand's early-colonising indigenous shrub and tree species to 5 years of age. *New Zealand Journal of Forestry Science*, *55,* 1–27. https://doi.org/10.33494/nzjfs552025x387x

Marden, M., Rowan, D., & Phillips, C. (2005). Stabilising characteristics of New Zealand indigenous riparian colonising plants. *Plant and Soil*, *278*(1–2), 95–105. https://doi.org/10.1007/s11104-004-7598-2

Masi, E. B., Segoni, S., & Tofani, V. (2021). Root reinforcement in slope stability models: a review. *Geosciences*, *11*(5), 212. https://doi.org/10.3390/geosciences11050212

McGregor, E., Mackay, A., Dodd, M., & Kemp, P. (1999). Silvopastoralism using tended poplars on New Zealand hill country: The opportunities. *Proceedings of the New Zealand Grassland Association, 61*, 85–89. https://doi.org/10.33584/jnzg.1999.61.2360

McIvor, I. (2023). *Poplar cultivation: a comparison of international and national activity*. Forest Growers Levy Trust. https://www.poplarandwillow.org.nz/documents/report-1-for-FGLT.pdf

McIvor, I. R., & Douglas, G. B. (2012). *Poplars and Willows in Hill Country-Stabilising Soils and Storing Carbon*. https://www.massey.ac.nz/~flrc/workshops/12/Manuscripts/McIvor_2012.pdf

McIvor, I. R., Douglas, G. B., & Benavides, R. (2009). Coarse root growth of Veronese poplar trees varies with position on an erodible slope in New Zealand. *Agroforestry Systems*, *76*(1), 251–264. https://doi.org/10.1007/s10457-009-9209-y

McIvor, I. R., Douglas, G. B., Hurst, S. E., Hussain, Z., & Foote, A. G. (2008). Structural root growth of young Veronese poplars on erodible slopes in the southern North Island, New Zealand. *Agroforestry Systems*, *72*(1), 75–86. https://doi.org/10.1007/s10457-007-9090-5

McIvor, I., Mackay-Smith, T., & Spiekermann, R. (2024). *Drivers and new opportunities for woody vegetation use in erosion management in pastoral hill country in New Zealand*. In S. Mahmood (Ed.), Soil erosion - Risk modeling and management. IntechOpen. https://doi.org/10.5772/intechopen.112241

Milledge, D. G., Bellugi, D., McKean, J. A., Densmore, A. L., & Dietrich, W. E. (2014). A multidimensional stability model for predicting shallow landslide size and shape across landscapes. *Journal of Geophysical Research: Earth Surface*, *119*(11), 2481–2504. https://doi.org/10.1002/2014JF003135

Murgia, I., Giadrossich, F., Mao, Z., Cohen, D., Capra, G. F., & Schwarz, M. (2022). Modeling shallow landslides and root reinforcement: A review. *Ecological Engineering*, *181,* 106671. https://doi.org/10.1016/j.ecoleng.2022.106671

Ngo, H. M., van Zadelhoff, F. B., Gasparini, I., Plaschy, J., Flepp, G., Dorren, L., Phillips, C., Giadrossich, F., & Schwarz, M. (2023). Analysis of Poplar's (Populus nigra ita.) Root Systems for Quantifying Bio-Engineering Measures in New Zealand Pastoral Hill Country. *Forests*, *14*(6), 1240. https://doi.org/10.3390/f14061240

Pacheco Quevedo, R., Velastegui-Montoya, A., Montalván-Burbano, N., Morante-Carballo, F., Korup, O., & Daleles Rennó, C. (2023). Land use and land cover as a conditioning factor in landslide susceptibility: a literature review. *Landslides, 20*(5), 967-982. https://doi.org/10.1007/s10346-022-02020-4

Page, M., Trustrum, N., & Gomez, B. (2000). Implications of a century of anthropogenic erosion for future land use in the Gisborne-East Coast Region of New Zealand. *New Zealand Geographer, 56*(2), 13–24. https://doi.org/10.1111/j.1745-7939.2000.tb01571.x

Phillips, C. J., Marden, M., & Suzanne, L. M. (2014). Observations of root growth of young poplar and willow planting types. *New Zealand Journal of Forestry Science*, *44*(1), 15. https://doi.org/10.1186/s40490-014-0015-6

Phillips, C., Bloomberg, M., Marden, M., & Lambie, S. (2023). Tree root research in New Zealand: a retrospective 'review' with emphasis on soil reinforcement for soil conservation and wind firmness. *New Zealand Journal of Forestry Science*, *53*, 6. https://doi.org/10.33494/nzjfs532023x177x

Phillips, C., Hales, T., Smith, H., & Basher, L. (2021). Shallow landslides and vegetation at the catchment scale: A perspective. *Ecological Engineering*, *173*, 106436. https://doi.org/10.1016/j.ecoleng.2021.106436

Quinlan, P. (2022). *A Practical Guide to Managing Tōtara on Private Land*. Tāne's Tree Trust. https://www.tanestrees.org.nz/site/assets/files/1069/complete_totara_manual_final_92dpi.pdf

Salekin, S., Roschak, C., & Steward, G. (2025). Development of a height-diameter model for New Zealand grown tōtara (Podocarpus totara G. Benn. ex D. Don). *New Zealand Journal of Forestry Science*, *55*, 11. https://doi.org/10.33494/nzjfs552025x426x

Satchell, D. (2018). *Report: Trees for steep slopes – Poplar.* Farm Forestry New Zealand. https://www.nzffa.org.nz/farm-forestry-model/why-farm-forestry/trees-for-erosion-controlsoil-conservation/report-trees-for-steep-slopes/tree-species/poplar/

Schwarz, M., Cohen, D., & Or, D. (2010a). Root-soil mechanical interactions during pullout and failure of root bundles. *Journal of Geophysical Research: Earth Surface*, *115*, F04035. https://doi.org/10.1029/2009JF001603

Schwarz, M., Cohen, D., & Or, D. (2011). Pullout tests of root analogs and natural root bundles in soil: Experiments and modeling. *Journal of Geophysical Research: Earth Surface*, *116*, F02007. https://doi.org/10.1029/2010JF001753

Schwarz, M., Cohen, D., & Or, D. (2012). Spatial characterization of root reinforcement at stand scale: Theory and case study. *Geomorphology*, *171–172*, 190–200. https://doi.org/10.1016/j.geomorph.2012.05.020

Schwarz, M., Giadrossich, F., & Cohen, D. (2013). Modeling root reinforcement using a root-failure Weibull survival function. *Hydrology and Earth System Sciences*, *17*(11), 4367–4377. https://doi.org/10.5194/hess-17-4367-2013

Schwarz, M., Lehmann, P., & Or, D. (2010b). Quantifying lateral root reinforcement in steep slopes - from a bundle of roots to tree stands. *Earth Surface Processes and Landforms*, *35*(3), 354–367. https://doi.org/10.1002/esp.1927

Schwarz, M., Phillips, C., Marden, M., McIvor, I. R., Douglas, G. B., & Watson, A. (2016). Modelling of root reinforcement and erosion control by 'Veronese' poplar on pastoral hill country in New Zealand. *New Zealand Journal of Forestry Science*, *46*(1), 1–17. https://doi.org/10.1186/s40490-016-0060-4

Schwarz, M., Preti, F., Giadrossich, F., Lehmann, P., & Or, D. (2010c). Quantifying the role of vegetation in slope stability: A case study in Tuscany (Italy). *Ecological Engineering*, *36*(3), 285–291. https://doi.org/10.1016/j.ecoleng.2009.06.014

Schwarz, M., Rist, A., Cohen, D., Giadrossich, F., Egorov, P., Büttner, D., Stolz, M., & Thormann, J. J. (2015). Root reinforcement of soils under compression. *Journal of Geophysical Research: Earth Surface*, *120*(10), 2103–2120. https://doi.org/10.1002/2015JF003632

Sidle, R. C., & Ziegler, A. D. (2017). The canopy interception-landslide initiation conundrum: Insight from a tropical secondary forest in northern Thailand. *Hydrology and Earth System Sciences*, *21*(1), 651–667. https://doi.org/10.5194/hess-21-651-2017

Spiekermann, R. I., McColl, S., Fuller, I., Dymond, J., Burkitt, L., & Smith, H. G. (2021). Quantifying the influence of individual trees on slope stability at landscape scale. *Journal of Environmental Management*, *286*, 112194. https://doi.org/10.1016/j.jenvman.2021.112194

Spiekermann, R. I., Smith, H. G., McColl, S., Burkitt, L., & Fuller, I. C. (2022a). Development of a morphometric connectivity model to mitigate sediment derived from storm-driven shallow landslides. *Ecological Engineering*, *180*, 106676. https://doi.org/10.1016/j.ecoleng.2022.106676

Spiekermann, R. I., Smith, H. G., McColl, S., Burkitt, L., & Fuller, I. C. (2022b). Quantifying effectiveness of trees for landslide erosion control. *Geomorphology*, *396*, 107993. https://doi.org/10.1016/j.geomorph.2021.107993

Spiekermann, R. I., van Zadelhoff, F., Schindler, J., Smith, H., Phillips, C., & Schwarz, M. (2023). Comparing physical and statistical landslide susceptibility models at the scale of individual trees. *Geomorphology*, *440*, 108870. https://doi.org/10.1016/j.geomorph.2023.108870

Stats NZ. (2025). *Geographic Boundary Viewer.* New Zealand Government. https://statsnz.maps.arcgis.com/apps/instant/sidebar/index.html?appid=3a406ce8fbb14367ab5caae21c07ab8b

Stokes, A., & Yildiz, A. (2023). The reinforcement of soil by plant roots. *Encyclopedia of soils in the environment, 5,* 115–122. https://doi.org/10.1016/B978-0-12-822974-3.00226-3

Sulaiman, Z. (2006). *Establishment and Silvopastoral Aspects of Willow and Poplar* [Doctoral dissertation, Massey University]. https://www.researchgate.net/publication/35146754_Establishment_and_silvopastoral_aspects_of_willow_and_poplar_a_thesis_presented_in_partial_fulfilment_of_the_requirements_for_the_degree_of_Doctor_of_Philosophy_Ph_D_in_Plant_Science_Institute_of_Natu

van Zadelhoff, F.B., Albaba, A., Cohen, D., Phillips, C., Schaefli, B., Dorren, L., Schwarz, M., 2022. Introducing SlideforMAP: a probabilistic finite slope approach for modelling shallow-landslide probability in forested situations. *Natural Hazards and Earth System Sciences 22*, 2611–2635. https://doi.org/10.5194/nhess-22-2611-2022

Vergani, C., & Graf, F. (2016). Soil permeability, aggregate stability and root growth: a pot experiment from a soil bioengineering perspective. *Ecohydrology*, *9*(5), 830–842. https://doi.org/10.1002/eco.1686

Vergani, C., Giadrossich, F., Buckley, P., Conedera, M., Pividori, M., Salbitano, F., Rauch, H. S., Lovreglio, R., & Schwarz, M. (2017). Root reinforcement dynamics of European coppice woodlands and their effect on shallow landslides: A review. *Earth-Science Reviews, 167*, 88–102. https://doi.org/10.1016/j.earscirev.2017.02.002

Vergani, C., Schwarz, M., Soldati, M., Corda, A., Giadrossich, F., Chiaradia, E. A., Morando, P., & Bassanelli, C. (2016). Root reinforcement dynamics in subalpine spruce forests following timber harvest: A case study in Canton Schwyz, Switzerland. *Catena*, *143*, 275–288. https://doi.org/10.1016/j.catena.2016.03.038

Walther, F. (2025). *Root Distribution of Kānuka (Kunzea ericoides) and Tōtara (Podocarpus tōtara) in Pastural Hill Landscape in New Zealand* [Master's thesis, Bern University of Applied Sciences].

Watson, A. J., & Marden, M. (2004). Live root-wood tensile strengths of some common New Zealand indigenous and plantation tree species. *New Zealand Journal of Forestry Science*, 34(3), 344–353. https://www.scionresearch.com/__data/assets/pdf_file/0020/59141/08_Watson_-and-_Marden.pdf

Watson, A., Phillips, C., & Marden, M. (1999). Root strength, growth, and rates of decay: Root reinforcement changes of two tree species and their contribution to slope stability. *Plant and Soil, 217*, 39–47. https://doi.org/10.1023/A:1004682509514

Wieczorek, G. F., & Glade, T. (2005). Climatic factors influencing occurrence of debris flows. In M. Jakob & O. Hungr (Eds.), *Debris-flow hazards and related phenomena* (pp. 325–362). Springer. https://doi.org/10.1007/3-540-27129-5_14

Wilkinson, A. G. (1999). Poplars and willows for soil erosion control in New Zealand. *Biomass and Bioenergy*, *16*, 263–274. https://doi.org/10.1016/S0961-9534(99)0007-0

Wu, T. H., McKinnell, W. P., III, & Swanston, D. N. (1979). Strength of tree roots and landslides on Prince of Wales Island, Alaska. *Canadian Geotechnical Journal, 16*(1), 19–33. https://doi.org/10.1139/t79-003

Yang, Y., Chen, L., Li, N., & Zhang, Q. (2016). Effect of root moisture content and diameter on root tensile properties. *PLoS ONE*, *11*(3), 0151791. https://doi.org/10.1371/journal.pone.0151791

Zhang, C., Zhou, X., Jiang, J., Wei, Y., Ma, J., & Hallett, P. D. (2019). Root moisture content influence on root tensile tests of herbaceous plants. *Catena*, *172*, 140–147. https://doi.org/10.1016/j.catena.2018.08.012

Appendix A
R Script Root Distribution Analysis

```
---
title: "RD_Analysis"
author: "Anne Fokker"
date: "2025-12-04"
output:  html_document: default
---
# ==== Setting Up ====
setwd("D:/Data Thesis/Distribution")
packages <- c(
  "tidyverse", "dplyr", "ggplot2", "lme4", "lmerTest", "car", "MuMIn")

for (pkg in packages) {
  if (!require(pkg, character.only = TRUE)) {
    install.packages(pkg, dependencies = TRUE)
  } library(pkg, character.only = TRUE)}

df <- read_csv("D:/Data Thesis/Distribution Data/Distribution_v_3010.csv")

# ==== Computing RAR ====
# 1. Set diameter cols
start_index <- which(names(df) == "1.5")
end_index <- which(names(df) == "249.5")
diameter_cols <- names(df)[start_index:end_index]

# 2. Extract numeric diameters from column names
diameters_mm <- as.numeric(diameter_cols)
diameters_cm <- diameters_mm / 10  # convert mm → cm

all_na_cols <- names(df)[apply(is.na(df), 2, any)]
print(all_na_cols)

# 3. Set root counts
root_counts <- df[, diameter_cols]

# 4. Calculate area per root diameter class (cm²)
areas_cm2 <- pi * (diameters_cm / 2)^2
areas_cm2 <- as.numeric(areas_cm2)

# 5. Multiply counts × area
area_matrix <- as.matrix(root_counts) %*% diag(areas_cm2)

# 6. Sum across root diameter classes → total root area per soil depth row (in m²)
df$Root_Area_m2 <- rowSums(area_matrix) / 10000  # cm² → m²

# 7. Segment area
df$r_tree <- (df$DBH_m / pi) * 1/2
df$r_wall <- (df$r_tree + df$Distance_m)
df$soil_area_row <- ifelse(
  df$Top_Depth_cm == 90 & df$Bottom_Depth_cm == 100,
  (df$r_wall * pi) * 1/8 * 0.10,
  (df$r_wall * pi) * 1/8 * 0.15)

# 8. Root Area Ratio (RAR, %) per soil section
```

```
df$RAR_row <- (df$Root_Area_m2 / df$soil_area_row) * 100

# 9. Summarize segment root area and segment soil area (per tree-sector-distance)
summary_totals <- df %>%
  group_by(Tree_Nr, Sector, Distance_m) %>%
  summarise(
    SegmentRootArea = sum(Root_Area_m2, na.rm = TRUE),
    SegmentSoilArea = sum(soil_area_row, na.rm = TRUE),
    .groups = "drop")  %>%
    mutate(RAR_segment = (SegmentRootArea / SegmentSoilArea) * 100)

# 10. Compute total root area of each tree nr
tree_totals <- summary_totals %>%
  group_by(Tree_Nr)  %>% summarise(TreeTotalRootArea = sum(SegmentRootArea, na.rm = TRUE), .groups =
"drop")

df <- df %>%
  left_join(summary_totals, by = c("Tree_Nr", "Sector", "Distance_m"))

# 12. Log transform RAR
df$log_RAR_row <- log(df$RAR_row + 0.01)

# 13. Log tranform counts
small_roots <- diameter_cols[diameters_mm < 6.5]
big_roots   <- diameter_cols[diameters_mm >= 6.5]

df <- df %>%
  mutate( all_counts = rowSums(across(all_of(diameter_cols)), na.rm = TRUE),
        small_roots = rowSums(across(all_of(small_roots)), na.rm = TRUE),
        big_roots = rowSums(across(all_of(big_roots)), na.rm = TRUE))

df$log_counts <- log(df$all_counts + 0.01)
df$log_counts_big <- log(df$big_roots + 0.01)
df$log_counts_small <- log(df$small_roots + 0.01)

# ==== Basic Tests ====

# Summarize per tree
tree_summary <- df %>%
  group_by(Soil_Type, Tree_Nr, Species) %>%
  summarise(
    DBH_m = first(DBH_m),
    TotalRootNumber = sum(rowSums(across(all_of(diameter_cols))), na.rm = TRUE),
    SmallRoots = sum(rowSums(across(all_of(small_roots)))),
    TotalRootArea_m2 = sum(Root_Area_m2, na.rm = TRUE),
    RAR_tree = sum(Root_Area_m2, na.rm = TRUE) / sum(soil_area_row, na.rm = TRUE) * 100, .groups = "drop"
  ) %>% arrange(Soil_Type, Tree_Nr)

# Total root count ~ species
aov_species_c <- aov(TotalRootNumber ~ Species, data = tree_summary)
summary(aov_species_c)

# Total root count ~ DBH
qqPlot(tree_summary$TotalRootNumber)
hist(tree_summary$TotalRootNumber, breaks = 20)
cor.test(tree_summary$DBH_m, tree_summary$RAR_tree, method = "spearman")
```

```
# ==== Linear Mixed Effect Models ====

# Check data for normality
qqPlot(df$log_counts) # COUNTS
qqPlot(df$log_RAR_row) # RAR

# Reference species rotation
df$Species <- relevel(factor(df$Species), ref = "Kānuka")

# ---- Vertical arrangement (depth) ----

# Model selection (repeat for counts)
mod1 <- lmer(log_RAR_row ~ Top_Depth_cm + (1 | Tree_Nr), data = df, REML = FALSE)
mod2 <- lmer(log_RAR_row ~ Top_Depth_cm + Soil_Type + (1 | Tree_Nr), data = df, REML = FALSE)
mod3 <- lmer(log_RAR_row ~ Top_Depth_cm + Soil_Type + Species + (1 | Tree_Nr), data = df, REML = FALSE)
mod4 <- lmer(log_RAR_row ~ Top_Depth_cm * Soil_Type + (1 | Tree_Nr), data = df, REML = FALSE)
mod5 <- lmer(log_RAR_row ~ Top_Depth_cm * Soil_Type * Species + (1 | Tree_Nr), data = df, REML = FALSE)
anova(mod1, mod2, mod3, mod4, mod5)

# Evaluation of selected model (repeat for counts)
mod_vert_RAR <- lmer(log_RAR_row ~ Top_Depth_cm * Species * Soil_Type + (1 | Tree_Nr), data = df)
hist((residuals(mod_vert_RAR)), breaks = 100)
shapiro.test(residuals(mod_vert_RAR))
anova(mod_vert_RAR)
summary(mod_vert_RAR)
r.squaredGLMM(mod_vert_RAR)

# ==== Lateral arrangement (distance) ====

# Model selection (repeat for counts)
mod1 <- lmer(log_RAR_row ~ Distance_m + (1 | Tree_Nr), data = df, REML = FALSE)
mod2 <- lmer(log_RAR_row ~ Distance_m + Soil_Type + (1 | Tree_Nr), data = df, REML = FALSE)
mod3 <- lmer(log_RAR_row ~ Distance_m + Soil_Type + Species + (1 | Tree_Nr), data = df, REML = FALSE)
mod4 <- lmer(log_RAR_row ~ Distance_m * Soil_Type + (1 | Tree_Nr), data = df, REML = FALSE)
mod5 <- lmer(log_RAR_row ~ Distance_m * Soil_Type * Species + (1 | Tree_Nr), data = df, REML = FALSE)
anova(mod1, mod2, mod3, mod4, mod5)

# Evaluation of selected model (repeat for counts)
mod_dis_RAR <- lmer(log_RAR_row ~ Distance_m * Species * Soil_Type + (1 | Tree_Nr), data = df)
hist(log(residuals(mod_dis_RAR)), breaks = 100)
shapiro.test(residuals(mod_dis_RAR))
summary(mod_dis_RAR)
anova(mod_dis_RAR)
r.squaredGLMM(mod_dis_RAR)

# ==== Lateral arrangement (sector) =====

# Model selection (repeat for counts)
mod1 <- lmer(log_RAR_row ~ Sector + (1 | Tree_Nr), data = df, REML = FALSE)
mod2 <- lmer(log_RAR_row ~ Sector + Soil_Type + (1 | Tree_Nr), data = df, REML = FALSE)
mod3 <- lmer(log_RAR_row ~ Sector + Soil_Type + Species + (1 | Tree_Nr), data = df, REML = FALSE)
mod4 <- lmer(log_RAR_row ~ Sector * Soil_Type + (1 | Tree_Nr), data = df, REML = FALSE)
mod5 <- lmer(log_RAR_row ~ Sector * Soil_Type * Species + (1 | Tree_Nr), data = df, REML = FALSE)
anova(mod1, mod2, mod3, mod4, mod5)

# Evaluation of selected model (repeat for counts)
mod_sec_RAR <- lmer(log_RAR_row ~ Sector * Species * Soil_Type + (1 | Tree_Nr), data = df)
```

```
hist(residuals(mod_sec_RAR), breaks = 100)
shapiro.test(residuals(mod_sec_count))
summary(mod_sec_RAR)
anova(mod_sec_RAR)
r.squaredGLMM(mod_sec_RAR)

# ---- Extra test up- versus downslope sectors (repeat for counts) ----

# Create new column
df <- df %>%
  mutate(Slope_Position = case_when(
    Sector %in% c(1, 2, 7, 8) ~ "upslope",
    Sector %in% c(3, 4, 5, 6) ~ "downslope",
    TRUE ~ NA_character_))

# Filter outer radii
RAR_sector <- df %>%
  filter(!(Distance_m %in% c(3.5, 4.5))) %>%
  group_by(Tree_Nr, Sector, Soil_Type, Species) %>%
  mutate(RAR_sector_1525 = sum(Root_Area_m2, na.rm = TRUE) / sum(soil_area_row, na.rm = TRUE) * 100,
.groups = "drop")

# Compute RAR inner radii
radial_RAR_data <- RAR_sector %>%
  group_by(Tree_Nr, Species, Soil_Type, Sector) %>%
  summarise(
    mean_root_RAR = mean(RAR_sector_1525, na.rm = TRUE), .groups = "drop")

RAR_sector$log_RAR_sector = log(RAR_sector$RAR_sector_1525 + 0.01)

# Subset for species and soil type (rotate for each; here Tōtara x UYM)
sector_sub_tot <- subset(RAR_sector, Species == "Tōtara" & Soil_Type == "Mottled Yellow Ultic Soil")
qqPlot(sector_sub_tot$RAR_sector_1525)
hist(RAR_sector$log_RAR_sector)
shapiro.test(sector_sub_tot$log_RAR_sector)

# t-test RAR across slope position
t.test(log_RAR_sector ~ Slope_Position, data = sector_sub_tot)
tot_test <- aov(log_RAR_sector ~ Sector, data = sector_sub_tot)
summary(tot_test)
```

Appendix B
R Script Mechanical Properties Analysis

```
---
title: "TS_Analysis"
author: "Anne Fokker"
date: "2025-12-04"
output: html_document
---
# ==== Setting up ====
setwd("D:/Data Thesis/Thesis")
packages <- c(
  "tidyverse","lme4",  "lmerTest",  "performance",  "ggeffects",  "car",  "corrplot",  "patchwork",  "minpack.lm",
"stats", "pracma")

for (pkg in packages) {
  if (!require(pkg, character.only = TRUE)) {
    install.packages(pkg, dependencies = TRUE)
  }
  library(pkg, character.only = TRUE)
}

# ==== Load Data ====

all_data <- read_csv("D:/Data Thesis/Tensile Strength Data/Final/Merged.csv")

# Create seperate dataset dropping poor quality
good_data <- all_data %>% filter(Test_quality != "Poor")

good_data <- mutate(
  good_data,
  Root_class = case_when(
    Diameter <= 5 ~ "Very fine",
    Diameter > 5 & Diameter <= 10 ~ "Fine",
    Diameter > 10 & Diameter <= 20 ~ "Medium",
    Diameter > 20 & Diameter <= 30 ~ "Large",
    Diameter > 30 ~ "Very large",
    TRUE ~ NA_character_
  ))

# ==== Basic Tests ====
qqPlot(good_data$MPa)
hist(good_data$MPa, breaks = 10)
cor.test(tree_summary$DBH_m, tree_summary$RAR_tree, method = "spearman")
aov_MPa_species <- aov(log(MPa) ~ Species, data = good_data)

qqPlot(good_data$Fmax)
hist(good_data$Fmax, breaks = 10)
good_data$log_Fmax <- log(good_data$F_max)

# ==== Linear Mixed Effects Model ====

    # Draft models
# Check Normal LM
normallm<-lm(log(F_max)~Diameter + Soil_Type + Species, data=good_data)
plot(normallm)
```

```
# ---- Compare LMER ----
mod0 <- lmer(log(F_max) ~ (1 | Species), data = good_data, REML = FALSE)
mod1 <- lmer(log(F_max) ~ Diameter + (1 | Species), data = good_data, REML = FALSE)
mod2 <- lmer(log(F_max) ~ Diameter + Soil_Type + (1 | Species), data = good_data, REML = FALSE)
mod3 <- lmer(log(F_max) ~ Diameter + Soil_Type + Species + (1 | Species), data = good_data, REML = FALSE)
mod4 <- lmer(log(F_max) ~ Diameter * Soil_Type + (1 | Species), data = good_data, REML = FALSE)
mod5 <- lmer(log(F_max) ~ Diameter * Soil_Type * Species + (1 | Species), data = good_data, REML = TRUE)
mod6 <- lmer(log(F_max) ~ Diameter * Soil_Type * Species + Soil_Moisture + (1 | Species), data = good_data,
REML = FALSE)
mod7 <- lmer(log(F_max) ~ Diameter * Soil_Type * Species * Soil_Moisture + (1 | Species), data = good_data,
REML = FALSE)
mod8 <- lmer(log(F_max) ~ Diameter + Species + (1 | Species), data = good_data, REML = FALSE)
mod9 <- lmer(log(F_max) ~ Diameter * Species + (1 | Species), data = good_data, REML = FALSE)
mod10 <- lmer(log(F_max) ~ Diameter * Species + Soil_Type (1 | Species), data = good_data, REML = FALSE)
mod10 <- lmer(log(F_max) ~ Diameter + Soil_Moisture + (1 | Species), data = good_data, REML = FALSE)
mod11 <- lmer(log(F_max) ~ Diameter * Soil_Moisture + (1 | Species), data = good_data, REML = FALSE)
mod12 <- lmer(log(F_max) ~ Diameter * Soil_Moisture * Species (1 | Species), data = good_data, REML = FALSE)
mod13 <- lmer(log(F_max) ~ Diameter * DBH_m + (1 | Species), data = good_data, REML = FALSE)
mod14 <- lmer(log(F_max) ~ Diameter * Soil_Type * DBH_m + (1 | Species), data = good_data, REML = FALSE)
mod15 <- lmer(log(F_max) ~ Diameter * DBH_m * Soil_Type * Species + (1 | Species), data = good_data, REML =
FALSE)

anova(mod0, mod1, mod2, mod3, mod4, mod5, mod8, mod9, mod10, mod11, mod12, mod13, mod14, mod15)

# Evaluation of selected model
mod5 <- lmer(log(F_max) ~ Diameter * Soil_Type * Species + (1 | Species), data = good_data, REML = TRUE)
shapiro.test(residuals(mod5))
summary(mod5)
anova(mod5)

# ==== Setting up parameter fitting ====
good_data$displ_m <- good_data$Rel_Displ_Fmax * 10^-3
good_data$k <- good_data$F_max / good_data$displ_m
no_outliers <- good_data[-c(110, 181),]

#colourcodes: "Tōtara" = "#F79646", "Kānuka" = "#1F497D", "Poplar" = "#9BBB59"

# ==== Fmax function ====
fit_species_model <- function(species_name, data) {
 cat("\n===== Fitting model for =====\n")
 print(species_name)

 df <- subset(data, Species == species_name)

 fit <- nlsLM(
  F_max ~ pnorm(Diameter_m, mean=c, sd=e) * F0 * Diameter_m^alpha,
  data = df,
  start = list(F0 = max(df$F_max), alpha = 1,
       c=mean(df$Diameter_m, na.rm = TRUE), e=sd(df$Diameter_m, na.rm = TRUE)),
  lower = c(F0 = 0, alpha = 0, c = 0.008, e = 0.00015),
  control = nls.lm.control(maxiter = 500)
 )

 preds <- predict(fit)
 residuals <- df$F_max - preds

 ss_res <- sum(residuals^2)
```

```
  ss_tot <- sum((df$F_max - mean(df$F_max))^2)
  r_squared <- 1 - ss_res / ss_tot
  fit$r_squared <- r_squared

  print(r_squared)
  print(summary(fit))

  # Plot data vs fitted
  plot(df$Diameter_m, df$F_max, pch = 16, col = "#808080",
      xlab = "Diameter (m)", ylab = "Maximum Force (N)",
      main = paste("Model Fit -", species_name))
  lines(sort(df$Diameter_m),
        predict(fit, newdata = df[order(df$Diameter_m), ]),
        col = "#9BBB59", lwd = 3)
  legend("topleft", legend = c("Measured", "Fitted"),
         col = c("#808080", "#9BBB59"), pch = c(16, NA), lwd = c(NA, 2))

  # Extract coefficients
  cf <- coef(fit)
  F0_val <- round(cf["F0"], 3)
  alpha_val <- round(cf["alpha"], 3)

  # Equation string
  eq_text <- bquote(F[max] == .(F0_val) %.% phi^.(alpha_val))

  # R² string
  r2_text <- bquote(R^2 == .(round(r_squared, 3)))

  usr <- par("usr")
  x_pos <- usr[1] + 0.03 * diff(usr[1:2])
  y_pos <- usr[4] - 0.05 * diff(usr[3:4])

  text(x_pos, y_pos, eq_text, adj = c(0,1), cex = 0.9)
  text(x_pos, y_pos - 0.04 * diff(usr[3:4]),
      r2_text, adj = c(0,1), cex = 0.9)

  # Return results
  return(fit)
}

# Apply to each species
fit_F_results <- lapply(species_list, fit_species_model, data = good_data)

# ==== Spring function ====

fit_spring_constant <- function(species_name, data) {
  cat("\n===== Fitting spring constant for=====\n")
  print(species_name)

  df <- subset(data, Species == species_name)
  df <- subset(df, !is.na(k) & k & Diameter_m > 0)

  fit <- nlsLM(
    k ~ k0 * Diameter_m^beta,
    data = df,
    start = list(k0 = mean(df$k, na.rm = TRUE), beta = 1),
    control = nls.lm.control(maxiter = 500)
```

```
  )

  preds <- predict(fit)
  residuals <- df$k - preds

  ss_res <- sum(residuals^2)
  ss_tot <- sum((df$k - mean(df$k))^2)
  r_squared <- 1 - ss_res / ss_tot
  cat("R² =", round(r_squared, 3), "\n")
  fit$r_squared <- r_squared

  print(summary(fit))

  # Plot
  plot(df$Diameter_m, df$k, pch = 16, col = "#808080",
      xlab = "Diameter (m)", ylab = "Spring constant k (N/m)",
      main = paste("Spring Constant Fit -", species_name))
  lines(sort(df$Diameter_m),
        predict(fit, newdata = df[order(df$Diameter_m), ]),
        col = "#1F497D", lwd = 2)
  legend("topleft", legend = c("Measured", "Fitted"),
         col = c("#808080", "#1F497D"), pch = c(16, NA), lwd = c(NA, 2))

  cf <- coef(fit)
  k0_val <- round(cf["k0"], 3)
  beta_val <- round(cf["beta"], 3)

  # Fit and r2
  eq_text <- bquote(k == .(k0_val) %.% phi^.(beta_val))
  r2_text <- bquote(R^2 == .(round(r_squared, 3)))

  usr <- par("usr")
  x_pos <- usr[1] + 0.03 * diff(usr[1:2])
  y_pos <- usr[4] - 0.10 * diff(usr[3:4])

  text(x_pos, y_pos, eq_text, adj = c(0,1), cex = 0.9)
  text(x_pos, y_pos - 0.04 * diff(usr[3:4]),
      r2_text, adj = c(0,1), cex = 0.9)

  return(fit)
}

k0_results <- lapply(species_list, fit_spring_constant, data = no_outliers)

# ==== Compute Normalised Displacement ====
names(fit_F_results) <- species_list
names(k0_results) <- species_list

# Repeat for each species:
fit_F_tōtara <- fit_F_results[["Tōtara"]]
F0_val_t    <- coef(fit_F_tōtara)["F0"]
alpha_val_t <- coef(fit_F_tōtara)["alpha"]

fit_k_tōtara <- k0_results[["Tōtara"]]
k0_val_t    <- coef(fit_k_tōtara)["k0"]
beta_val_t <- coef(fit_k_tōtara)["beta"]
```

```
tōtara_df$fitted_x <- (F0_val_t / k0_val_t) * tōtara_df$Diameter_m^(alpha_val_t - beta_val_t)
tōtara_df$bling <- tōtara_df$Rel_Displ_Fmax / tōtara_df$fitted_x

# ==== Calculate Ranking ====

# Repeat for each species:
tōtara_df <- tōtara_df %>%
 arrange(bling) %>%
 mutate(n = row_number(), N  = n(), S = 1 - (n / N)
 ) %>%
 ungroup()

# ==== Fit Survival Function ====
fit_survival <- function(species_name, data) {
 cat("\n===== Fitting model for =====\n")
 print(species_name)

 df <- subset(data, Species == species_name)

 fit <- nlsLM(
  S ~ exp( - (bling / lambda)^omega ),
  data = df,
  start = list(lambda = median(df$bling), omega = 1),
  control = nls.lm.control(maxiter = 1000)
 )

 df$S_pred <- predict(fit)

 residuals <- df$S - df$S_pred
 ss_res <- sum(residuals^2)
 ss_tot <- sum((df$S - mean(df$S))^2)
 r_squared <- 1 - ss_res / ss_tot
 fit$r_squared <- r_squared

 print(r_squared)
 print(summary(fit))

 # ---- Plot ----
 plot(df$bling, df$S,
     pch = 16, col = "#808080",
     xlab = "Normalized Displacement (-)",
     ylab = "Survival Function (-)",
     main = paste("Weibull Survival Fit -", species_name),
     ylim = c(0,1))
 lines(sort(df$bling),
      df$S_pred[order(df$bling)],
      col = "#F79646", lwd = 2)
 legend("topright", legend=c("Measured S","Fitted S"),
       col=c("#808080","#F79646"), pch=c(16,NA), lwd=c(NA,2))

 cf <- coef(fit)
 lambda_val <- round(cf["lambda"], 3)
 omega_val  <- round(cf["omega"], 3)

 # Equation in plot
 text(
  x = par("usr")[2] - 0.05 * diff(par("usr")[1:2]),
```

```
   y = par("usr")[4] - 0.15 * diff(par("usr")[3:4]),
   labels = bquote(
     S(x^"*") == exp( - ( x^"*" / .(lambda_val) )^.(omega_val) )
   ),
   adj = c(1,1),
   cex = 1.0
  )

  # R2 in plot
  text(
   x = par("usr")[2] - 0.05 * diff(par("usr")[1:2]),
   y = par("usr")[4] - 0.25 * diff(par("usr")[3:4]),
   labels = bquote(R^2 == .(round(r_squared, 3))),
   adj = c(1,1),
   cex = 1.0
  )

  return(fit)
}

# Obtain for each species:
S_results_t <- fit_survival("Tōtara", tōtara_df)
```

Appendix C

Chemical Composition of the Soil of Root Distribution Trees

Sample	pH	K[a]	Ca[a]	Mg[a]	Na[a]	CEC[b]	Base Sat. (%)	Vol. Weight (g/mL)	PAN[c] (g/mL)	Org. M (%)	Tot. C (%)	Tot. N (%)	C/N (-)
HP1	7.3	0.43	34.6	1.38	0.18	37	100	0.86	296	10.1	5.8	0.44	13.1
HP2	5.9	0.56	9.3	3.76	0.27	21	67	0.79	318	13.2	7.7	0.52	14.9
TK2	5.6	0.45	10.2	2.4	0.23	22	59	0.84	369	14.1	8.2	0.51	16
TK1	5.6	0.46	10.9	2.25	0.27	25	55	0.73	349	14.4	8.3	0.58	14.4
TT1	6.2	0.75	12.6	2.23	0.18	23	69	0.73	348	12.3	7.1	0.56	12.6
TT2	5.7	0.71	11.2	3.78	0.22	26	62	0.78	355	12.4	7.2	0.56	12.8
MK1	6.1	0.53	19.3	2.7	0.39	34	67	0.61	364	13.2	7.7	0.62	12.4
MK2	5.2	1.95	10.8	8.89	1.29	35	65	0.72	202	7.6	4.4	0.42	10.5
MT1	6	0.42	12.6	1.81	0.26	23	65	0.8	402	14.8	8.6	0.49	17.6
MT2	5.7	0.86	11.6	6.95	0.25	30	66	0.72	344	16.7	9.7	0.57	17
MP1	5.9	1.14	10.3	5.36	0.27	25	68	0.82	316	10.2	5.9	0.54	11
MP2	6	1.03	12.1	8.86	0.56	29	78	0.91	202	7.6	4.4	0.36	12.3

Note. Chemical analysis of the soil was provided by Verdantia Research, New Zealand.

[a] Available cations; units in milliequivalents100 g^{-1} soil

[b] Cation Exchange Capacity; unit in milliequivalents 100 g^{-1} soil

[c] Plant-available Nitrogen

Appendix D
Interactions of the Linear Mixed Effect Models for the Root Distribution

Figure D1

Model Fit of log_counts ~ Top_Depth_cm * Species * Soil_Type + (1 | Tree_Nr)

```
> anova(mod_vert_count)
Type III Analysis of Variance Table with Satterthwaite's method
                            Sum Sq Mean Sq NumDF   DenDF  F value    Pr(>F)
Top_Depth_cm                265.587 265.587     1 2670.00 466.9483 < 2.2e-16 ***
Species                      16.185   8.093     2    7.51  14.2284  0.002788 **
Soil_Type                     1.771   1.771     1    7.51   3.1145  0.118040
Top_Depth_cm:Species          5.075   2.538     2 2670.00   4.4615  0.011631 *
Top_Depth_cm:Soil_Type        5.339   5.339     1 2670.00   9.3871  0.002207 **
Species:Soil_Type             1.764   0.882     2    7.51   1.5509  0.273005
Top_Depth_cm:Species:Soil_Type  14.634   7.317     2 2670.00  12.8643 2.753e-06 ***
---
Signif. codes:  0 ‘***’ 0.001 ‘**’ 0.01 ‘*’ 0.05 ‘.’ 0.1 ‘ ’ 1
> summary(mod_vert_count)
Linear mixed model fit by REML. t-tests use Satterthwaite's method ['lmerModLmerTest']
Formula: log_counts ~ Top_Depth_cm * Species * Soil_Type + (1 | Tree_Nr)
   Data: df

REML criterion at convergence: 6215.9

Scaled residuals:
     Min       1Q   Median       3Q      Max
-10.7761  -0.4388   0.1227   0.6036   2.0001

Random effects:
 Groups   Name        Variance Std.Dev.
 Tree_Nr  (Intercept) 0.04551  0.2133
 Residual             0.56877  0.7542
Number of obs: 2688, groups:  Tree_Nr, 12

Fixed effects:
                                                          Estimate Std. Error         df t value Pr(>|t|)
(Intercept)                                              3.952e+00  1.639e-01  7.512e+00  24.105 2.18e-08 ***
Top_Depth_cm                                            -1.034e-02  1.188e-03  2.670e+03  -8.702  < 2e-16 ***
SpeciesKanuka                                           -2.394e-01  2.319e-01  7.512e+00  -1.032  0.33394
SpeciesTotara                                            5.104e-01  2.319e-01  7.512e+00   2.201  0.06101 .
Soil_TypeTypic Yellow Ultic Soil                        -5.696e-01  2.319e-01  7.512e+00  -2.457  0.04139 *
Top_Depth_cm:SpeciesKanuka                              -2.467e-03  1.680e-03  2.670e+03  -1.469  0.14198
Top_Depth_cm:SpeciesTotara                              -2.416e-03  1.680e-03  2.670e+03  -1.438  0.15049
Top_Depth_cm:Soil_TypeTypic Yellow Ultic Soil           -3.464e-03  1.680e-03  2.670e+03  -2.062  0.03929 *
SpeciesKanuka:Soil_TypeTypic Yellow Ultic Soil           4.971e-01  3.279e-01  7.512e+00   1.516  0.17038
SpeciesTotara:Soil_TypeTypic Yellow Ultic Soil           5.030e-01  3.279e-01  7.512e+00   1.534  0.16596
Top_Depth_cm:SpeciesKanuka:Soil_TypeTypic Yellow Ultic Soil  1.194e-02  2.375e-03  2.670e+03   5.027 5.31e-07 ***
Top_Depth_cm:SpeciesTotara:Soil_TypeTypic Yellow Ultic Soil  7.364e-03  2.375e-03  2.670e+03   3.100  0.00196 **
---
Signif. codes:  0 ‘***’ 0.001 ‘**’ 0.01 ‘*’ 0.05 ‘.’ 0.1 ‘ ’ 1

Correlation of Fixed Effects:
            (Intr) Tp_Dp_ SpcsKn SpcsTt S_TYUS T_D_:SK T_D_:ST T_D_:S_YUS SK:YUS ST:YUS T_D_:SKYUS
Top_Dpth_cm -0.326
SpeciesKank -0.707  0.231
SpeciesTotr -0.707  0.231  0.500
Sl_TypTyYUS -0.707  0.231  0.500  0.500
Tp_Dpth_:SK  0.231 -0.707 -0.326 -0.163 -0.163
Tp_Dpth_:ST  0.231 -0.707 -0.163 -0.326 -0.163  0.500
T_D_:S_TYUS  0.231 -0.707 -0.163 -0.163 -0.326  0.500   0.500
SpK:S_TTYUS  0.500 -0.163 -0.707 -0.354 -0.707  0.231   0.115   0.231
SpT:S_TTYUS  0.500 -0.163 -0.354 -0.707 -0.707  0.115   0.231   0.231      0.500
T_D_:SK:YUS -0.163  0.500  0.231  0.115  0.231 -0.707  -0.354  -0.707     -0.326 -0.163
T_D_:ST:YUS -0.163  0.500  0.115  0.231  0.231 -0.354  -0.707  -0.707     -0.163 -0.326  0.500
```

Note. Above: the ANOVA test of the model. Below: Summary of the model effects. Poplar was set as reference species in the displayed fit of the linear mixed effects model.

Figure D2

Model Fit of log_RAR_row ~ Top_Depth_cm * Species * Soil_Type + (1 | Tree_Nr)

```
> anova(mod_vert_RAR)
Type III Analysis of Variance Table with Satterthwaite's method
                            Sum Sq Mean Sq NumDF   DenDF  F value    Pr(>F)
Top_Depth_cm                965.64  965.64     1 2670.00 492.8244 < 2.2e-16 ***
Species                      25.95   12.97     2   10.58   6.6218 0.0136558 *
Soil_Type                    55.23   55.23     1   10.58  28.1887 0.0002840 ***
Top_Depth_cm:Species         18.32    9.16     2 2670.00   4.6747 0.0094051 **
Top_Depth_cm:Soil_Type       22.03   22.03     1 2670.00  11.2407 0.0008114 ***
Species:Soil_Type            68.53   34.27     2   10.58  17.4877 0.0004429 ***
Top_Depth_cm:Species:Soil_Type  19.77    9.89     2 2670.00   5.0455 0.0064997 **
---
Signif. codes:  0 ‘***’ 0.001 ‘**’ 0.01 ‘*’ 0.05 ‘.’ 0.1 ‘ ’ 1
> summary(mod_vert_RAR)
Linear mixed model fit by REML. t-tests use Satterthwaite's method ['lmerModLmerTest']
Formula: log_RAR_row ~ Top_Depth_cm * Species * Soil_Type + (1 | Tree_Nr)
   Data: df

REML criterion at convergence: 9519.8

Scaled residuals:
    Min      1Q  Median      3Q     Max
-2.7899 -0.6888 -0.1154  0.6206  3.5579

Random effects:
 Groups   Name        Variance Std.Dev.
 Tree_Nr  (Intercept) 0.05128  0.2264
 Residual             1.95940  1.3998
Number of obs: 2688, groups:  Tree_Nr, 12

Fixed effects:
                                                          Estimate Std. Error         df t value Pr(>|t|)
(Intercept)                                              5.166e-01  1.996e-01  1.058e+01   2.588 0.025963 *
Top_Depth_cm                                            -2.243e-02  2.204e-03  2.670e+03 -10.175  < 2e-16 ***
SpeciesKanuka                                           -1.709e+00  2.823e-01  1.058e+01  -6.054 9.74e-05 ***
SpeciesTotara                                           -5.854e-01  2.823e-01  1.058e+01  -2.074 0.063395 .
Soil_TypeTypic Yellow Ultic Soil                        -2.133e+00  2.823e-01  1.058e+01  -7.557 1.40e-05 ***
Top_Depth_cm:SpeciesKanuka                               3.250e-03  3.118e-03  2.670e+03   1.042 0.297319
Top_Depth_cm:SpeciesTotara                              -4.951e-03  3.118e-03  2.670e+03  -1.588 0.112409
Top_Depth_cm:Soil_TypeTypic Yellow Ultic Soil            1.173e-02  3.118e-03  2.670e+03   3.763 0.000171 ***
SpeciesKanuka:Soil_TypeTypic Yellow Ultic Soil           2.336e+00  3.993e-01  1.058e+01   5.850 0.000130 ***
SpeciesTotara:Soil_TypeTypic Yellow Ultic Soil           1.469e+00  3.993e-01  1.058e+01   3.678 0.003880 **
Top_Depth_cm:SpeciesKanuka:Soil_TypeTypic Yellow Ultic Soil -1.351e-02  4.409e-03  2.670e+03  -3.065 0.002196 **
Top_Depth_cm:SpeciesTotara:Soil_TypeTypic Yellow Ultic Soil -3.576e-03  4.409e-03  2.670e+03  -0.811 0.417400
---
Signif. codes:  0 ‘***’ 0.001 ‘**’ 0.01 ‘*’ 0.05 ‘.’ 0.1 ‘ ’ 1

Correlation of Fixed Effects:
            (Intr) Tp_Dp_ SpcsKn SpcsTt S_TYUS T_D_:SK T_D_:ST T_D_:S_YUS SK:YUS ST:YUS T_D_:SKYUS
Top_Dpth_cm -0.497
SpeciesKank -0.707  0.351
SpeciesTotr -0.707  0.351  0.500
Sl_TypTyYUS -0.707  0.351  0.500  0.500
Tp_Dpth_:SK  0.351 -0.707 -0.497 -0.248 -0.248
Tp_Dpth_:ST  0.351 -0.707 -0.248 -0.497 -0.248  0.500
T_D_:S_TYUS  0.351 -0.707 -0.248 -0.248 -0.497  0.500   0.500
SpK:S_TTYUS  0.500 -0.248 -0.707 -0.354 -0.707  0.351   0.176   0.351
SpT:S_TTYUS  0.500 -0.248 -0.354 -0.707 -0.707  0.176   0.351   0.351      0.500
T_D_:SK:YUS -0.248  0.500  0.351  0.176  0.351 -0.707  -0.354  -0.707     -0.497 -0.248
T_D_:ST:YUS -0.248  0.500  0.176  0.351  0.351 -0.354  -0.707  -0.707     -0.248 -0.497  0.500
```

Note. Above: the ANOVA test of the model. Below: Summary of the model effects. Poplar was set as reference species in the displayed fit of the linear mixed effects model.

Figure D3

Model Fit of log_counts ~ Distance_m * Species * Soil_Type + (1 | Tree_Nr)

```
> anova(mod_dis_count)
Type III Analysis of Variance Table with Satterthwaite's method
                          Sum Sq Mean Sq NumDF  DenDF F value    Pr(>F)
Distance_m                19.187 19.1874     1 2670.0 29.3151 6.699e-08 ***
Species                    1.802  0.9008     2   12.4  1.3763   0.28852
Soil_Type                  0.066  0.0662     1   12.4  0.1011   0.75584
Distance_m:Species        36.319 18.1594     2 2670.0 27.7446 1.186e-12 ***
Distance_m:Soil_Type       2.122  2.1219     1 2670.0  3.2419   0.07189 .
Species:Soil_Type          1.779  0.8897     2   12.4  1.3593   0.29258
Distance_m:Species:Soil_Type  4.054  2.0268     2 2670.0  3.0967   0.04536 *
---
Signif. codes:  0 ‘***’ 0.001 ‘**’ 0.01 ‘*’ 0.05 ‘.’ 0.1 ‘ ’ 1
> summary(mod_dis_count)
Linear mixed model fit by REML. t-tests use Satterthwaite's method ['lmerModLmerTest']
Formula: log_counts ~ Distance_m * Species * Soil_Type + (1 | Tree_Nr)
   Data: df

REML criterion at convergence: 6551.3

Scaled residuals:
     Min       1Q   Median       3Q      Max
-10.6296  -0.4435   0.1481   0.6147   2.3408

Random effects:
 Groups   Name        Variance Std.Dev.
 Tree_Nr  (Intercept) 0.04512  0.2124
 Residual             0.65452  0.8090
Number of obs: 2688, groups:  Tree_Nr, 12

Fixed effects:
                                                          Estimate Std. Error         df t value Pr(>|t|)
(Intercept)                                                3.42612    0.18585   12.39982  18.435  2.2e-10 ***
Distance_m                                                 0.02024    0.03419 2670.00000   0.592 0.553793
SpeciesKanuka                                             -0.53834    0.26284   12.39982  -2.048 0.062326 .
SpeciesTotara                                             -0.13443    0.26284   12.39982  -0.511 0.618014
Soil_TypeTypic Yellow Ultic Soil                          -0.28041    0.26284   12.39982  -1.067 0.306373
Distance_m:SpeciesKanuka                                   0.06264    0.04835 2670.00000   1.296 0.195207
Distance_m:SpeciesTotara                                   0.17872    0.04835 2670.00000   3.696 0.000223 ***
Distance_m:Soil_TypeTypic Yellow Ultic Soil                -0.14836    0.04835 2670.00000  -3.069 0.002172 **
SpeciesKanuka:Soil_TypeTypic Yellow Ultic Soil              0.60653    0.37171   12.39982   1.632 0.127854
SpeciesTotara:Soil_TypeTypic Yellow Ultic Soil              0.37942    0.37171   12.39982   1.021 0.326878
Distance_m:SpeciesKanuka:Soil_TypeTypic Yellow Ultic Soil   0.14265    0.06838 2670.00000   2.086 0.037046 *
Distance_m:SpeciesTotara:Soil_TypeTypic Yellow Ultic Soil   0.15166    0.06838 2670.00000   2.218 0.026631 *
---
Signif. codes:  0 ‘***’ 0.001 ‘**’ 0.01 ‘*’ 0.05 ‘.’ 0.1 ‘ ’ 1

Correlation of Fixed Effects:
            (Intr) Dstnc_ SpcsKn SpcsTt S_TYUS Ds_:SK Ds_:ST D_:S_YUS SK:YUS ST:YUS D_:SKYUS
Distance_m  -0.552
SpeciesKank -0.707  0.390
SpeciesTotr -0.707  0.390  0.500
Sl_TypTyYUS -0.707  0.390  0.500  0.500
Dstnc_m:SpK  0.390 -0.707 -0.552 -0.276 -0.276
Dstnc_m:SpT  0.390 -0.707 -0.276 -0.552 -0.276  0.500
Ds_:S_TTYUS  0.390 -0.707 -0.276 -0.276 -0.552  0.500  0.500
SpK:S_TTYUS  0.500 -0.276 -0.707 -0.354 -0.707  0.390  0.195  0.390
SpT:S_TTYUS  0.500 -0.276 -0.354 -0.707 -0.707  0.195  0.390  0.390    0.500
D_:SK:S_YUS -0.276  0.500  0.390  0.195  0.390 -0.707 -0.354 -0.707   -0.552 -0.276
D_:ST:S_YUS -0.276  0.500  0.195  0.390  0.390 -0.354 -0.707 -0.707   -0.276 -0.552  0.500
```

Note. Above: the ANOVA test of the model. Below: Summary of the model effects. Poplar was set as reference species in the displayed fit of the linear mixed effects model.

Figure D4

Model Fit of log_RAR_row ~ Distance_m * Species * Soil_Type + (1 | Tree_Nr)

```
> anova(mod_dis_RAR)
Type III Analysis of Variance Table with Satterthwaite's method
                         Sum Sq Mean Sq NumDF   DenDF  F value    Pr(>F)
Distance_m               739.50  739.50     1 2670.00 359.9582 < 2.2e-16 ***
Species                   33.52   16.76     2   26.39   8.1578  0.001744 **
Soil_Type                  7.51    7.51     1   26.39   3.6547  0.066827 .
Distance_m:Species         5.87    2.94     2 2670.00   1.4296  0.239585
Distance_m:Soil_Type       3.81    3.81     1 2670.00   1.8533  0.173513
Species:Soil_Type         58.91   29.45     2   26.39  14.3367 6.098e-05 ***
Distance_m:Species:Soil_Type  22.92   11.46     2 2670.00   5.5774  0.003827 **
---
Signif. codes:  0 ‘***’ 0.001 ‘**’ 0.01 ‘*’ 0.05 ‘.’ 0.1 ‘ ’ 1
> summary(mod_dis_RAR)
Linear mixed model fit by REML. t-tests use Satterthwaite's method ['lmerModLmerTest']
Formula: log_RAR_row ~ Distance_m * Species * Soil_Type + (1 | Tree_Nr)
   Data: df

REML criterion at convergence: 9606.7

Scaled residuals:
    Min      1Q  Median      3Q     Max
-2.7013 -0.7463 -0.0953  0.6904  3.6397

Random effects:
 Groups   Name        Variance Std.Dev.
 Tree_Nr  (Intercept) 0.05085  0.2255
 Residual             2.05441  1.4333
Number of obs: 2688, groups:  Tree_Nr, 12

Fixed effects:
                                                    Estimate Std. Error         df t value Pr(>|t|)
(Intercept)                                          1.11033    0.25106   26.39091   4.423  0.00015 ***
Distance_m                                          -0.53435    0.06057 2670.00000  -8.822  < 2e-16 ***
SpeciesKanuka                                       -2.33941    0.35505   26.39091  -6.589 5.09e-07 ***
SpeciesTotara                                       -0.92162    0.35505   26.39091  -2.596  0.01522 *
Soil_TypeTypic Yellow Ultic Soil                    -1.66078    0.35505   26.39091  -4.678 7.62e-05 ***
Distance_m:SpeciesKanuka                             0.25882    0.08566 2670.00000   3.022  0.00254 **
Distance_m:SpeciesTotara                             0.03781    0.08566 2670.00000   0.441  0.65892
Distance_m:Soil_TypeTypic Yellow Ultic Soil           0.01841    0.08566 2670.00000   0.215  0.82980
SpeciesKanuka:Soil_TypeTypic Yellow Ultic Soil       2.67776    0.50212   26.39091   5.333 1.34e-05 ***
SpeciesTotara:Soil_TypeTypic Yellow Ultic Soil       1.12894    0.50212   26.39091   2.248  0.03312 *
Distance_m:SpeciesKanuka:Soil_TypeTypic Yellow Ultic Soil  -0.31678    0.12114 2670.00000  -2.615  0.00897 **
Distance_m:SpeciesTotara:Soil_TypeTypic Yellow Ultic Soil   0.05956    0.12114 2670.00000   0.492  0.62298
---
Signif. codes:  0 ‘***’ 0.001 ‘**’ 0.01 ‘*’ 0.05 ‘.’ 0.1 ‘ ’ 1

Correlation of Fixed Effects:
            (Intr) Dstnc_ SpcsKn SpcsTt S_TYUS Ds_:SK Ds_:ST D_:S_YUS SK:YUS ST:YUS D_:SKYUS
Distance_m  -0.724
SpeciesKank -0.707  0.512
SpeciesTotr -0.707  0.512  0.500
Sl_TypTyYUS -0.707  0.512  0.500  0.500
Dstnc_m:SpK  0.512 -0.707 -0.724 -0.362 -0.362
Dstnc_m:SpT  0.512 -0.707 -0.362 -0.724 -0.362  0.500
Ds_:S_TTYUS  0.512 -0.707 -0.362 -0.362 -0.724  0.500  0.500
SpK:S_TTYUS  0.500 -0.362 -0.707 -0.354 -0.707  0.512  0.256  0.512
SpT:S_TTYUS  0.500 -0.362 -0.354 -0.707 -0.707  0.256  0.512  0.512    0.500
D_:SK:S_YUS -0.362  0.500  0.512  0.256  0.512 -0.707 -0.354 -0.707   -0.724 -0.362
D_:ST:S_YUS -0.362  0.500  0.256  0.512  0.512 -0.354 -0.707 -0.707   -0.362 -0.724  0.500
```

Note. Above: the ANOVA test of the model. Below: Summary of the model effects. Poplar was set as reference species in the displayed fit of the linear mixed effects model.

Figure D5

Model Fit of log_counts ~ Sector * Species * Soil_Type + (1 | Tree_Nr)

```
> anova(mod_sec_count)
Type III Analysis of Variance Table with Satterthwaite's method
                       Sum Sq Mean Sq NumDF   DenDF F value    Pr(>F)
Sector                 0.1447  0.1447     1 2670.00  0.2169  0.641443
Species               12.4843  6.2422     2    9.21  9.3601  0.006043 **
Soil_Type              0.0179  0.0179     1    9.21  0.0269  0.873370
Sector:Species         7.5317  3.7659     2 2670.00  5.6469  0.003571 **
Sector:Soil_Type       1.0998  1.0998     1 2670.00  1.6492  0.199182
Species:Soil_Type      0.5486  0.2743     2    9.21  0.4113  0.674365
Sector:Species:Soil_Type 19.8854  9.9427     2 2670.00 14.9091 3.639e-07 ***
---
Signif. codes:  0 ‘***’ 0.001 ‘**’ 0.01 ‘*’ 0.05 ‘.’ 0.1 ‘ ’ 1
> summary(mod_sec_count)
Linear mixed model fit by REML. t-tests use Satterthwaite's method ['lmerModLmerTest']
Formula: log_counts ~ Sector * Species * Soil_Type + (1 | Tree_Nr)
   Data: df

REML criterion at convergence: 6609.9

Scaled residuals:
     Min       1Q   Median       3Q      Max
-10.6522  -0.4548   0.1570   0.6144   2.1396

Random effects:
 Groups   Name        Variance Std.Dev.
 Tree_Nr  (Intercept) 0.04507  0.2123
 Residual             0.66689  0.8166
Number of obs: 2688, groups:  Tree_Nr, 12

Fixed effects:
                                                    Estimate Std. Error         df t value Pr(>|t|)
(Intercept)                                          3.34021    0.17252    9.20978  19.361 8.95e-09 ***
Sector                                               0.03259    0.01684 2670.00000   1.935   0.0531 .
SpeciesKanuka                                       -0.22033    0.24398    9.20978  -0.903   0.3895
SpeciesTotara                                        0.54917    0.24398    9.20978   2.251   0.0503 .
Soil_TypeTypic Yellow Ultic Soil                    -0.16833    0.24398    9.20978  -0.690   0.5072
Sector:SpeciesKanuka                                -0.02891    0.02381 2670.00000  -1.214   0.2249
Sector:SpeciesTotara                                -0.03277    0.02381 2670.00000  -1.376   0.1690
Sector:Soil_TypeTypic Yellow Ultic Soil              -0.12382    0.02381 2670.00000  -5.199 2.15e-07 ***
SpeciesKanuka:Soil_TypeTypic Yellow Ultic Soil       0.31095    0.34504    9.20978   0.901   0.3905
SpeciesTotara:Soil_TypeTypic Yellow Ultic Soil       0.12480    0.34504    9.20978   0.362   0.7257
Sector:SpeciesKanuka:Soil_TypeTypic Yellow Ultic Soil  0.16079  0.03368 2670.00000   4.774 1.90e-06 ***
Sector:SpeciesTotara:Soil_TypeTypic Yellow Ultic Soil  0.15769  0.03368 2670.00000   4.682 2.98e-06 ***
---
Signif. codes:  0 ‘***’ 0.001 ‘**’ 0.01 ‘*’ 0.05 ‘.’ 0.1 ‘ ’ 1

Correlation of Fixed Effects:
            (Intr) Sector SpcsKn SpcsTt S_TYUS Sct:SK Sct:ST S:S_YUS SK:YUS ST:YUS S:SKYUS
Sector      -0.439
SpeciesKank -0.707  0.311
SpeciesTotr -0.707  0.311  0.500
Sl_TypTyYUS -0.707  0.311  0.500  0.500
Sctr:SpcsKn  0.311 -0.707 -0.439 -0.220 -0.220
Sctr:SpcsTt  0.311 -0.707 -0.220 -0.439 -0.220  0.500
Sct:S_TTYUS  0.311 -0.707 -0.220 -0.220 -0.439  0.500  0.500
SpK:S_TTYUS  0.500 -0.220 -0.707 -0.354 -0.707  0.311  0.155  0.311
SpT:S_TTYUS  0.500 -0.220 -0.354 -0.707 -0.707  0.155  0.311  0.311   0.500
S:SK:S_TYUS -0.220  0.500  0.311  0.155  0.311 -0.707 -0.354 -0.707  -0.439 -0.220
S:ST:S_TYUS -0.220  0.500  0.155  0.311  0.311 -0.354 -0.707 -0.707  -0.220 -0.439  0.500
```

Note. Above: the ANOVA test of the model. Below: Summary of the model effects. Poplar was set as reference species in the displayed fit of the linear mixed effects model.

Figure D6

The Mean Root Count for Individual Trees Across Sector and Soil Type

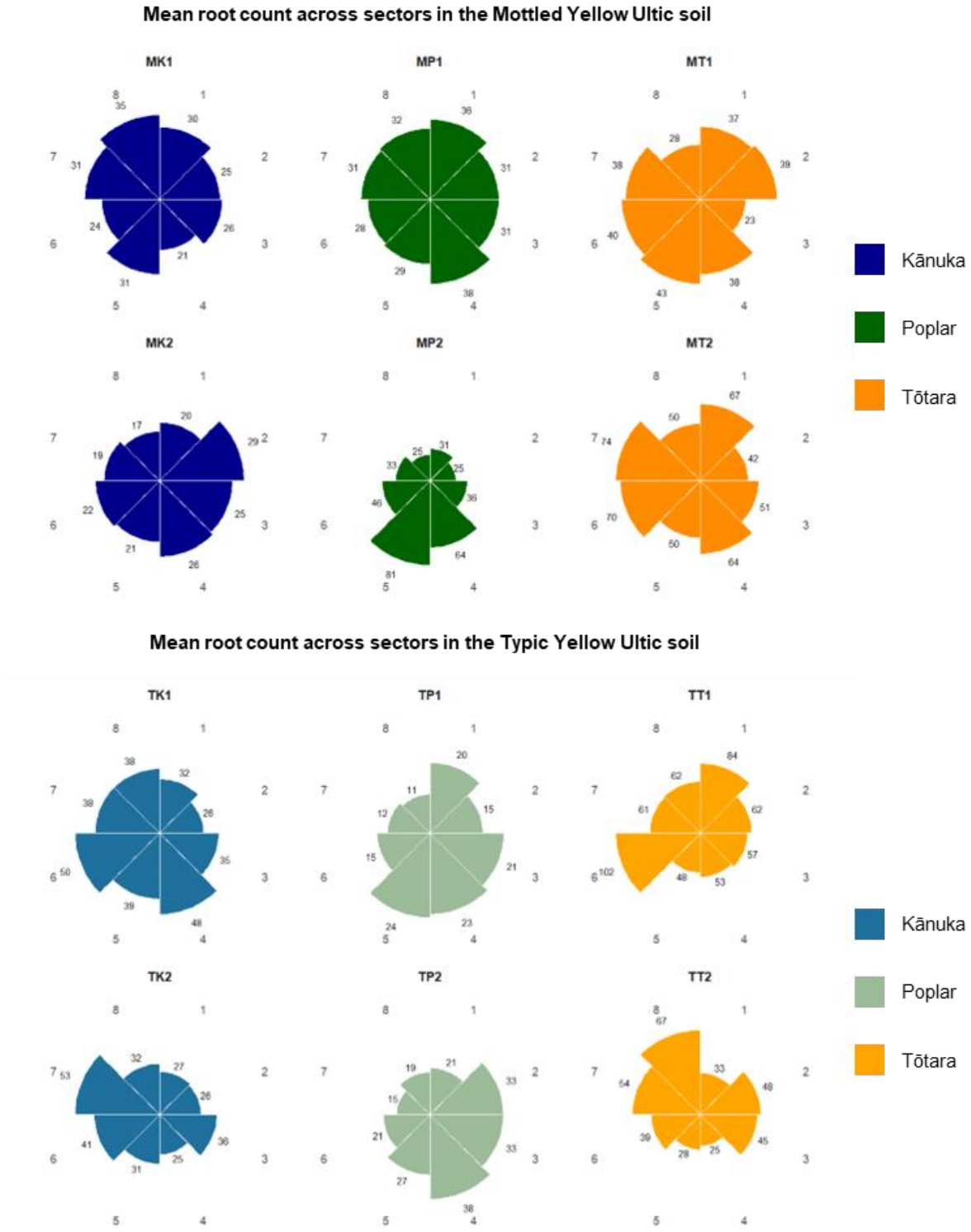

Note. The root counts are presented for radii 1.5 m and 2.5 m, the outer two radii were filtered out for display purposes.

Figure D7

Model Fit of log_RAR_row ~ Distance_m * Species * Soil_Type + (1 | Tree_Nr)

```
> anova(mod_sec_RAR)
Type III Analysis of Variance Table with Satterthwaite's method
                       Sum Sq Mean Sq NumDF   DenDF F value    Pr(>F)
Sector                  1.993  1.9928     1 2670.00  0.8593 0.3540149
Species                52.942 26.4710     2   16.62 11.4145 0.0007590 ***
Soil_Type              24.294 24.2941     1   16.62 10.4758 0.0049628 **
Sector:Species         22.426 11.2128     2 2670.00  4.8351 0.0080158 **
Sector:Soil_Type        0.002  0.0016     1 2670.00  0.0007 0.9788912
Species:Soil_Type       7.047  3.5235     2   16.62  1.5194 0.2477381
Sector:Species:Soil_Type 41.048 20.5240     2 2670.00  8.8501 0.0001476 ***
---
Signif. codes:  0 ‘***’ 0.001 ‘**’ 0.01 ‘*’ 0.05 ‘.’ 0.1 ‘ ’ 1
> summary(mod_sec_RAR)
Linear mixed model fit by REML. t-tests use Satterthwaite's method ['lmerModLmerTest']
Formula: log_RAR_row ~ Sector * Species * Soil_Type + (1 | Tree_Nr)
   Data: df

REML criterion at convergence: 9938.9

Scaled residuals:
    Min      1Q  Median      3Q     Max
-2.7609 -0.7327 -0.1228  0.5961  3.9808

Random effects:
 Groups   Name        Variance Std.Dev.
 Tree_Nr  (Intercept) 0.04967  0.2229
 Residual             2.31906  1.5228
Number of obs: 2688, groups:  Tree_Nr, 12

Fixed effects:
                                                  Estimate Std. Error         df t value Pr(>|t|)
(Intercept)                                     -5.291e-01  2.236e-01  1.662e+01  -2.367 0.030382 *
Sector                                           8.079e-03  3.140e-02  2.670e+03   0.257 0.796976
SpeciesKanuka                                   -1.448e+00  3.162e-01  1.662e+01  -4.579 0.000282 ***
SpeciesTotara                                   -6.586e-01  3.162e-01  1.662e+01  -2.083 0.053003 .
Soil_TypeTypic Yellow Ultic Soil                -9.192e-01  3.162e-01  1.662e+01  -2.907 0.009983 **
Sector:SpeciesKanuka                            -2.563e-02  4.441e-02  2.670e+03  -0.577 0.563812
Sector:SpeciesTotara                            -3.324e-02  4.441e-02  2.670e+03  -0.748 0.454276
Sector:Soil_TypeTypic Yellow Ultic Soil          -1.525e-01  4.441e-02  2.670e+03  -3.435 0.000602 ***
SpeciesKanuka:Soil_TypeTypic Yellow Ultic Soil    7.590e-01  4.471e-01  1.662e+01   1.698 0.108236
SpeciesTotara:Soil_TypeTypic Yellow Ultic Soil    2.260e-01  4.471e-01  1.662e+01   0.506 0.619817
Sector:SpeciesKanuka:Soil_TypeTypic Yellow Ultic Soil  2.152e-01  6.280e-02  2.670e+03   3.427 0.000620 ***
Sector:SpeciesTotara:Soil_TypeTypic Yellow Ultic Soil  2.404e-01  6.280e-02  2.670e+03   3.827 0.000133 ***
---
Signif. codes:  0 ‘***’ 0.001 ‘**’ 0.01 ‘*’ 0.05 ‘.’ 0.1 ‘ ’ 1

Correlation of Fixed Effects:
            (Intr) Sector SpcsKn SpcsTt S_TYUS Sct:SK Sct:ST S:S_YUS SK:YUS ST:YUS S:SKYUS
Sector      -0.632
SpeciesKank -0.707  0.447
SpeciesTotr -0.707  0.447  0.500
Sl_TypTyYUS -0.707  0.447  0.500  0.500
Sctr:SpcsKn  0.447 -0.707 -0.632 -0.316 -0.316
Sctr:SpcsTt  0.447 -0.707 -0.316 -0.632 -0.316  0.500
Sct:S_TTYUS  0.447 -0.707 -0.316 -0.316 -0.632  0.500  0.500
SpK:S_TTYUS  0.500 -0.316 -0.707 -0.354 -0.707  0.447  0.223  0.447
SpT:S_TTYUS  0.500 -0.316 -0.354 -0.707 -0.707  0.223  0.447  0.447   0.500
```

Note. Above: the ANOVA test of the model. Below: Summary of the model effects. Poplar was set as reference species in the displayed fit of the linear mixed effects model.

Figure D8

The Mean Root Area Ratio for Individual Trees Across Sector and Soil Type

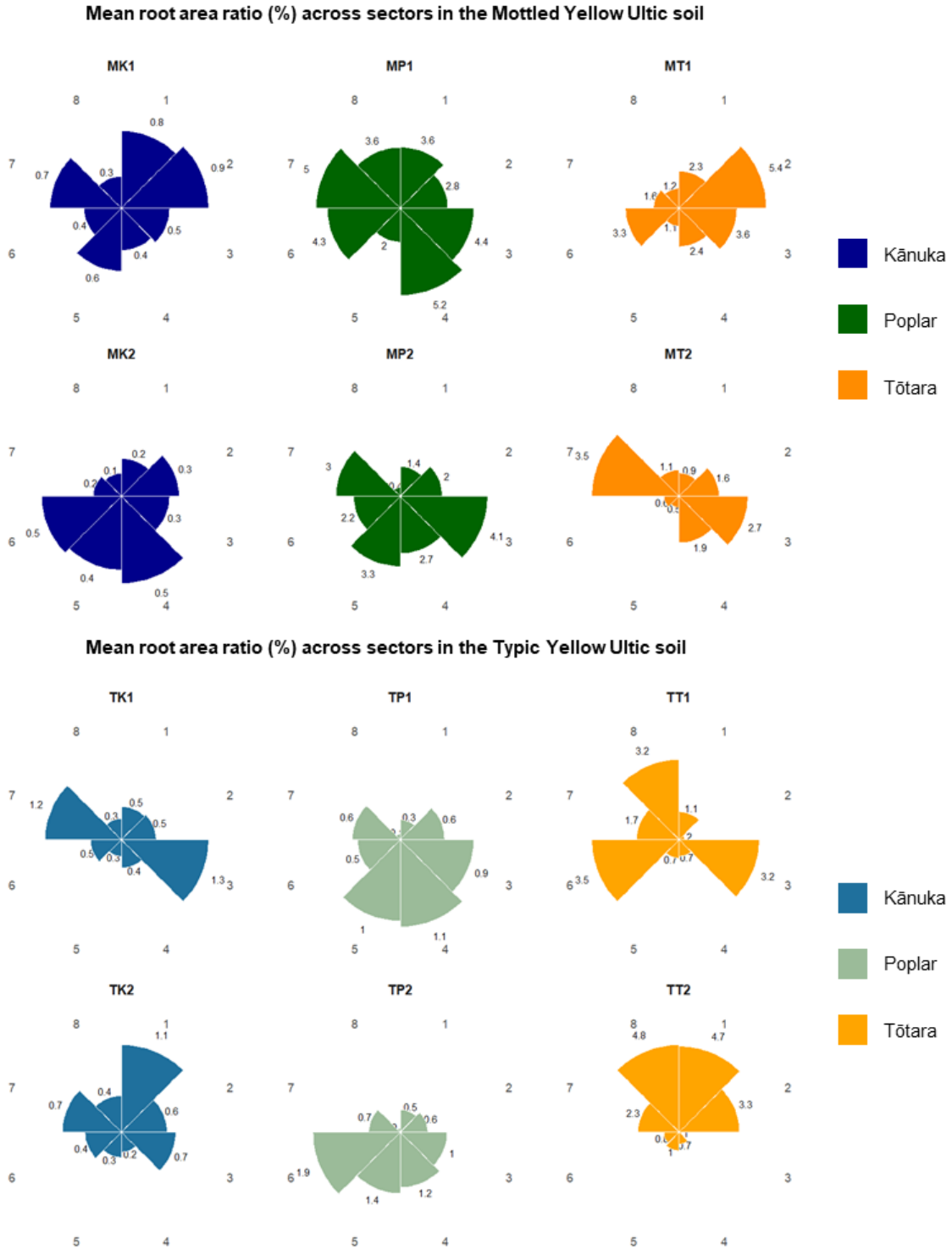

Note. The Root Area Ratio is presented for radii 1.5 m and 2.5 m, the outer two radii were filtered out for display purposes.

Appendix E

Interactions of the Linear Mixed Effect Model for the Root Tensile Strength

```
> anova(mod5)
Type III Analysis of Variance Table with Satterthwaite's method
                         Sum Sq Mean Sq NumDF DenDF  F value    Pr(>F)
Diameter                157.249 157.249     1   202 335.0749 < 2.2e-16 ***
Soil_Type                 4.037   4.037     1   202   8.6026  0.003745 **
Species                   1.142   0.571     2     0   1.2168  1.000000
Diameter:Soil_Type        0.103   0.103     1   202   0.2201  0.639476
Diameter:Species          0.267   0.134     2   202   0.2847  0.752568
Soil_Type:Species         2.530   1.265     2   202   2.6957  0.069925 .
Diameter:Soil_Type:Species  0.880   0.440     2   202   0.9379  0.393160
---
Signif. codes:  0 ‘***’ 0.001 ‘**’ 0.01 ‘*’ 0.05 ‘.’ 0.1 ‘ ’ 1
> summary(mod5)
Linear mixed model fit by REML. t-tests use Satterthwaite's method ['lmerModLmerTest']
Formula: log(F_max) ~ Diameter * Soil_Type * Species + (1 | Species)
   Data: good_data

REML criterion at convergence: 487.9

Scaled residuals:
    Min      1Q  Median      3Q     Max
-3.2674 -0.6012  0.0261  0.7085  2.6786

Random effects:
 Groups   Name        Variance Std.Dev.
 Species  (Intercept) 0.02801  0.1673
 Residual             0.46929  0.6851
Number of obs: 214, groups:  Species, 3

Fixed effects:
                                                        Estimate Std. Error         df t value Pr(>|t|)
(Intercept)                                            4.541e+00  3.010e-01  3.684e-09  15.085 1.000000
Diameter                                               1.163e-01  1.941e-02  2.020e+02   5.992 9.37e-09 ***
Soil_TypeTypic Yellow Ultic Soil                       1.099e+00  3.214e-01  2.020e+02   3.420 0.000758 ***
SpeciesPoplar                                          6.136e-01  4.112e-01  3.207e-09   1.492 1.000000
SpeciesKanuka                                          9.922e-01  3.983e-01  2.824e-09   2.491 1.000000
Diameter:Soil_TypeTypic Yellow Ultic Soil              -1.645e-02  2.308e-02  2.020e+02  -0.713 0.476805
Diameter:SpeciesPoplar                                 -1.634e-02  2.416e-02  2.020e+02  -0.676 0.499586
Diameter:SpeciesKanuka                                 -9.049e-05  2.314e-02  2.020e+02  -0.004 0.996884
Soil_TypeTypic Yellow Ultic Soil:SpeciesPoplar         -7.264e-01  4.568e-01  2.020e+02  -1.590 0.113337
Soil_TypeTypic Yellow Ultic Soil:SpeciesKanuka         -9.841e-01  4.329e-01  2.020e+02  -2.273 0.024052 *
Diameter:Soil_TypeTypic Yellow Ultic Soil:SpeciesPoplar  4.458e-02  3.255e-02  2.020e+02   1.370 0.172345
Diameter:Soil_TypeTypic Yellow Ultic Soil:SpeciesKanuka  2.226e-02  2.937e-02  2.020e+02   0.758 0.449354
---
Signif. codes:  0 ‘***’ 0.001 ‘**’ 0.01 ‘*’ 0.05 ‘.’ 0.1 ‘ ’ 1

Correlation of Fixed Effects:
            (Intr) Diamtr Sl_TTYUS SpcsPp SpcsKn Dm:S_TTYUS Dmt:SP Dmt:SK S_TTYUS:SP S_TTYUS:SK D:S_TTYUS:SP
Diameter    -0.720
Sl_TypTyYUS -0.647  0.674
SpeciesPplr -0.732  0.527  0.474
SpeciesKank -0.756  0.544  0.489    0.553
Dmt:S_TTYUS  0.605 -0.841 -0.850   -0.443 -0.457
Dmtr:SpcsPp  0.578 -0.803 -0.542   -0.704 -0.437  0.675
Dmtr:SpcsKn  0.604 -0.839 -0.565   -0.442 -0.681  0.705      0.674
Sl_TTYUS:SP  0.455 -0.474 -0.704   -0.602 -0.344  0.598      0.633  0.398
Sl_TTYUS:SK  0.480 -0.501 -0.742   -0.352 -0.595  0.631      0.402  0.627  0.522
D:S_TTYUS:SP -0.429  0.596  0.603    0.522  0.324 -0.709     -0.742 -0.500 -0.859     -0.448
D:S_TTYUS:SK -0.476  0.661  0.668    0.348  0.537 -0.786     -0.531 -0.788 -0.470     -0.841      0.557
```

Note. Above: the ANOVA test of the model. Below: Summary of the model effects. Tōtara was set as reference species in the displayed fit of the linear mixed effects model.